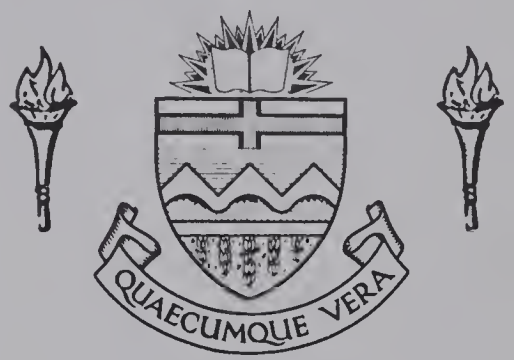

The University of A
Printing Departm
Edmonton, Alber

THE UNIVERSITY OF ALBERTA

A LANDSLIDE NEAR EDMONTON

by

© EBERHARD F. LORBERG

A THESIS

SUBMITTED TO THE FACULTY OF GRADUATE STUDIES

IN PARTIAL FULFILMENT OF THE REQUIREMENTS FOR THE DEGREE

OF MASTER OF SCIENCE

DEPARTMENT OF GEOLOGY

EDMONTON, ALBERTA

SPRING, 1971

THE UNIVERSITY OF ALBERTA

FACULTY OF GRADUATE STUDIES

The undersigned certify that they have read, and recommend to the Faculty of Graduate Studies for acceptance, a thesis entitled A LANDSLIDE NEAR EDMONTON, submitted by Eberhard F. Lorberg in partial fulfilment of the requirements for the degree of Master of Science.

ABSTRACT

A landslide on an abandoned cutbank along the North Saskatchewan River was investigated. Standard procedures were employed and conventional equipment and instruments were used to arrive at and compile a large-scale surficial materials, structure and contour map, a cross-section along the longitudinal axis of the slide, and lithologic sections in bedrock and slide material.

The principal materials involved in the slide area, are from top to bottom: Lake Edmonton silts and clays, two tills, bentonitic, partly concretionary beds of shale and sandstone, and a seam of coal from the Edmonton Formation. Surficial expressions, vegetal regrowth and auger hole logs indicate the occurrence of an earlier slide. The shear zone of the more recent slide is shallow and material displacement is large. The mass probably descended quite rapidly.

Probable causes of this slope failure are: additional consolidation of all materials due to the load of glacial ice and subsequent differential rebound, under-cutting by the river, a fault trending normal into the bank, lateral expansion and fissuring of bedrock near the surface, swelling pressure of clays, the increase of hydrostatic pressure in open fractures due to seasonal meltwater, and the removal of gravel from the toe by man.

ACKNOWLEDGEMENT

The author acknowledges with gratitude all assistance offered by staff of the Department of Geology and Civil Engineering, notably Dr. A.J. Broscoe under whose direction this work was initiated, Dr. S. Thomson and Dr. E.W. Brooker who offered valuable suggestions on mechanical aspects of slope stability, Dr. J. Toth who pointed out some of the effects of fine grained rock on groundwater motion, and Dr. J.S. Bell under whose kind and tolerant supervision this work was completed. Both departments offered their facilities. Through the Department of Geology, the University assisted financially. A student, B. Smith, tirelessly assited in field and laboratory work. For the compiling of drawings, D. Seibt, M.J. Oosting, and E.W. Spofford offered their experience. I would also like to express my gratitude to the Water Resources Division of the Department of The Environment and it's personnel for their assistance.

TABLE OF CONTENTS

TABLE OF CONTENTS, CONT'D

Title, Cont'd

LIST OF FIGURES

LIST OF FIGURES, CONT'D

LIST OF FIGURES, CONT'D

LIST OF TABLES

LIST OF PLATES

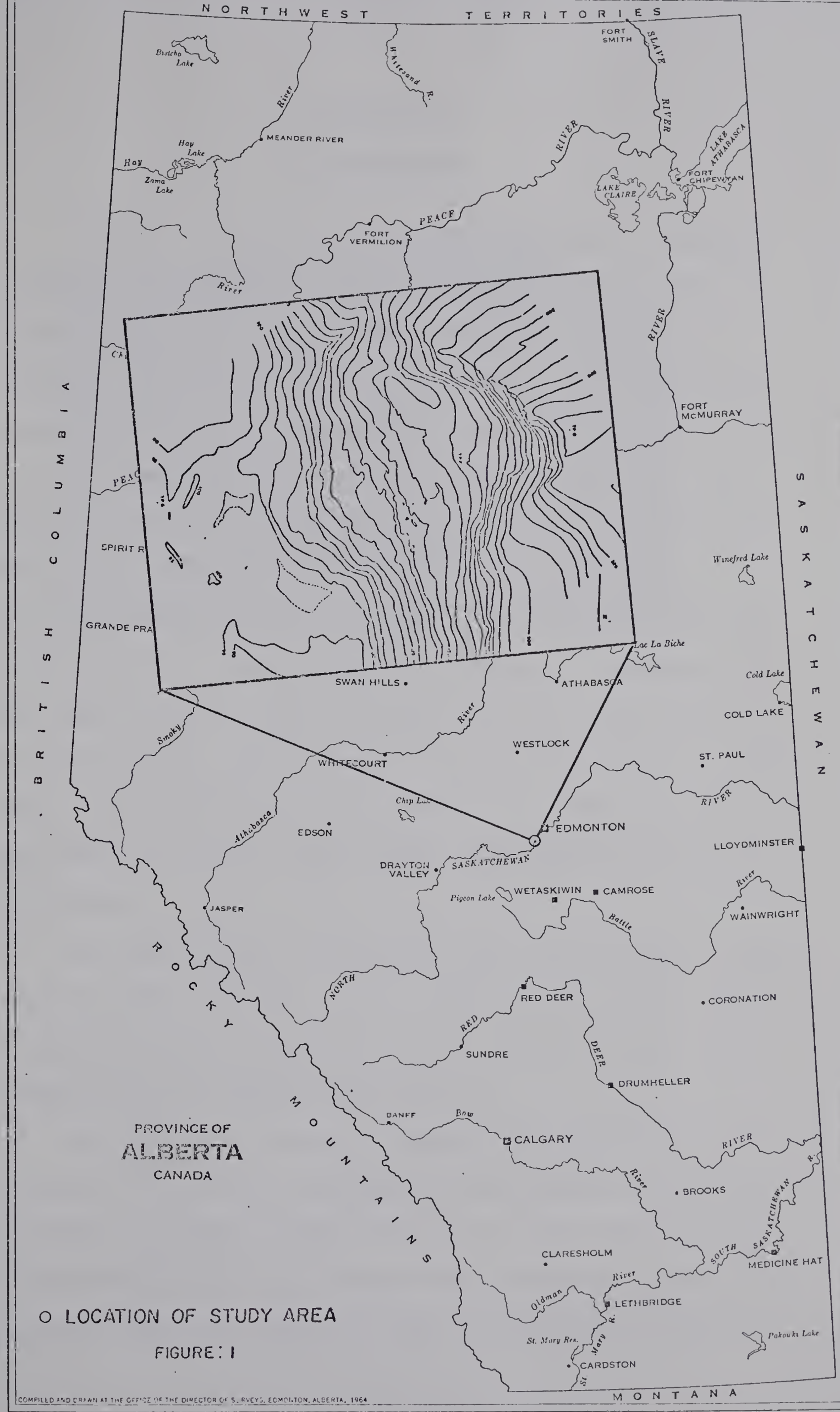
NORTHWEST TERRITORIES
FORT SMITH
SLAVE RIVER
Bistcho Lake
Hottesend R.
River
MEANDER RIVER
Hay Lake
Hay
Zama Lake
RIVER
LAKE ATHABASCA
FORT CHIPEWYAN
LAKE CLAIRE
PEACE
FORT VERMILION
River
RIVER
FORT McMURRAY
BRITISH COLUMBIA
PEAC
SPIRIT R
GRANDE PRA
Winefred Lake
Lac La Biche
SWAN HILLS
ATHABASCA
Cold Lake
COLD LAKE
River
Smoky
WESTLOCK
ST. PAUL
WHITECOURT
Chip Lake
RIVER
Athabasca
EDSON
EDMONTON
LLOYDMINSTER
DRAYTON VALLEY
SASKATCHEWAN
Pigeon Lake
WETASKIWIN
CAMROSE
River
JASPER
Battle
WAINWRIGHT
ROCKY MOUNTAINS
NORTH
RED DEER
CORONATION
RED
SUNDRE
DEER
DRUMHELLER
BANFF
Bow
CALGARY
RIVER
River
BROOKS
SOUTH SASKATCHEWAN R.
CLARESHOLM
MEDICINE HAT
River
Oldman
LETHBRIDGE
St. Mary Res.
St. Mary R.
Pakowki Lake
CARDSTON
MONTANA
PROVINCE OF
ALBERTA
CANADA
O LOCATION OF STUDY AREA
FIGURE: 1
COMPILED AND DRAWN AT THE OFFICE OF THE DIRECTOR OF SURVEYS, EDMONTON, ALBERTA, 1964

CHAPTER ONE

INTRODUCTION

In Webster's Third New International Dictionary, a landslide or landslip is defined as "(1) the rapid downward movement under the influence of gravity of a mass of rock, earth or artificial fill on a slope, (2) the mass that moves or has moved." This investigation is primarily devoted to the second definition. Terzaghi (1929) differentiates between the shearing slide or slump and the flow slide. A slump is a "downward slipping of a mass of rock or unconsolidated material of any size, moving as a unit or as several subsidiary units, usually with backward rotation on a more or less horizontal axis parallel to the cliff or slope from which it descends. Displacement is usually small relative to the size of the block. The slip surface is deep and spoonshaped. Most slumps move slowly and intermittently over a long period of time but some are completed in a single rapid slip" (Sharpe 1938, p.65). While a flow slide involves only a skin of surficial material.

The landslide under investigation falls under Terzaghi's group of shearing slides or slumps. It is a shallow slump of large displacement and rapid movement that spills over the lip of its shear surface and grades into an earthflow towards the toe.

The slide area is located in NW¼ Sec. 28, Tp. 51, Rg. 23, W 4 Mer., close to "Big Island", eight aerial miles southwest of the University Campus in Edmonton, Alberta (Figure 1). The slide material has slid out westward from a steep cutbank into an abandoned channel of the North Saskatchewan River (Figures 2 & 3). To the north of the slide

Figure 2. Landslide after drilling. View eastward from floodplain.

is a wooded area exhibiting progressive wedge or block sliding, to the east a hummocky belt that abruptly yields to a gently undulating plain, to the south a steep slope that is sparingly vegetated, and to the west a gravel-covered low terrace, "Big Island," and the River.

Until two centuries ago little was known about landslides. Collin (1846) published a detailed report on the geometry of failed slopes in clays and postulated causes of their failure, which marked the beginning of geomechanics. But this significant work was largely ignored and forgotten until Terzaghi (1925) injected renewed enthusiasm into research on slope failure. Since then a large number of workers have produced volumes of valuable material on this topic. Among them Sharpe (1938, 1960) summarized the types of slides and their relation-

Figure 3. Landslide. View downslope from the crown.

ship to other forms of mass wasting; and Terzaghi (1951) grouped the causes of slope failure into two categories: those that are directly responsible and those that are indirectly responsible for a slide. In 1958 the U.S. Highway Research Board Landslide Committee published the Special Report No. 29 entitled Landslides and Engineering Practice which summarized all work , currently accepted definitions, and forms. of slope failure. Because of its concise, comprehensive and logical presentation, material from Plate 1 and Table 1 of this particular report served as a basis for the terms and scales used in this study.

Relatively little has been published on slope stability in the overconsolidated bentonitic rock that typically outcrops on valley sides in the Edmonton area. This rock is jointed, poorly cemented, thin bedded, lenticular bentonitic sandstone and shale of continental origin and of Upper Cretaceous age (Ower, 1958). Tills and lacustrine deposits overlie this succession. Scott and Brooker (1968) have approached the problem of slope stability in bentonitic shales that typically outcrop for many miles along streams in the Prairies, and Bruce (1966) has studied slope failure in a similar succession, the bentonitic Pierre Shales of South Dakota. In addition some research has been undertaken recently by the University of Alberta staff on aspects of slope stability, however, little has yet been published.

In the present study the slide is mainly in bentonite-rich sandstone some of which have a salt-and-pepper appearance, and shales of the Upper Edmonton Formation, which are covered with two sheets of till and beds of Lake Edmonton silts and clays. The object of this study was to map all features of the slide area, to establish the shear surface of the slide, to estimate displacements of surficial slide material, to determine some engineering properties of the materials in-

volved, and to determine the more significant factors responsible for this slide. It is emphasized that this is a geomorphic study.

CHAPTER TWO

METHOD OF INVESTIGATION

Field Work

Since both general and detailed surficial expressions of the slide are of prime significance in estimating the character of the landslide, an accurate topographic map (Plate 1) with one-foot contour intervals was required. To establish a control grid, 185 labelled pegs were placed at topographically and lithologically strategic points. Almost all pegs were surveyed with a transit by triangulation and checked with a chain to with $\pm$0.1 feet in elevation and $\pm$0.5 feet in plan. The ground elevation at TPA on the flood plain gravels was chosen as an arbitrary datum of 100 feet in elevation, roughly 2100 feet above mean sea level; the location itself was the end of a baseline. Pegs within the slide area proper were marked with numbers and pegs along both ends of the slide were labelled with prefixes CL and TL, (Plate 1) meaning cliff line and toe line. The pegs were 5 to 30 feet, or an average of 20 feet, apart and provided good control for visual mapping. Then, with an optical alidade and plane table, points an average of 3 feet apart were surveyed and plotted. On an overlay of this plot of points, the elevation countours, at one foot interval, were closely estimated in the field, thus ensuring that all prominent and almost all small features were included. Small features, such as protrusions and depressions, having less than 1/2 foot of relief were ignored. To ensure against excessive crowding of contour lines a scale of 1 inch to 10 feet was chosen.

On the countour map an outline of surficial materials, their attitudes and fractures, and the location of surface material samples were plotted (Plate 1). Later, the locations of drill holes and trenches were added to this map.

One hundred bag samples, prefixed with an S, (Table 3) were collected from the surface, located on the map (Plate 1), and later matched with those recovered from the subsurface investigation.

The subsurface investigation involved drilling seven power auger holes along the line of greatest estimated movement, (Plate I1 to IX), denoted as line C-C and one auger hole D-1, (Plate X), in a graben below the northern scarp. Both disturbed and undisturbed samples were recovered at one foot intervals. The tool was always driven to refusal.

The lithology of in-place bedrock was logged from two manually dug trenches. The trench along line A-A (Plate XI), follows the grade up the cut-slope just south of the slide. An averager of 6 feet, and up to 10 feet, of weathered material had to be removed before undisturbed bedrock was reached. The trench along line B-B, (Plate XII), is an offset continuation of trench A. It, too, follows a straight line, but within the slide near the southern end of the main scarp. Because of its recent exposure, weathering was relatively shallow so that less than 2 feet of material needed removing.

Attitudes of probable joint planes were measured in till outcropping along the northern scarp (Table 2, Figure 50). No such planes

were found in the same till on the southern scarp where fabric measurements were done (Table 1, Figure 49). All field work was completed in the winter and spring of 1968.

Laboratory Work

In order to establish the mineralogy and engineering properties of the materials involved in the slide, one or more tests were performed on each of the 436 samples collected. The results are tabulated in Table 3 and plotted in part on Plates III to XII. Three dozen thinsections were prepared and examined under the petrographic microscope and photographed but were not found to be useful in this study. Two dozen of these photomicrographs are illustrated in Figure 37 (in Appendix C). The clay fraction, of particle size not exceeding 1 micron, of 8 rock samples was prepared for, and subjected to X-ray diffraction analysis. The results are illustrated in Table 4.

Essentially all rock material disintegrated readily with agitation in water and could therefore be subjected to testing procedures suited for soils. Hence, complete mechanical analyses were performed on 300 samples, and Atterberg limits on 135 samples. The natural moisture content was measured on 395 samples. The results were used mainly for lithologic correlation of slide material with that in-situ.

Most undisturbed, or shelby tube, samples from the auger holes were cut axially and photographed (Figure 36). Carbonate content determinations were performed on 321 samples (Table 3 and Plates III to XII).

Essentially all rock material disintegrated readily with agitation in water and could therefore be subjected to testing procedures suited for soils. Hence, complete mechanical analyses were performed on 300 samples, and Atterberg limits on 135 samples. The natural moisture content was measured on 395 samples. The results were used mainly for lithologic correlation of slide material with that in situ.

Most undisturbed, or shelby tube, samples from the auger holes were cut axially and photographed (Figure 36). Carbonate content determinations were performed on 321 samples (Table 3 and Plates III to XII).

CHAPTER THREE

RESULTS OF SURFACE INVESTIGATIONS

Field and laboratory data were compiled in the following forms: several small-scale outline and indicator maps (Figures 39 to 46), a large-scale composite map (Plate I), a cross-section through the slide along line C-C (Plate II), and logs from auger holes and trenches (Plates III to XII). Tables 1 to 4 list all data. Figure 46 indicates the location and scope of Figures 3 to 33. Figure 51 contains the legend to the log plates.

Morphology of the Slide

The slide surface exhibits the following features (Figure 40): a V-shaped crown and flanks, a bisected main scarp the foot of which is largely covered with talus, a slightly backward rotated head, a number of drifted-apart and forward-tilted blocks below the head, three major and several minor transverse ridges on the back of the outflowing slide material, a rimmed halfmoon-shaped toe and onlapping tip. Visible shear and tension fractures are common in many parts of the slide material (Figure 41).

The Crown

The crown spreads across the highest area of the main scarp. At its edge it breaks abruptly through the turf with no visible fractures and little bevelling. Between pegs CL-6 and CL-7 (Plate I) a small scarp trends easterly. The ends of the crown-line turn westerly quite abruptly and continue in cliff-lines. As seen on the shear slope

the material under the crown is water-deposited silts and clays of glacial Lake Edmonton, with the proportion of silt increasing with depth. The contact with till is conformal without transition (figures 4, 5 & 6).

The Flanks

The surfaces of the two flanks differ considerably from each other (Figure 2). The northern flank is covered with a stand of young deciduous trees and moderately dense underbrush. Trees close to the scarp, particularly those higher up the flank, are stunted or dried out, clearly indicating a lack of soil moisture. The slope is exposed to the north. Except for the two anomalies at the faults (Plate 1), it is fairly smooth. A few old tree stumps lean up to ten degrees into the slope and the lower parts of some trunks are bent outwards from the slope. The slope ends at CL-16 in old, progressive slide material.

The southern flank which is exposed to the southwest, is free of shrubs and trees but is covered with grass. Its inclination varies with the type of underlying materials. The slope is shallower in the lacustrine silts, clays, and in the highly fissile black shales under the tills, and steeper in the tills. The cliff-line, or edge, is bevelled between CL-4 and CL-6 and is increasingly separated into parallel enechelon turf strips as one approaches the scarp. No cracks are visible further down the cliff-line.

In plan the crest, or crown-line, together with both cliff-lines, resembles a right-angle V with its axis pointing northeast. Its total length is approximately 180 feet. In more detail the entire crest projects as a series of concave inward lines, each spanning

Figure 4. Central section of scarp and crown.

Figure 5. Columnar till and lacustrine silts and clays on northern scarp.

Figure 6. Upper central and southern scarp.

a section of material of different properties. The ends merge imperceptibly with the slopes. The southern limb of the crest projects as a shallow zig-zag pattern to CL-1 and disperses beyond peg 20. All points that lie south of a straight line that connects CL-1 and TPB on the northern limb deviate little from a straight line.

The Scarp

It was indicated earlier that different materials underlie the flanks and crown. The upper members of the Edmonton Formation, till and

glacio-lacustrine deposits are clearly exposed along much of the 50-foot high scarp and control the angle of repose. However, this scarp is structurally interrupted along a long talus slope between TPB and TPF (Figure 4), a point on the highest part of the slide head. A talus wedge, the thickness of which is largely related to the quantity of debris available, skirts much of the scarp and obscures the contact line with the head.

The slope of the scarp changes for each type of material exposed. The central portion increases with silt content from 35 degrees at the top to 45 degrees at the till contact (Figure 6). In the area between CL-6 and peg 2 the slope is steeper and appears to have sagged considerably. Cracks and large voids between blocks of till seem to point to a disturbed zone beneath the surface (Figure 7). Indeed, a vertical displacement of almost 8 feet was measured where material to the south is on the upthrown side.

South of CL-8 is another crease, where a downward displacement of 4 inches with respect to material to the north could be measured. The silt beds immediately above the till point between CL-8 and peg 4 stand vertically for several feet before they grade into clayey beds that assume an average angle of repose that ranges from 25 to 40 degrees (Figure 5). The ground surface east of CL-8 is irregular. Thus a large block has dropped between CL-6 and CL-8. It is worth noting that the surface between CL-6 and CL-7 has dropped 2 feet only, and not 8 feet as measured on the scarp.

A relatively major shear fault zone due to earlier sliding was exhumed west of peg 2 and between pegs 3 and 5 (Figure 7). This fault is in line with and is the cause of the depression trending east through CL-7. It is dipping steeply to the north and disappears

Figure 7. Fault zone below peg 2; left portion of photograph.

under the talus slope below.

The contact between the silt beds and the tills below is sharp and conformable. It is dipping several degrees southeast on the north side and one to two degrees on the south side of the scarp. The upper till is tough, medium grey, desiccated on the surface, and 7 to 9 feet thick. It rests on a thin irregular sheet of well-sorted sand, probably the Tofield Sands. On the south scarp it is a vertical continuous wall but on the north scarp it is columnar (Figures 4 & 5).

The lower till is dark grey and lightly stained, weak and finely fissured and rests at angles of between 35 and 55 degrees. It is mostly covered with fine debris. The contact with the Edmonton Formation below is nonconformable (Figures 8 & 9).

The attitude of the Edmonton Formation outcropping below the tills is also very difference on both sides of the scarp. On the north side sandstone beds striking northeast and dipping 18 to 20 degrees easterly make an unconformable contact with the tills (Figure 10). Between pegs 44 and 46 a wedge of till, sandstone and tuffaceous shales has slid down some ten feet (Figures 10 & 11). The exposed triangle within CL-16, pegs 44 and 54 is covered with bentonitic deeply weathered light grey shales and clay-ironstone pebbles (Figure 33). This surface appears to be paralleling a continuation of the cutbank along trench A. Dragged-along material of the same type is found below this triangle.

On the south scarp the Edmonton Formation reaches a higher elevation and exhibits finely fissured mauve shales and buff to light grey bentonitic and tuffaceous shales above the salt-and-pepper sandstone. These beds dip 6 to 8 degrees to the east. The contact with the tills above is nonconformable. The scree-covered shales rest with a slope of 42 to 45 degrees whereas the sandstone bulges to stand up to 80 degrees east of peg 13 (Figure 12). In the middle of the bentonite-rich sandstone is a porous, calcite-cemented, erosionally resistant, cross-bedded sandstone which does not yet protrude.

A striking feature is a thick lens of sandstone within the shales above the sandstone beds between pegs 10 and 11 (Figure 10). Its beds and contact planes strike east-west and dip 23 degrees north. The upper contact is nonconformable with shales but the lower contact

Figure 8. Paraconformable contact between till and sandstone on northern scarp. Note difference in slope between tills.

Figure 9. Upper till, lower till and sandstone. Note deformed layers of silt embedded in lower till, rills on talus apron.

Figure 10. Till-sandstone contact exposed along northern scarp.

Figure 11. Wedge of till above sandstone and tuffaceous shale on northern scarp.

Figure 12. Sandstone and overlying fissured shales of southern scarp.

is unconformable, seperated from the shales by a 1/2 inch thick zone of slickensided shales. The shales below this thin zone are dipping 6 to 8 degrees to the east. At both ends is a sequence of interfingered wedges, dipping under talus to the north and bending down to the south to conform with the locally prevailing attitudes.

Much of the centre portion of the scarp is covered with a silt- and till, sandstone and shale talus apron of increasing thickness downslope (Figures 4 & 7). The location of formation contact planes and the fault zone could be guessed only. Similarly, much of the contact along the top of the head is concealed under a wedge of this debris. The largest particles fringe the lowest strip of the debris cone.

The Head

There is one large, voluminous head below the scarp. No minor scarps were noticed elsewhere on this head. Its surface is generally sloping downhill at low angles. Shrubs and trees often indicate the amount of tilting due to sliding. In plan it is halfmoon shaped and breaks off sharply to the west along the 157-foot contour line. The maximum downward displacement of the head is 60 feet, its lateral displacement westward some 70 feet, and its backward rotation at least 7 degrees, as measured from the till-silt contact under TPF.

On the northern part of the head large, curvilinear shear and separation fractures are common (Figure 13). Till underlies most of the area, and lake deposits cap the east-central area. A 3-foot deep graben clearly marks the northernmost edge of the head and disappears under the talus. It does not reappear on the south side. Going southeast, from peg 54 the graben is at first 10 feet wide and 6 feet deep, then it widens to 25 feet in a depression at auger hole D-1, and then it rises until it finally disperses somewhere between pegs 30 and 31.

The Body

One half of the entire area within the slide is occupied by a broad body of much-deformed, broken slide material. Its widest section spans 220 feet between CL-16 and peg 74, and over 120 feet in plan along line C-C, between the 157-foot and 98-foot contour lines. Its average slope is 25 degrees.

The topography allows the body to be divided into two distinct sections: a smaller section in the northern area (Figure 14) and a larger section in the central and southern area (Figure 15). The upper

Figure 13. Tension cracks common on northern part of slide head that is underlain by till.

portion of this northern area has a steeper and more variable slope than the lower portion. Its surface is fractured and quite rough, with blocks of sandstone outcropping, as for example around peg 57 (Figure 16). The strip between TL 22-23 and peg 56 is also quite steep, but the disturbed shales that outcrop here dip southerly at 25 to 28 degrees and are not completely disjointed (Figure 17). The lower portion is relatively smooth, evenly sloped, and lightly vegetated (Figure 14).

A 30 to 50-foot wide, very sandy and evenly sloping strip south

Figure 14. Northern section of slide.

Figure 15. Central section of slide.

Figure 16. Outward wedged blocks of sandstone and bentonitic shales.

Figure 17. Outward wedged and dipping beds of bitum¡nous, bentonitic shales that are not completely disjointed.

of the area just described is a transition zone to the major and later slide. It is marked with a slight topographic indentation and with a few low diagonal ridges traversing its upper part (Figure 14). Sandstones mixed with light grey bentonitic shales are present here. In the middle, between pegs 86 and 92, are a few blocks of vegetated till. The lower portion steepens to 44 degrees down to peg 121 but levels out at peg 123. The principal surficial rock is salt-and-pepper sandstone of the Edmonton Formation, interspersed with fragments of light buff bentonitic shales.

Quite distinct from the outcropping slope materials described so far is much of the surficial material on both sides of line C-C (Figure 15). Most of it, in the upper portion, is till that thins out in a veneer of vegetated tilley debris downslope, and has occasional windows of silt and shale. The lowest strip exhibits highly disturbed shales, sandstones and clay-ironstone concretions but no till. All surface material has drifted and separated to some extent.

The edge of the head north of line C-C is distinct and straight but becomes indistinct and interrupted to the south of this line. Downslope the topographic contours become more and more curved, convex outward, with three transverse ridges evident. From the indistinct edge of the head, the till has drifted apart as thick blocks in a southwesterly direction (Figure 18), and rapidly wedges out to the south. The mauve shales and buff Lake Edmonton deposits outcrop at only two locations. Downward from the black shale window around peg 80 the till in its original state wedges out and carries on as a wasted, vegetated veneer almost to the toe near peg 110. Below the edge of the

Figure 18. Blocks of till separating from edge of slide head.

veneer, shales and sandstone can hardly be distinguished at the surface. Later, bulldozer cuts revealed a maze of variably tilted blocks dipping generally towards line C-C.

The uneven southern edge grades indistinctly into relatively undisturbed rock. Only near pegs 20, 73, 74, 101, and 103 do shear and tension fractures delimit the margin of the slide. A distinct scarp between pegs 97 and 120 clearly delineates a short section of the boundary (Figure 19). The contact with the foot, however, is almost everywhere clearly defined as a near horizontal line which is the result of the intersection of the sloping body surface and the essentially level foot surface. This boundary line ends at peg 103 to the south and peg 123 to the north. A variety of surface and freshly exposed near-surface materials is illustrated in Figures 20 to 26.

Figure 19. A sharp break (left) between the transition zone and the main section of the slide body.

Figure 20. Shale pinnacles near foot of slide. The outcropping rock mass appears disrupted and mixed.

Figure 21. Mixture of shales and calcareous sandstone on lower transverse ridge.

Figure 22. Shales and fractured sandstone just below surface of lower transverse ridge. Here, the rock mass is fractured only.

Figure 23. Bentonitic shale and till exposed in main section of body.

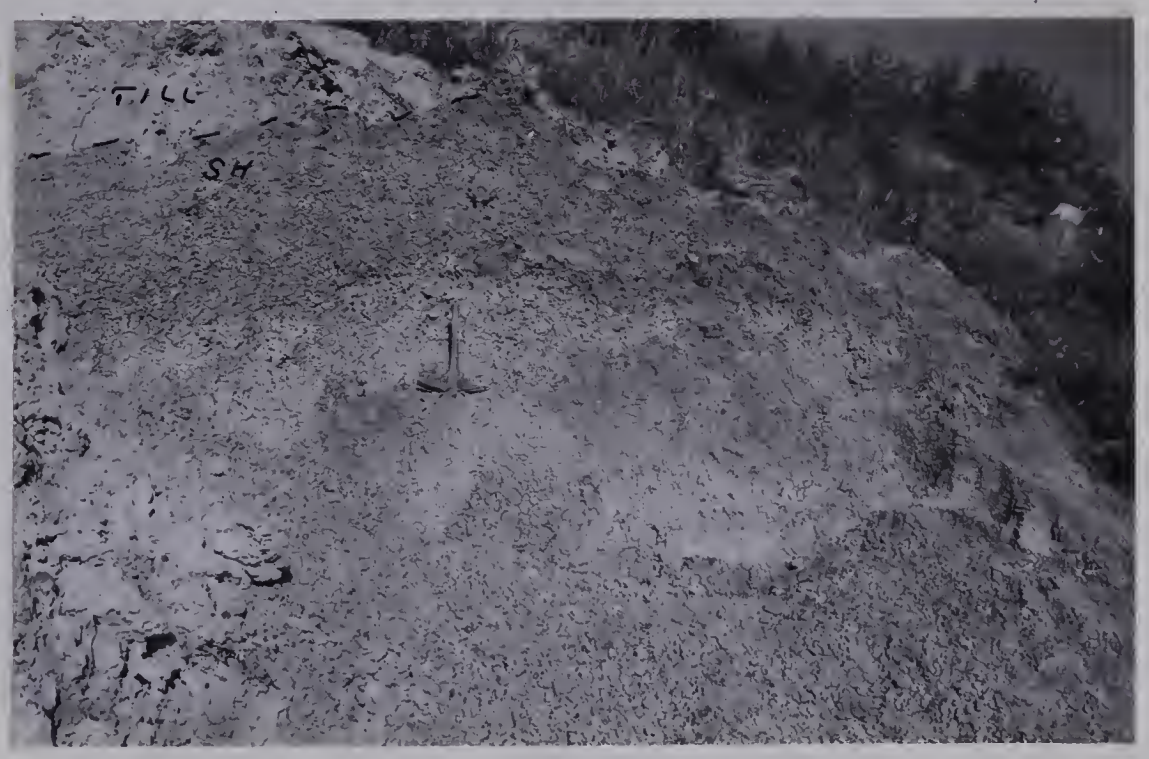

Figure 24. Bentonitic shales exposed in upper main section of body.

Figure 25. Bentonitic and tuffaceous shales exposed under veneer of till.

Figure 26. Shales and sandstone exposed in centre of main section of body.

The Foot

The foot rests entirely in the abandoned stream channel. It is quarter moon shaped in plan, it holds two shallow bodies of water in the large inner depressions, and its elevated but broken toe, or rim, tucks into both sides of the major slide. The surface is weathered such that all the more elevated knolls or swales clearly exhibit tension fractures (Figures 27 to 30), and loose fine grained sediments is washed into depressions, often burying the original surface (Figures 31 & 32). The ponded water is surface runoff and is therefore constantly turbid, with colloidal bentonite clays that do not settle sufficiently before the next downpour of rain washes more clay sized particles into these ponds. During the winter season evaporation and seepage has been observed to reduce this water level by more than 8 inches. Vegetation in the foot area is young and scant.

Surficial material is generally moister and softer than material anywhere else in the slide. It is also well mixed and perhaps remolded in places. Sandstone, shales, concretions, and calcicemented sandstones are present as an unsorted disoriented mass of blocks (Figure 30). Coal outcrops in noticeable quantity south of peg 133 only (Figure 28 & 32). It is derived from the coal seam exhumed at the 120-125 foot level in the A-line trench. Partings of coal derived from very thin lenses under the sandstone member are found around pegs 139 and 126. Clay-ironstone fragments appear to have been scattered like seed grain over many parts of the foot and buoyed up in other areas without forming a clearly decipherable pattern.

It is worth noting that the toe along the northern end is rough, steep and overlaps earlier slide material as is indicated by overrun shrubs, whereas along the southern end of the foot undisturbed

Figure 27. Fractured swale on foot of the slide.

Figure 28. Open fracture on foot. Coal seam is exposed.

Figure 29. Open fracture on foot filled with stagnant muddy surface water.

Figure 30. Fractured low relief knoll on swale of slide foot.

Figure 31. Mud filled cracks around partially disintegrated swale blocks.

Figure 32. Disintregrated coal and bentonitic shales on foot of slide.

vegetation gradually increases with proximity to a body of standing water towards which the ground slopes fairly gently and evenly so that the two materials could not be clearly differentiated. The western strip of the toe drops only slightly because it onlaps sharply against a broad ridge of gravel tailings.

Observation of Precipitation, Runoff, and Infiltration

Snow accumulated most and remained longest in depressions not directly exposed to sunlight. Larger and deeper snowpacks occur between TL-9 and TL-10, TL-1 and peg 103, around pegs 10, 12, 24, and 53 and between pegs 28 and 54, 97 and 120. These areas remained quite moist until the end of spring. Groundwater seepage near peg 7 under the talus slope was most pronounced right into July, at which time this source of moisture also dried up. A spring-runoff rivulet discharged over the edge of the head, at peg 70, and dispersed between the blocks of till below. No other running or ponded water was observed except that on the foot as described above.

It was observed that after a moderate rain shower a thin sheet of water carried grains of sand and some clay readily some distance downslope on exposed surface. Because the clays swelled quite readily upon wetting and thus sealed the pores (Figure 33), infiltration was less than 1/2 inch on shales but up to 1/2 inch in bentonitic sandstone. After a week of damp weather, water infiltrated no further than one inch.

Another feature worth noting here are the deep hair line cracks in the surficial soils of the original cutbank. Though invisible at the surface these cracks were exposed and traced into the bedrock in trench A. They are almost vertical, thin wet ribbons

Figure 33. Exposed bentonitic shales on most northern end of scarp.

widely spaced but concentrated in portions of deepest overburden. They don't appear to aid soil creep very much; instead, outward rotation, some toppling over and slumping in behind the cracks seems to be a preferred mechanism of motion.

Frost penetration during the winter was not measured, as frozen ground could not be penetrated with hand tools.

RESULTS OF SUBSURFACE INVESTIGATIONS

Auger Hole and Trench Data

In order to establish a section for correlating bedrock material from the 8 auger holes, trenches A and B were dug. On Plate XI, which illustrates Section A, the shales and sandstones below a five-foot thick coal seam, at elevation 120 to 125 feet, are quite silty, whereas those above the coal are clayey and often rusty. Clay-ironstone beds are common at elevations of 98, 125, 140, 156, 161-162, and 171 feet. All shales are highly fissile with steeply inclined cracks. Within the large body of shale above the coal bed pure, continuous bentonite seams 1/2 to 1 inch thick were encountered at elevations of 130 and 166 feet. Sandstone outcrops above the 174-foot level. Its matrix is largely bentonite clays. The bedrock is illustrated in Figure 34. The base of the same sandstone is at the 171-foot level in section B (Plate XII). Here it is 11½ feet thick. In the middle the sandstone is a hard, calcicemented, porous, one-foot thick bed. The matrix contains little clay. Above the sandstone in section B are some 15 feet of mauve, tuffaceous shales with a one-inch seam of tuff at the 196-foot level. This tuff and the mauve shales are absent from the north side of the slide. Some material of the lower portion of this section is illustrated in Figure 35.

Field inspection of samples recovered from auger holes afforded a crude appraisal of the lithology within the slide material (Plates III to X and Figure 36). Generally, the degree of fracturing, shearing, separating and mixing of material was observed to be directly

proportional to the distance travelled downslope from the edge of the head. Material within the head has moved essentially as a single, large block as the structure of undisturbed samples from auger holes C-6, C-7 and D-1 indicated.

Nowhere does the shear surface dip into the slope nor is it uniformly curved. Instead, it consists of as many straight segments as there are types of material along it. The lip, or the lower end line of the shear surface, is 20 feet above the surface of the standing body of water just south of the foot.

Below this lip, material of an earlier slide was encountered. It is sandwiched between material of the later slide above it and the undisturbed cutbank and alluvium bed below. All of this earlier slide material is broken up and mixed at the contact with the slide material above.

Laboratory Data

All results from tests performed on collected samples are tabulated in Table 3 and plotted with a few exceptions alongside the lithology on Plates III to XII. A direct-shear test on the salt-and-pepper sandstone yielded no conclusive results; but the bentonitic shale just below this sandstone produced consistent results under similar testing conditions. Cohesive strength is low and the residual angle of shear averages 11 degrees. The average angle of rest of the slide mass is 25 degrees whereas the cutbank rests at 42 to 43 degrees.

It may be noted that the natural moisture content in the slide material is slightly higher than that in the undisturbed material (Plates III to XII). The largest gain in moisture content was found in

shear zone samples where material is remolded. Moisture content was invariably below the plastic limit in undisturbed material but often at or even above this limit in disturbed material.

Because of distinctive test results found in the various materials both the Atterberg limits and the grainsize distributions were largely relied upon to correlate material from the auger holes with material from the two trenches. In other words, lithologic correlation depended much on mechanical properties and this allowed the internal displacements of the slide to be estimated.

Although the clay-mineral assemblage of rock and soils in the Edmonton area have been established (W. Pettapiece, personal communication, Aug., 1968) clays from a few rock samples were subjected to X-ray diffraction analysis. It was found that montmorillonite was invariably the predominant constituant, followed by chlorite and illite. (Table 4). The bentonitic seams at the 130 and 166-foot levels consist almost entirely of montmorillonite. Liquid limits of bentonite from these seams also indicate a high percentage of this swelling sensitive clay. Although the montmorillonite content of the clay matrix in the sandstone was high, the proportion of sand, with respect to the total mass of a sample, was too high to permit Atterberg Limits to be run.

CHAPTER FOUR

INTERPRETATION OF RESULTS

Surficial Morphology

Sufficient data were gathered and observations made to allow an interpretation of many of the surficial features. The major parts of the slide are discussed below and their areal extent is shown on Figure 40.

General Environment

To the south of the slide, the cutbank is now stable as compared to the cutbank to the north of the slide where material from above the 130-foot level bentonite seam has flowed out and been removed through stream erosion.

East of the crown the undulating topography might be due in-part to sliding material. Some indication of earlier movement in this area is provided by the dip of the rocks which is generally steeper than the regional dip.

On the north flank a zone of slumped and actively creeping blocks was noticed. Three north dipping shear zones were observed that are believed to be related to the above movements. In contrast to this, no sign of internal movement was noticed on the south flank which is therefore considered relatively undisturbed.

Scarp

The scarp is basically a spoon-shaped surface bounded on the uphill side by a sinuous crestline. As the map shows the crestline is actually made up of a series of linked crescents which are concave

downslope. The junction between crescents corresponds to boundaries between rock types suggesting that the crestline configuration is related to the present state of internal stress of each of the rock types.

The scarp is recessed into the normally consolidated lacustrine silts and clays that rest on top of the tills. The major reason for this indentation into the middle of the cliff is probably the lack of adequate lateral support of the weak material in the two shear zones that run through CL-7 and CL-8. The larger one of these zones also affects the tills, the shales, and the sandstones below.

The difference in appearence of the upper till between the two sides of the scarp is due to several factors. As noted earlier material on the north side is slumped and therefore more likely to be fractured internally. This allows deeper infiltration of surface water, particularly through the upper till into the clean sands below. Greater exposure to the sun's radiation and thus losses of moisture from the surface is much more pronounced on the north scarp than on the south scarp. Furthermore, trees on the north flank draw large quantities of water during the growth season thus tending to lower the moisture content of the till.

The sand layer between the tills is unconfined laterally at the scarp surface so that the first row of columns can shift and tilt enough to open joints and shear planes, and water can move more easily down into the sand. Staining and slaking was observed more than four feet deep into the flank.

In contrast, the upper till exposed on the south scarp revealed no more than small desiccation fractures at the surface of fissured, moist material. It is exposed to little radiation of the sun. Grasses only draw from its moisture during the growth season.

The lower till is softer and more fissured than the upper till and rests at a moderate slope. This could be attributed to the release of internal stresses in the probably overconsolidated material. The same interpretation likely applies to the shales below this till on the south scarp because of the same texture and slope.

The sandstone below the tills is not fissured and appears stable at a steep angle because the loadbearing silica framework can absorb and release relatively large stresses with little change in volume. The clay matrix probably shares little if any of the load and is thus inactive with regard to stress changes within the rock mass. Except for the thin bed of hard, calcicemented, porous sandstone the clay matrix closes the pores on wetting and the soft sandstone turns into an aquiclude. From water wells in the Edmonton area it is known that this sandstone yields water from open fractures only.

Head

The large head has moved as a single block with little internal displacement. The graben to the north is created by a slight southward shift when the whole mass moved down to the west.

The cracks in the northern portion of the head would indicate that the till is quite thick and was no moister than the same material on the north flank at the time of slope failure. The low area around peg 68 indicated a slipout of softer and probably already disturbed bedrock, which probably came from an area near CL-8. Similarly, the low bay west of a line between pegs 25 and 69 indicates a slipout of weak material under the till. The upward turn of the silt-till contact correlates well with the upward turn of that same contact below peg 2. Thus, the large east-west trending block fault is in part responsible for the large depression on the southern part of the

head. In addition, the western edge is ill-defined here; it is shallow and disrupted.

Northern Portion of Slide Area

The triangular area east of CL-16 and peg 54 is believed to represent the scar of surficial slip. The extent of weathering and vegetal growth (Figure 45) supports this interpretation. It is possible that this area is an irregular part of the cutbank.

Immediately west of this area is a zone of blocky, fractured and sheared material from the Edmonton Formation. It appears that the head has dragged along and wedged-outward adjacent material. No subsurface investigation was conducted here so that the configuration of subsurface shear and bedding planes remains unknown. However, judging from the stable talus material below TL-19 to TL-20 and from a mature, not displaced deciduous tree near TL-20, the slide wedge and slide surface are not as deep here as to the south along line C-C below TPF.

Transition Zone

Subsurface investigations were not conducted in the transition zone (Figure 40) but, with the deep head above, the plane of failure is expected to be at a depth of approximately 30 feet, which is a relatively great depth.

The diagonal ridges striking northwest (Figure 3) are interpreted as resulting from lateral spreading during sliding.

Central and Southern Portion of Slide Body

The surface is generally convex slope-downward and crossed by three transverse ridges. These ridges closely respond to the internal geometry slope downward beneath them (Figure 40, Plates I and II). One or perhaps two such ridges could be expected to develop during a single slide but the third, and lowest, ridge appears to be due to an earlier slide. Part of this material was later bulldozed along and mixed with the material of the most recent slide.

Considering the shallow depth and slope of the scarp the slumped material from either slide cannot be thick. The total thickness of slumped material is probably less than 50 feet and half that thick under the foot. Thus, the slide surface is shallow enough to allow it to be roughly visualized from the surface configuration. As Plate II shows the shear planes are more frequently encountered farther downslope. The sheared material is believed to rest on the original cutbank and on the wedge-shaped plane of failure of this slide on which the head rests. This interpretation is based on the cross-section (Plate ii) discussed further in a following section.

Foot

The morphological configuration of the foot suggests that the availability of water in the abandoned channel contributed substantially to the spreading and thorough mixing of chunks and fragments of bentonitic sandstone and shale. The lateral spreading of the larger chunks is especially well documented in the low interripted outer rim. The high degree of mixing is evident with the absence of any stratigraphic pattern, however faint, on the surface.

Ponded water and a confining bank of worked terrace alluvials are largely responsible for the almost level surface of the foot.

Coal, from the 120-125 foot level seam, outcrops near peg 133 and provides the only measurable displacement of material from undisturbed beds in the cutbank. The absence of this coal elsewhere on the surface of the foot suggests that the coal was buried by slide materials from above the seam. The erratic spatter of coal found in the northern area of the foot is associated with sandstone that is exposed in the north scarp near peg 34.

Anomalous Sandstone Lens

The peculiarly downward-bent sandstone lens between pegs 10 and 11 does not appear to have been deformed by recent stress changes. It could hardly be attributed to slumping because the stresses to cause such a large deformation are believed to be much greater than could possibly be provided under present conditions. Alternatively, ice pressure during glaciation seems to be a more plausible factor. Under streses of several thousand feet of ice, softer material would yield, deform and consolidate more readily than a harder material, particularly in locally anomalous facies. It is thus speculated that perhaps the entire failed area to the north of the slide area was somewhat altered during glaciation and weakened more when variable strains on rebound would have induced differential stresses. Therefore, the east-west trending shear zone, for example, through CL-7 could in part be attributable to this initial weakening of rock material, and the anomalous sandstone lens below is evidence of a large differential shift in this material.

Stress Relief

Material near the surface is fissured and slickensided. Much of this is caused by a significant reduction of lateral confining pressure and accompanying strain. Water entering the fissures is adsorbed by swelling clays that then exert a swelling pressure against confining material.

It was found that the natural moisture content was slightly higher in the slide material below the till than in undisturbed bedrock. (Plates III to XII). This is mainly attributed to increased porosity created by a general major stress relief and accompanying strain expansion in the compressed rock material. Skempton (1948) referred to it as strain softening.

Subsurface

The cross-section C-C (Plate II) was constructed from auger hole data. The correlation of the strata between holes and definition of the subsurface structure was achieved mostly by the use of texture, color, and Atterberg limits. In addition, the surface morphology significantly assisted in delineating the trend and especially the frequency of shear planes between the wedges and slices below the head. Unfortunately, no reconstruction of the internal structure of the slide west and a little east of hole C-4 was possible, but the surface configuration of form and material suggests that no very large blocks are left intact.

The plane of failure is well below the weathered zone which is 6 feet deep, extends east almost horizontally from the cutbank surface into the slope for about 70 feet when it meets the scarp surface that has a grade of 55 degrees from the horizontal. It is not a simple plane of failure of a fixed or uniformly varying

radius of curvature, as is commonly observed in failed slopes of homogeneous or isotropic material. It also should be noted that nowhere is the plane of failure dipping into the slope. This is mainly due to the horizontal, saturated, bentonite-rich zone of shale. Only active earth pressures and large, resisting friction stresses can account for the steep angle of the plane of failure of the scarp. The probable absence of excess pore water pressure allows for such steep angles. It is probable also that the shear plane has maintained the steep angle through the lower till and become vertical through the upper till and the lacustrine deposits. These have then collapsed to deposit the talus apron on the scarp above the head and to leave a stable slope below the crest.

From the description above it is evident that failure of the slope here originated within the highly overconsolidated bentonitic shales of the Edmonton Formation. The high internal stresses and heterogeneous lithology prevented the plane of failure from reaching a great depth. In addition, it is emphasized that the varying internal friction stresses, the load stresses, and stresses due to pore water, just before and at the instant of slope failure, determine in essence the configuration of the plane of failure.

Groundwater

In the absence of data on groundwater its involvement in this landslide remains speculative. No water was found except in Holes C-1, C-2, and C-3. This data was far from sufficient to even guess at the water table location and configuration anywhere within the slope, not to mention groundwater motion.

Instead, the bedrock structure and estimated relative porosity of the material were used in order to arrive at some workable model of groundwater motion and its effects on the medium

under various conditions. Calcicemented sand and rust staining are indicators of active groundwater movement. Open joints in the coal bed can readily transmit groundwater. Shaley beds and lenses of very low permeability separate beds of higher permeability which are usually identified with rust staining or noticeable clay-ironstone concretion content. This alternate bedding is quite frequent though unequally spaced. When montomorillonite clay is hydrated with water, it tends to swell and seal pores, exsert pressure on surrounding material so as to assist slope failure. Thus, if the effects of meltwater or groundwater was among the final factors triggering this landslide, slope failure most likely occurred during or after a wet spring.

Future Slope Failure

There are no signs within the immediate slide area that point to another massive slope failure in the immediate future since the toe is loaded while the head and crests to the south are low. The weaker zones appear to be sufficiently stable, on the one hand, to safeguard against failure, making the slide mass, at least, temporarily stable. On the other hand, there is ample evidence that mass wasting on a smaller scale takes place. Largely as a result of agents that influence surficial weathering and mass wasting, debris, scales and occasionally a block of sandstone or column of till break loose from the scarp and come to rest on the talus apron. Pieces of sod also drift a little from time to time and material on the north flank is creeping. Within the slide mass only the recently cut banks are shifting into a stable position. During the cold season no shifting of any material was detected.

Removal of any material from the bottom of the cutbank however, will tend to make the slope unstable again.

CHAPTER FIVE

EVOLUTION OF THE SLIDE

The internal stress history of the materials studied is: 1) compression due to loading of sediments deposited during late Cretaceous and early Tertiary times; 2) partial release of these stresses by removal of overburden through extensive land erosion; 3) recompression by a thick ice sheet; followed by 4) some stress release when the Pleistocene ice melted away; and 5) the release of stress, laterally was produced by a channel that was rapidly carved out by meltwater from the ice. This channel is now occupied by the North Saskatchewan River (Figure 38.1).

The slide scar, to the north of the slide area, is believed to predate a terrace at its foot, because no slide material was found on the terrace. The terrace, which is wide, gravel capped, and about 25 feet above the present river level, has been dated as at least 6500 years old (Westgate, 1969). The water table in the slide area remains low throughout the year, showing only slight seasonal fluctuations. It is, however, above the terrace level, as indicated by the ponded groundwater in the depressions on the terrace. The water table is highest during the frost free period.

Approximately 25 years ago, based on the appearance of the pit, gravel was removed from the toe of the slope, probably, when the ground was unfrozen. This removal of the toe load, at a time when the groundwater table and therefore the hydrostatic pressure are high, probably was the triggering mechanism for the landslide. The mass slid horizontally, slope-outward, on a weak, bentonite-rich zone, at the piezometric surface. As the mass slid outward, sections on the west

side collapsed into the water-filled gravel pit. The east side of the uppermost portion of the wedge block collapsed into the open space behind it (Figures 38.2 to 38.5). Some material from the cliff, and partcularly from the crown, has since broken away and formed the talus apron.

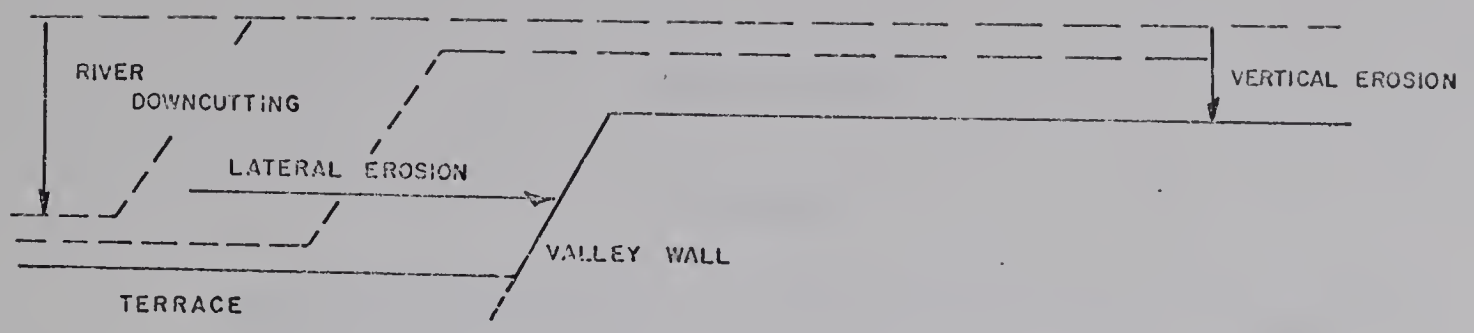

Figure 38.1

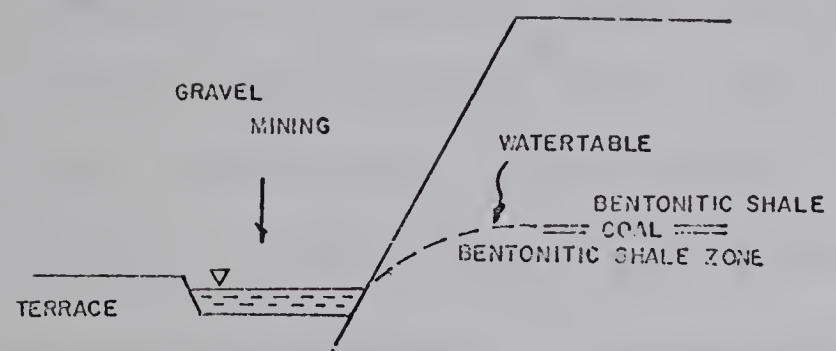

Figure 38.2

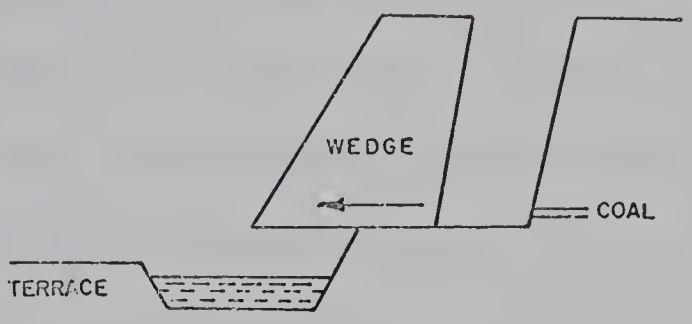

Figure 38.3

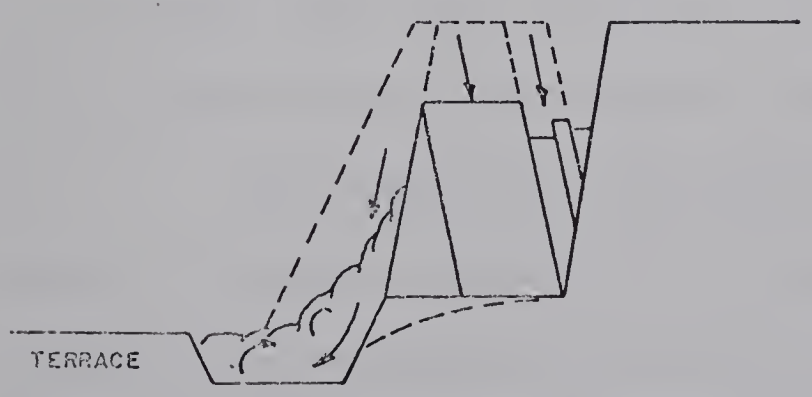

Figure 38.4

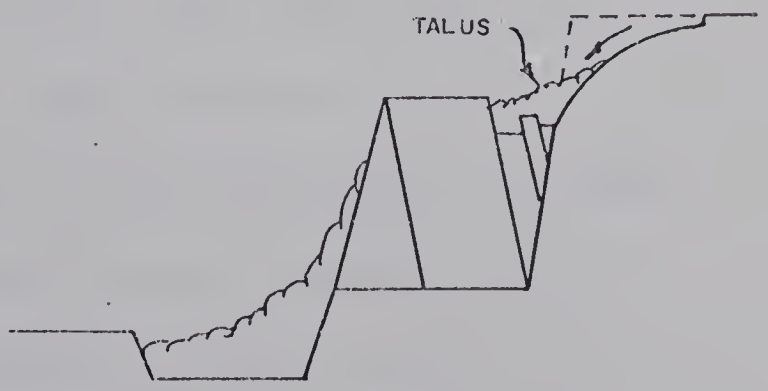

Figure 38.5

EVOLUTION OF THE SLIDE

CHAPTER SIX

SUMMARY

With detailed mapping of surficial materials, topographic and structural features, followed up by trenching, drilling and logging, and finally by tests on over four hundred samples, the motion of the slide with respect to its surficial expressions could be established. Factors causing this slope failure were suggested.

The slide area is located eight miles southwest of Edmonton, Alberta, on an abandoned cutbank of the North Saskatchewan River. The 150-foot high slope faces west. The slide is 220 feet wide, 320 feet long in plan and up to 50 feet thick. The large head has descended 60 feet into a graben, moved outward 70 feet, and tilted backward 10 degrees as indicated by shrubs, and trees as well as borehole information, and the study of surficial material. The few cracks on its northern surface indicate minor internal shearing. Depressions along the southern edge of the head, point to material with greater displacement some distance below the surface. A graben is formed only along the northern rim, which indicates predominant movement away from the scarp. Some material has also wedged outward in the northern portion. The sharp edge of the head is related to the lower end of the shear surface, encountered near the bottom of the auger hole C-4.

The bulk of the slide material is beyond the edge of the head. This is the body on which there are three transverse ridges, or swales, with only the lowest one clearly exhibiting a variety of tension fractures on exposed subsurface material. Till blocks have slid down to almost the lowest ridge.

The moon-shapped foot and toe which rest almost horizontally in the water-filled trench, is encompassed by a broken and tension-fractured, rim.

The materials involved in this landslide are, from top to bottom, Lake Edmonton silts and clays, a columnar, desiccated upper till, a softer and fissured lower till, and from the Edmonton Formation black, mauve and bentonitic shales that are absent under the north flank tills, a thick bed of bentonitic sandstone, a thick sequence of thin-bedded, fissile, bentonitic, concretionary, and sometimes silty shales, a 5 foot thick bed of coal, and silty, sandy and sometimes bentonitic shales below this coal.

Several factors are thought to have influenced the stability of the material in this area. An early and major factor responsible for setting the stage for slope failure, is overconsolidation of rock material that now tends to release presumably large stresses and becomes strain softened. Added to this state of stress, are the stresses left from differential reconsolidation by a thick sheet of ice that has melted away at the close of the Pleistocene Epoch.

Among the more recent and readily detectable factors affecting slope stability are stream cutting that formed the cutbank, fissuring and weathering of exposed material, and some minor local faulting. The steepness of the slope certainly is a major factor contributing here to slope instability. A fault zone trending orthogonally through the upper central portion of the scarp, not only interrupted and thus weakened the slope, but also allowed meltwater to accumulate and build up a hydrostatic head in its large open spaces, probably during spring thaw. Furthermore, montmorillonite clay tends to swell on addition of water, but in a confined environment it converts part of its ability

to expand into pressure that readily weekens its resistance to shear stresses. Removal of the toe load is in this case credited with triggering the slide.

Slope failures in overconsolidated heterogeneous material are typically shallow and wedge-shaped. Borings along a central line have not entirely confirmed this assumption here, but investigations of slides in central Alberta invariably demonstrate a wedge-slide pattern.

A carefully instrumented slope with observation records over many years and continuous sampling of material from many strategically placed holes would reduce guesswork and permit mathematical treatment of the problem. It is estimated that the large outlay for such an undertaking might be feasible in the case of a slope which is about to fail and threatens the safety of a structure such as a bridge abutment or some other property.

SELECTED REFERENCES

Alden, W.C., (1928): Landslide and Flood at Gros Ventre, Wyoming; Amer. Inst. Mining and Metallurgical Eng., Technical Public. No. 140, Trans., Vol. 76, pages 347-361.

Aronovici, V.S., (1947): The Mechanical Analysis as an Index of Subsoil Permeability; Proc. Amer. Soc. Soil Science, Vol. II, pages 137-141.

Baker, R.F. and R. Chieruzzi, (1959): Regional Concept of landslide occurrence; Highway Res. Board Buil. 216, pages 1-16.

Barton, R.H., E.A. Christiansen, W.O. Kupsch, W.H. Mathews, C.P. Gravenor, and L.A. Bayrock, (1964): Quaternary; In Geological History of Western Canada, Alberta Soc. Petrol. Geol., pages 195-200

Bayrock, L.A. and G.M. Hughes, (1962): Surficial Geology of the Edmonton District, Alberta; Res. Council of Alberta, Preliminary Rept. 62-6.

Beatty, C.B., (1956): Landslide and Slope Exposure; Jour. of Geology, Vol. 64(1), pages 70-74.

Bishop, A.W., and N. Morgenstern, (1960): The Stability Coefficients in Earth Slopes; Geotechnique, Vol. 10. No. 4.

Bjerrum, L., (Sept. 1967): Progressive Failure; Amer. Soc. Civil. Eng. Journal of Soil Mechanics and Foundation Div., Vol. 93, SM5.

Brooker, E.W., Aug. (1967): Strain Energy and Behavior of Overconsolidated Soils; Canadian Geotechnical Journal, Vol. IV. No.3.

Brooker, E.W., and H.O. Ireland, (1964): Earth Pressures related to Stress History; Can. Geotech. Jour. Vol. 2, No. 1.

Broscoe, A.J., and S. Thomson, (1968): The Devon Landslide, Edmonton, Alberta; University of Alberta, Edmonton, Unpubl. Report.

Bruce, R.L., (1966): Landslides in the Pierre Shale of South Dakota; Proc., 17 th Annual Highway Geology Symposium.

Carrigy, M.A., and G.B. Mellon, (1964): Authigenic Clay Minerai Cements, Alberta; Jour. Sed. Petrology, Vol. 34, No. 3, pages 461-472.

Casagrande, A., (1948): Classification and Identification of Soils; Trans. Amer. Soc. Civil Eng. Vol. 113, page 901.

Collin, A., (1846): Landslides in Clays; translated by W.R. Schiever, University of Toronto Press, 1956, 160 pages.

Department of Civil Engineering, (1968): Report on River bank Stability; University of Alberta, Edmonton, Unpublished.

Elliott, R.H.J., (1958): Subsurface Correlation of the Edmonton Formation; Edmonton Geol. Scc. Quart., Vol. 2, No. 2, pages 1-8.

Elson, J.A., (1960): The Geology of Tills; Fourteenth Canadian Soil Mechanics Conference, Proc. Techn. Mem. No. 69, pages 5-35.

Freeze, R.A., and P.A. Witherspoon, (1967): Theoretical Analysis of Regional Groundwater flow. II: Effect of Water-Table Configuration and Subsurface Permeability Variation; Water Resources Research, Vol. 3.

Grim, R.E., (1949): Mineralogical Composition in Relation to the Properties of Certain Soils; Geotechnique, Vol. 1, No. 3. Pages 139-147.

Hardy, R.M., (Sept. 1957): Engineering Problems Involving Preconsolidated Clay Shales; Trans. Eng. Inst. Can.

_____., (1963): The Peace River Highway Bridge-A Failure in Soft Shales; Highway Research Record, No. 17.

_____.'' E.W. Brooker, and W.E. Curtis, (1962): Landslides in Over-Consolidated Clays; Engineering Journal, Montreal, Vol. 45, pages 81-89.

Hemwell, J.B. and P.F. Low, (1956): Hydrostatic Repulsive Force in Clay Swelling; Soil Science Soc. Amer., Vol. 82, pages 135-145.

Henkel, D.J., and A.W. Skempton, (1955): A landslide at Jackfield, Shropshire, in a Heavily Over-Consolidated Clay; Geotechnique, Vol. 5, pages 131-137.

Kenny, T.C., (1963): Permeability ratio of repeatedly layered soils; Geotechnique, Vol. 13(4), pages 325-333.

Ladd, C.C., (1959): Mechanism of Swelling by Compacted Clay. Highway Research Board Bull. 245, Pages 10-26.

Locker, J.G., (1969): The Petrographic and Engineering Properties of Fine-Grained Sedimentary Rocks of Central Alberta; Unpublished Ph.D. Thesis, Univ. of Alberta.

Mitchell, R.H., (1941): An Unusual Landslide; Jour. of Geol., Vol. 49, pages 382-391.

Mocum, J. and I.I. Rosenquist, (1961): The Mechanical Properties of Montmorillonite and Illite Clays related to Electrolytes of the Pore Water; Proc. 5th Intern. Conf. Soil Mech. and Found. Eng. Vol. 1, pages 263-367.

Ower, J.R., (1958): The Edmonton Formation; Edmonton Geol. Soc. Quart., Vol. 2, No. 1, pages 3-11.

Painter, W.P., (1965): An investigation of the Lesueur Landslide; Unpublished M.Sc. Thesis, University of Alberta.

Peck, R.B., (July 1967): Stability of Natural Slopes; Amer. Soc. Civil Eng. Jour. of Soil Mech. and Found. Div., Vol. 96, SM4.

Pennell, D.G., (1969): Residual Strength Analysis of Five Landslides; Unpublished Ph.D. Thesis, Univ. of Alberta.

Peterson, R., J.L. Jasper, P.J. Rivard, and N.L. Iverson, (1960): Limitations of Laboratory Shear Strength in Evaluating Stability of Highly Plastic Clays; ASCE Research Conf. on the Shear Strength of Clays, Denver, Colo. pages 765-791.

Scott, J.S., (1965): Landslide Investigations, Saskatchewan and Alberta; In Jenness, S.E. (Comp.), Geol. Surv. Can., Paper 65-1, pages 85-87.

Scott, J.S. and E.W. Brooker, (1968): Geological and Engineering Aspects of Upper Cretaceous Shales in Western Canada; Geol. Surv. of Canada, Paper 66-37, 75 pages.

Seed, H.B., J.K. Mitchell, and C.K. Chan, (1962): Studies of Swell and Swell pressure Characteristics of Compacted Clays; Highway Research Board Bull. 313, pages 12-39.

Sharpe, C.F.S., (1938): Landslides and Related Phenomena; Columbia University Press, New York, N.Y., pages 83-87.

Sharpe, C.F.S., (1960): Landslides and related Phenomena; Pageant Books, Inc. N.J., 137 pages.

Sinclair, S., E.W. Brooker, (1967): The Shear Strength of Edmonton Shale; Proc. of the Geotechnical Conference, Oslo, Vol. 1, pages 295-299.

Skempton, A.W., (1948): The Rate of Softening in Stiff, Fissured Clays, with special Reference to London Clay; Proc. of 2nd Intern. Conf. on Soil Mech. and Found. Eng. Rotterdam, Vol. 2, pages 50-53.

_____., (1961): Horizontal Stresses in an Overconsolidated Eocene Clay; Proc. 5th Intern. Conf. on Soil Mech. and Found. Eng. Vol. 1, page 351.

Terzaghi, K., (1925): Erdbaumechanik; Leipzig, physics, and Vienna, Franz Denticke, pages 353-357 and 382-384.

_____., (1929): The Mechanics of Shear Failures on Clay Slopes and the Creep of Retaining Walls; Public Road, Vol. 10, No. 10, pages 177-192.

_____., (1950): Mechanism of Landslides; In Application of Geology to Engineering Practice; Berkey Volume, Geol Soc. of America, pages 83-123.

_____., and R.B. Peack, (1967): Soil Mechanics in Engineering Practice; John Wiley and Sons, Inc., N.Y. pages 232-255.

Thomson, S., (1963): Effects of Salt Content and Adsorbed Cations on the Shear Strength of a Remolded Highly Plastic Clay Soil; Unpubl. Ph.D. Thesis, University of Alberta.

_____., (1971): The Lesueur Landslide, a Failure in Upper Cretaceous Clay Shale; Ninth Annual Symposium on Engineering Geology and Soils Engineering, Boise, Idaho, April 1971, pages 1-25.

Varnes, D.J., (1958): Landslide Types and Processes; In Landslides and Engineering Practice; Highway Res. Board Spec. Report 29, pages 23-26 and 42-45.

Ward, W.H., (1945): The Stability of Natural Slopes; Geog. Jour. London, Vol. 105, No. 5-6, pages 17-197.

Warkentin, B.P., G.H. Bolt, and R.D. Miller, (1957): Swelling Pressure of Montmorillonite. Soil Science Soc. Amer., Proc., Vol. 21, pages 495-497.

Weeks, E.P., (1964): Field Methods for determining vertical permeability and aquifer anisotropy. U.S.G.S. Prof. Paper 501D, pages 193-199.

Westgate, J.A., (1969): Notes on the Quaternary Geology of the Edmonton Area, Alberta. Field Guide Book, Symposium on Pedology and Quaternary Research, Edmonton, May, 1969. pages 31-55.

Williams, G.D, and C.F. Burke, Jr., (1964): Upper Cretaceous; In Geological History of Western Canada, McCrossan, R.G., and R.P. Glaister (editors). Alberta Soc. Petrol. Geol., Pages 168-189.

Young, R.N., and B.P. Warkentin, (1965): Studies of the Mechanism of Failure Under Expansive Soils; Int. Res. and Eng. Conf. on Expansive Soils, August 1965, Vol. II, Texas A and M. Univ.

Yong, R.N., and B.P. Warkentin, (1966): Introduction to Soil Behavior; MacMillan Co., N.Y., pages 151-390

Young, A., P.F. Low, and A.S. McLatchie, (1964): Permeability Studies of Argillaceous rocks; Jour. Geophys. Res., Vol. 69, pages 4237-4247.

APPENDIX A

PHOTOGRAPHS OF TRENCH A AND B

Figure 34. Trench A. Exhumed sequence of most of bedrock underlying slide.

Figure 34. Trench A. Exhumed sequence of most of bedrock underlying slide.

Figure 34. Trench A. Exhumed sequence of most of bedrock underlying slide.

Figure 35. Trench B. Exhumed shale - sandstone contact under slip surface.

APPENDIX B

PHOTOGRAPHS OF AXIALLY CUT SHELBY TUBE SAMPLES

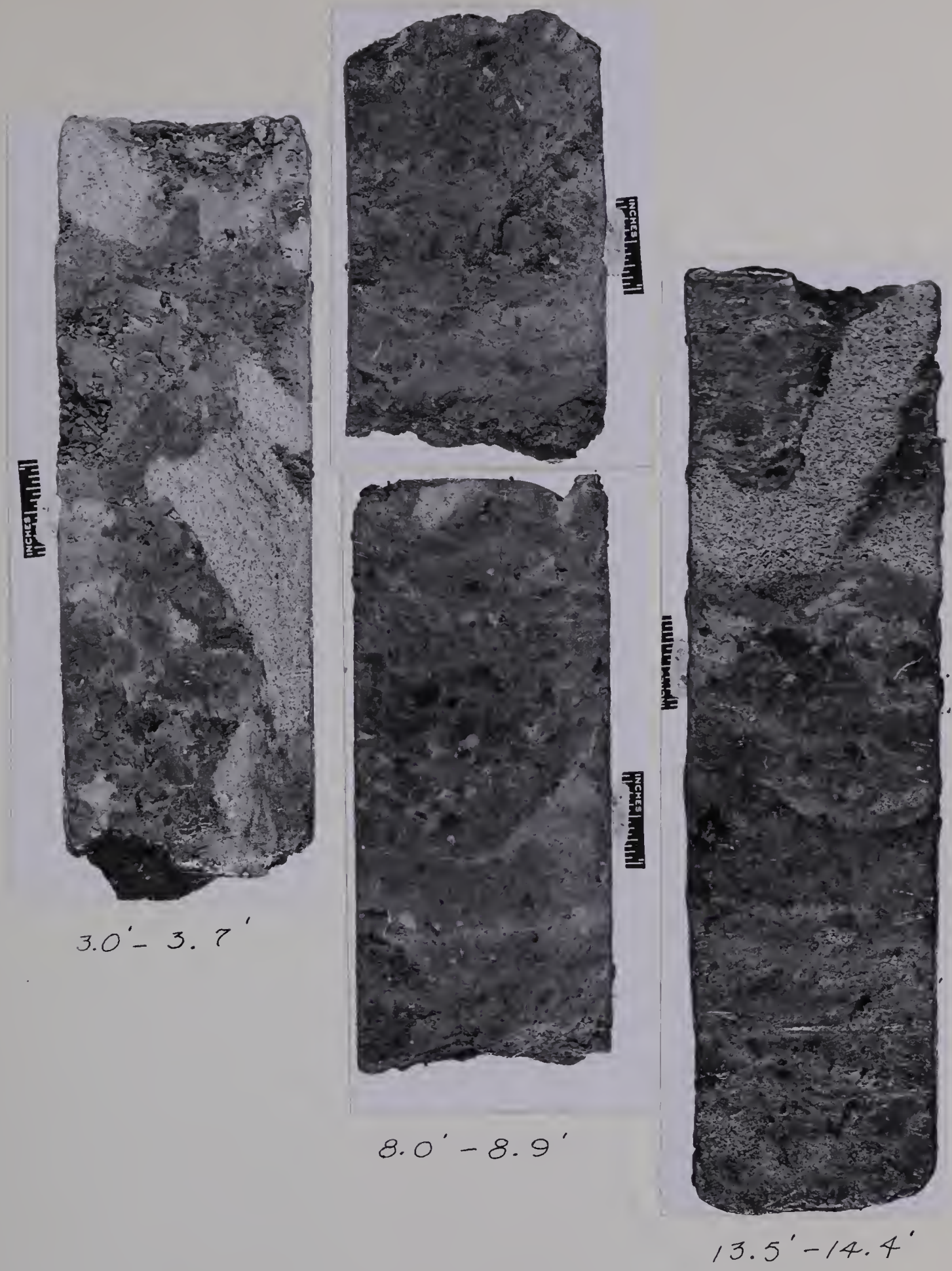

Figure 36.01. Auger hole C-1; axially cut shelby tube samples.

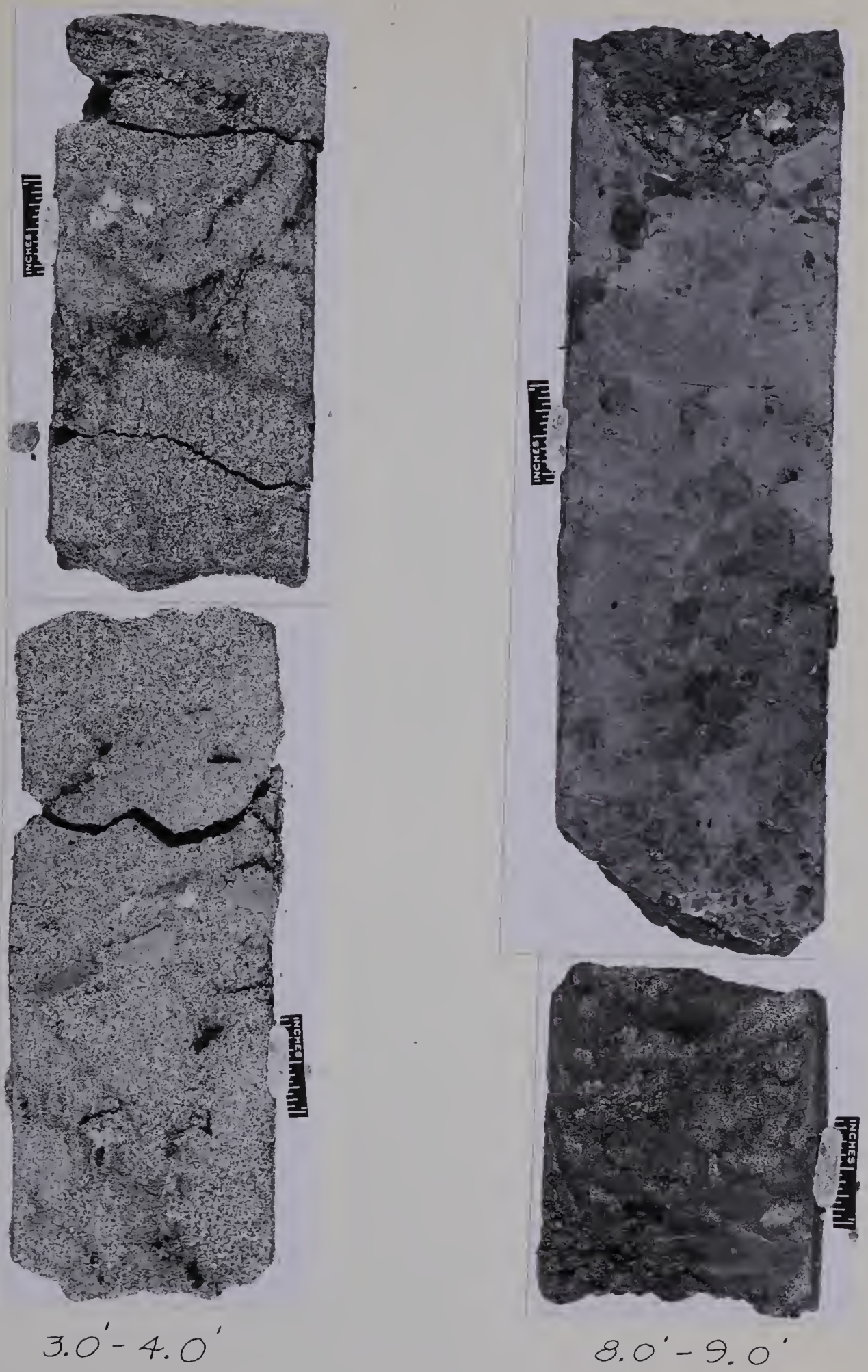

Figure 36.02. Auger hole C-2; axially cut shelby tube samples.

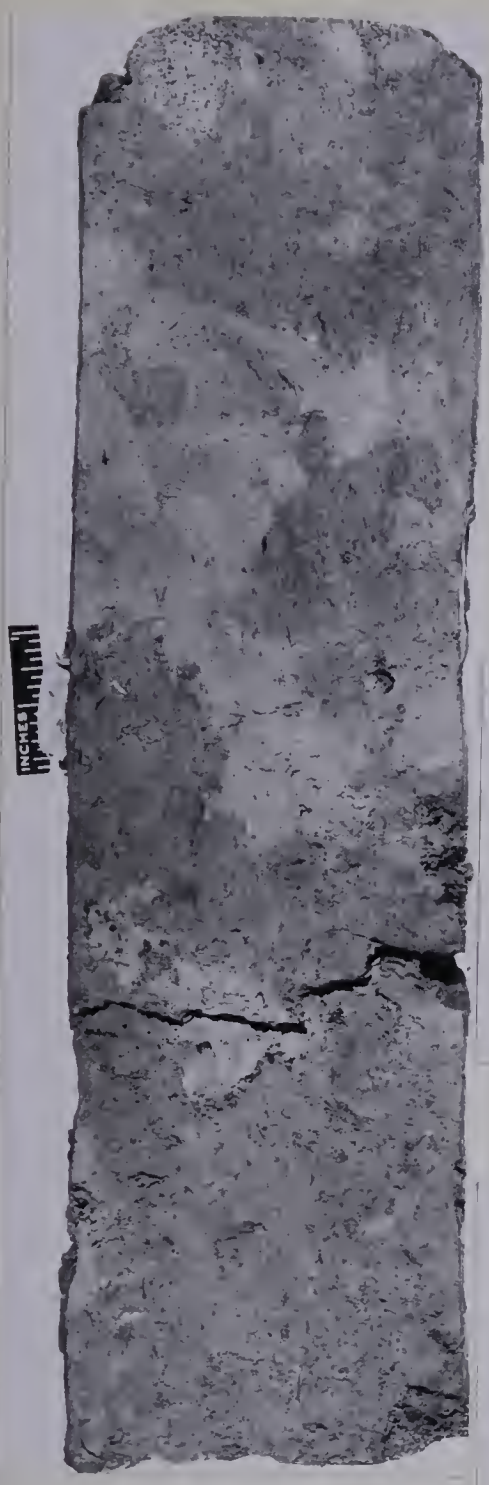

3.0' - 3.8'

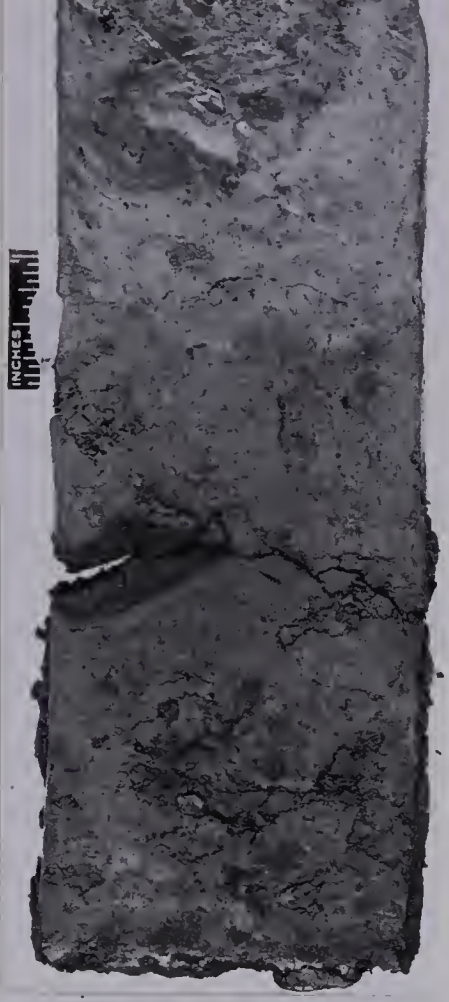

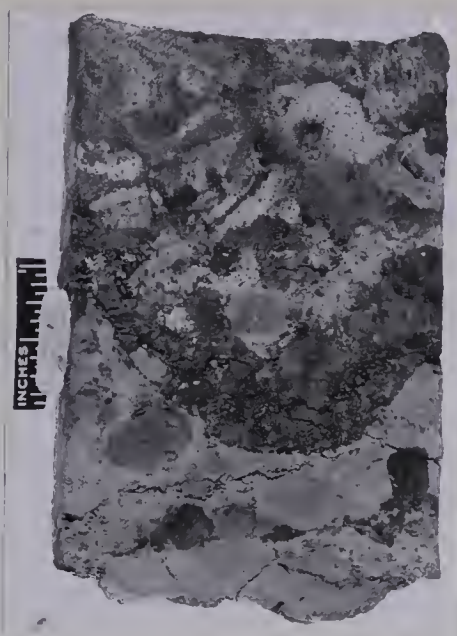

18.1' - 18.5'

28.0' - 28.5'

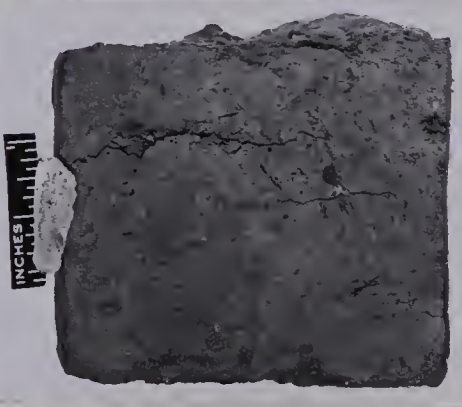

8.0' - 8.8'

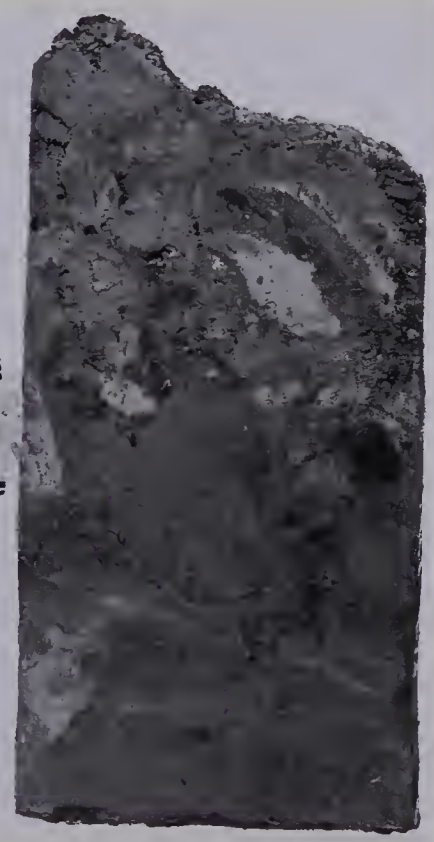

13.1' - 13.7'

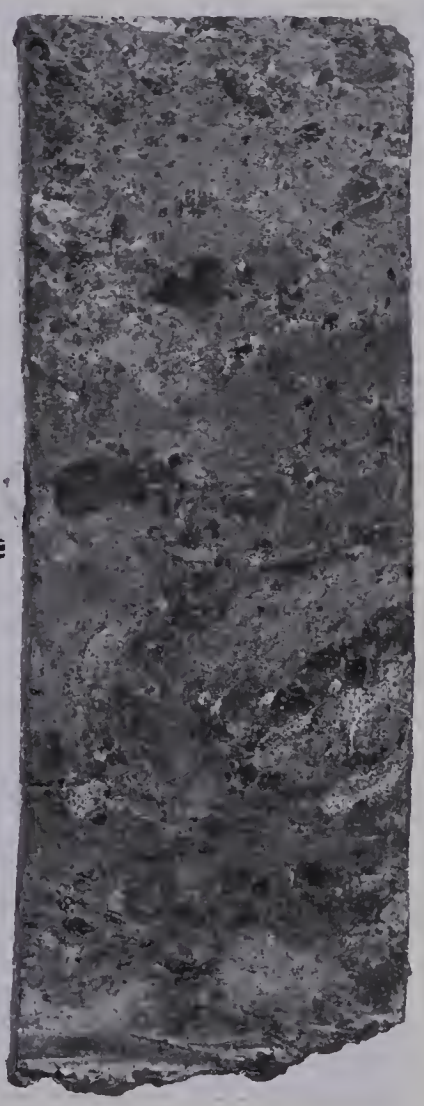

23.0' - 23.6'

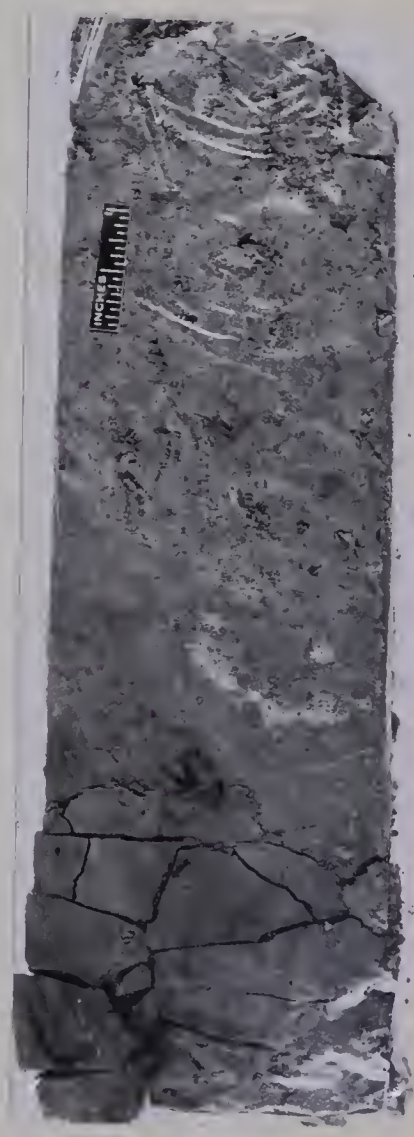

33.0' - 33.8'

Figure 36.03. Auger hole C-3; axially cut shelby tube samples.

Figure 36.04. Auger hole C-4; axially cut shelby tube samples.

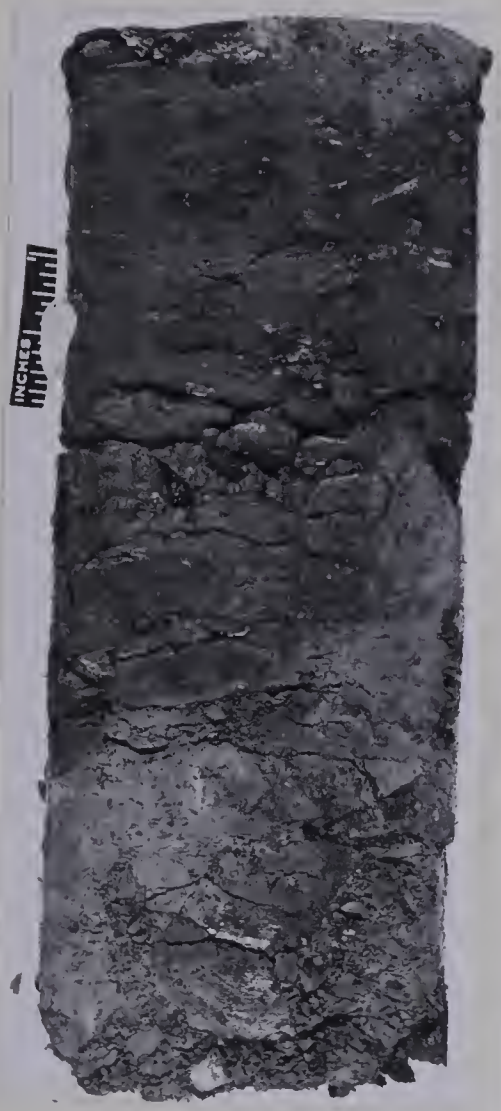

3.0' - 3.6'

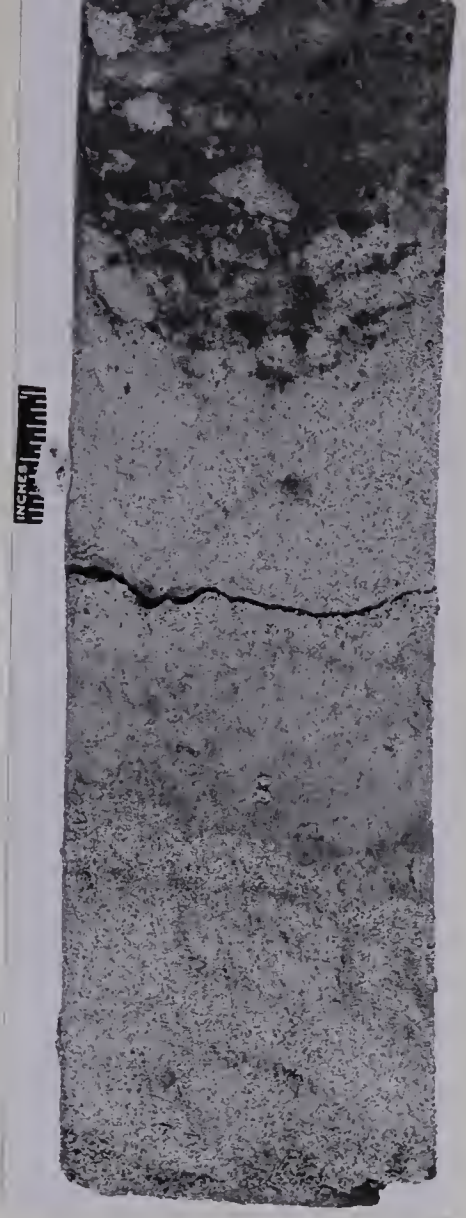

8.0' - 8.8'

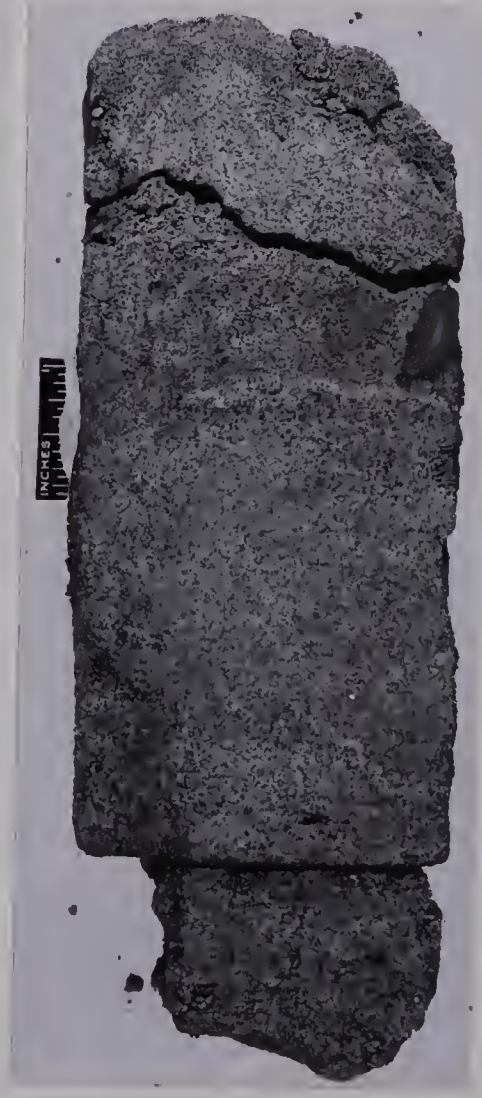

12.2' - 12.8'

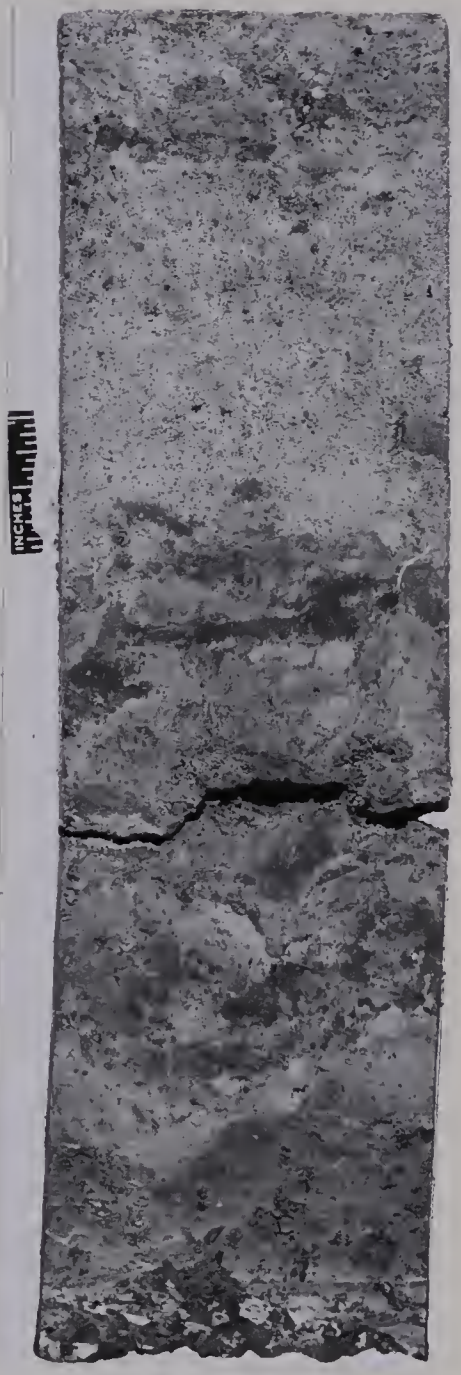

17.0' - 17.8

Figure 36.05. Auger hole C-5; axially cut shelby tube samples.

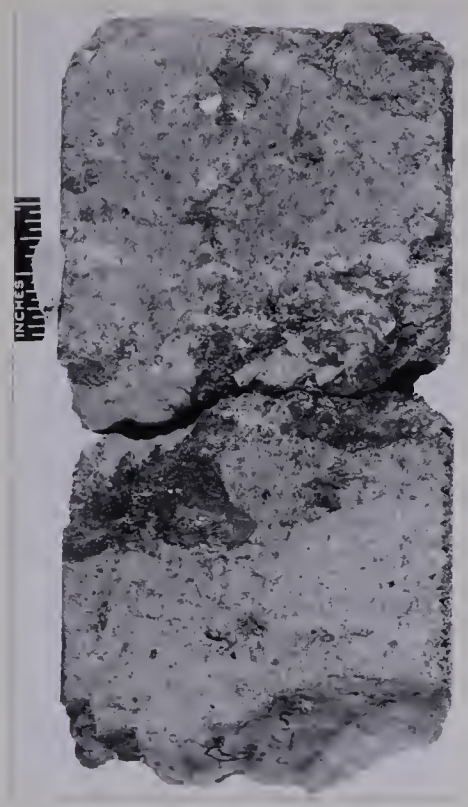

4.0' - 4.4'

22.0' - 22.6'

17.0' - 17.8'

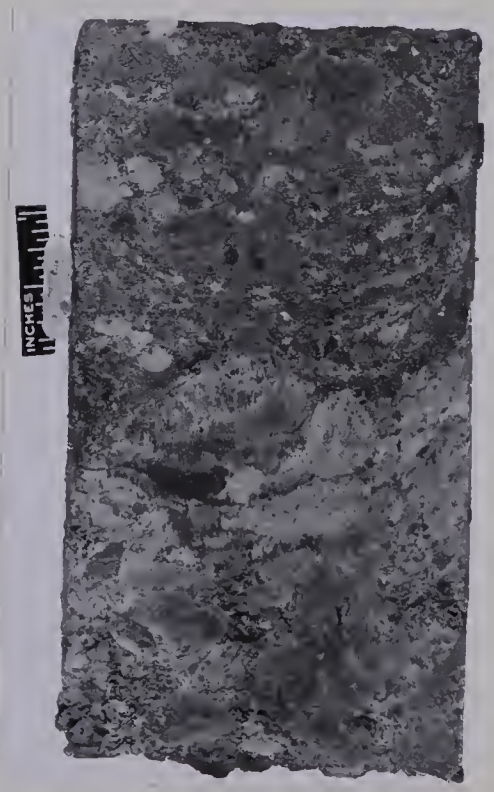

26.0' - 26.5'

Figure 36.06. Auger hole C-6; axially cut shelby tube samples.

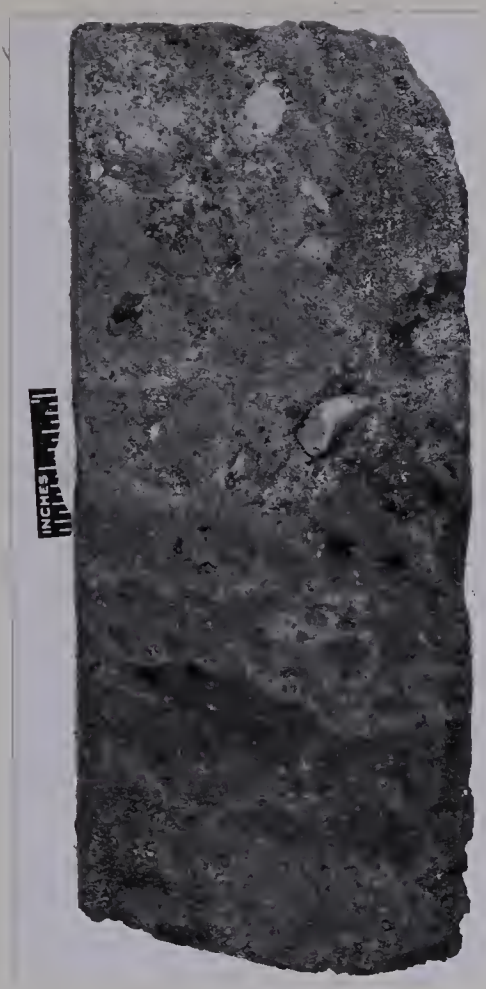

C-7 8.0' - 8.5'

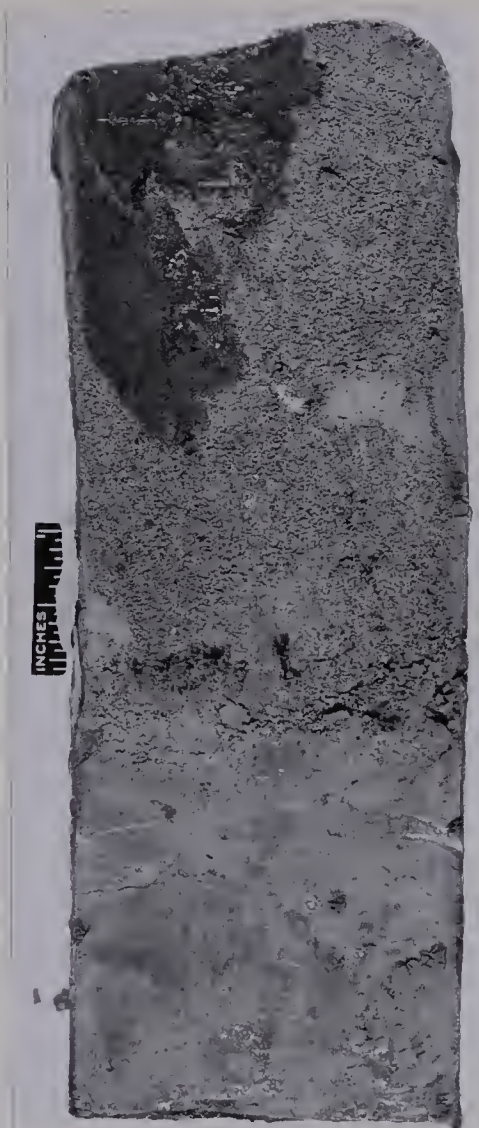

D1 13.0' - 13.6'

D1 18.0' - 18.6'

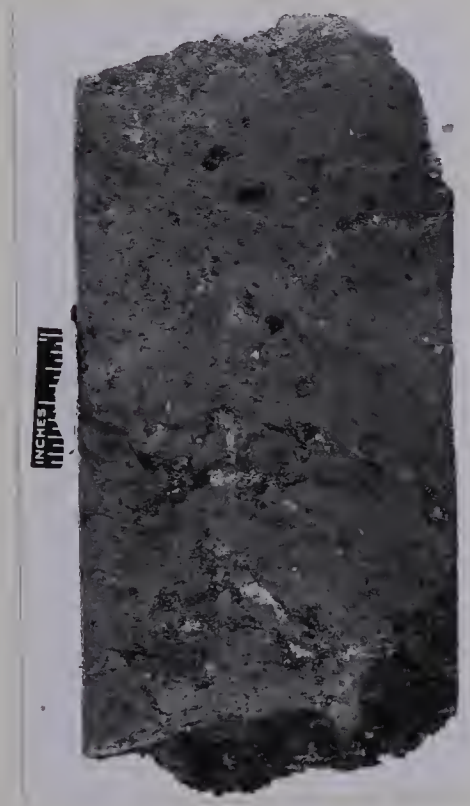

D1 8.1' - 8.6'

Figure 36.07. Auger holes C-7 and D-1; axially cut shelby tube samples.

APPENDIX C

PHOTOMICROGRAPHS OF THINSECTIONS OF BEDROCK

Figure 37.01. Sample A108.1, 40X. Shale, fine grained poorly sorted poorly structured siliceous calcareous bitumenous.

Figure 37.02. Sample A115.0, 100X. Shale, very fine textured massive.

Figure 37.03. Sample A119.3, 40X. Shale, fine textured poorly sorted poorly bedded calcareous.

Figure 37.04. Sample A125.1, 100X. Clay-ironstone concretion, fine textured calcareous unstructured.

Figure 37.05. Sample A132.9, 40X. Shale, very fine textured finely laminated bentonitic siliceous very fine coally partings.

Figure 37.06. Sample A138.2, 100X. Shale, very fine textured bedded concretionary calcareous some coally fragments.

Figure 37.07. Sample A146.8, 40X. Shale, fine textured poorly sorted disturbed laminated bitumenous ferrugenous.

Figure 37.08. Sample A152.1, 100X. Shale, medium-fine textured bedded siliceous coally fragments.

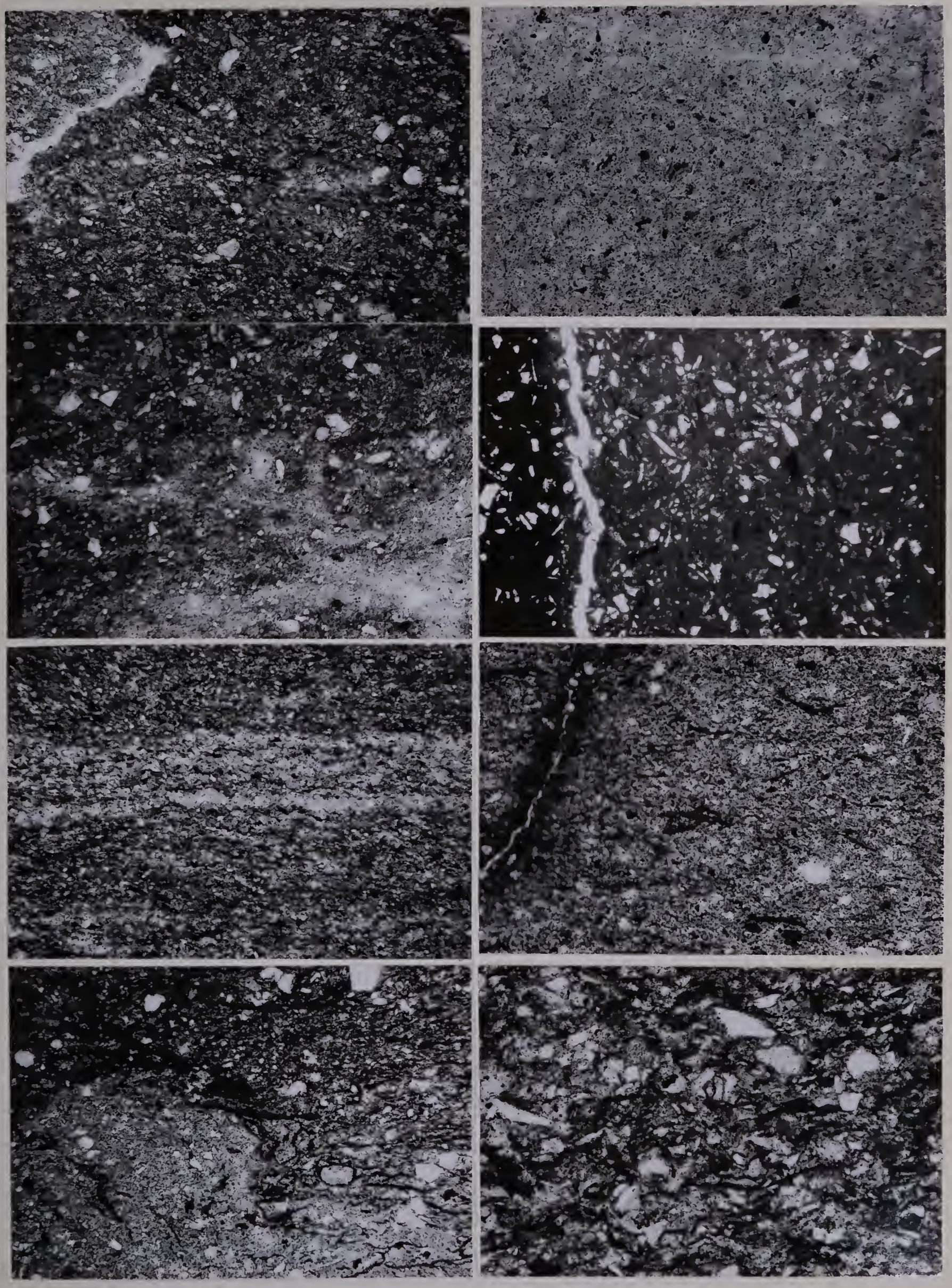

Figures 37.01 to 37.08. Photomicrographs of thinsections of bedrock.

Figure 37.09. Sample A158.0, 40X. Shale, medium-fine textured poorly structured large and small coal fragments siliceous feldspathic poorly sorted.

Figure 37.10. Sample A165.6, 40X. Shale, medium-fine textured poorly sorted laminated bentonitic very fine coal particles.

Figure 37.11. Sample A168.0, 128X. Shale, very fine textured laminated bentonitic common coal particles.

Figure 37.12. Sample A172.3, 40X. Shale, very fine grained laminated bentonitic common coal fragments.

Figure 37.13. Sample A172.3, 40X. Shale, very fine grained laminated common coal partings bentonitic.

Figure 37.14. Sample A172.3, 40X. Shale, very fine textured massive bentonitic siliceous feldspathic minor coal fragments.

Figure 37.15. Sample A173.7, 40X. Shale, very fine grained laminated bentonitic minor coal particles.

Figure 37.16. Sample B190.0, 40X. Shale, medium to very fine textured tuffaceous slightly calcareous.

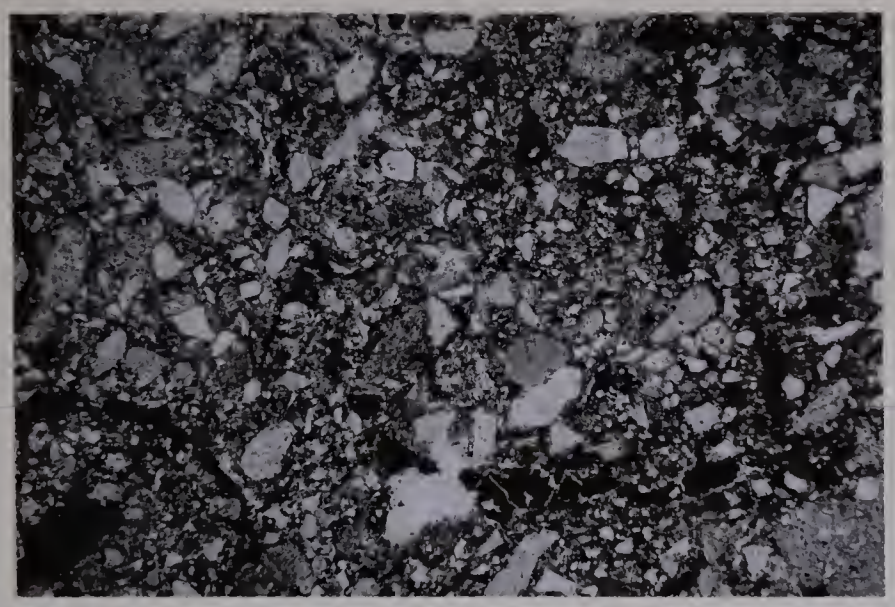

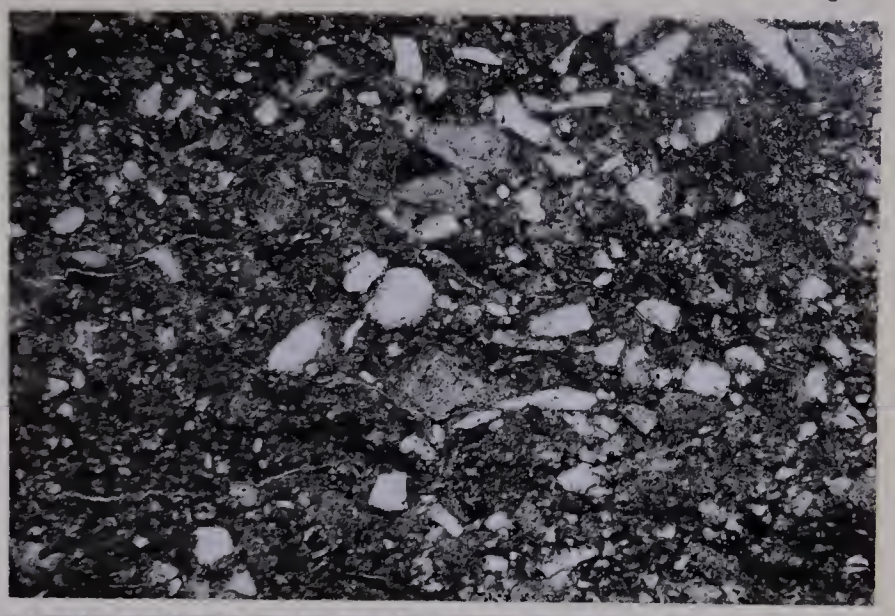

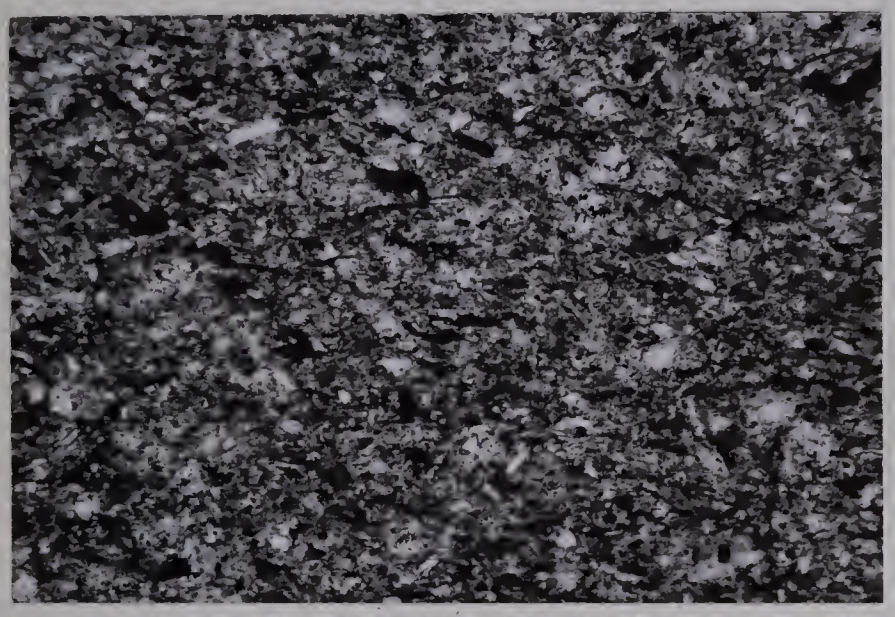

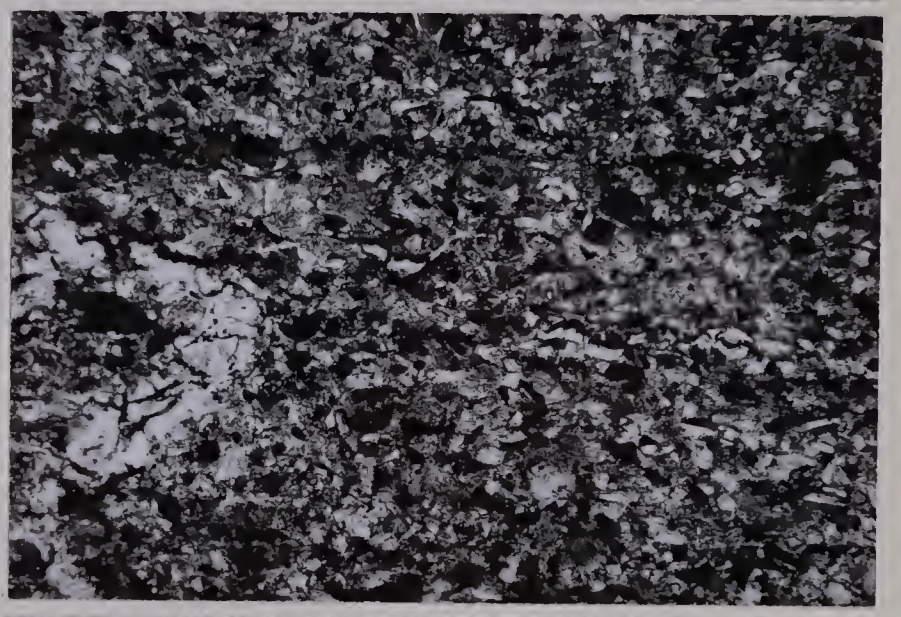

Figures 37.09 to 37.16. Photomicrographs of thinsections of bedrock.

Figure 37.17. Sample A174.2, 40X. Figure 37.18. Sample A174.2, 40XNic. Sandstone, medium textured poorly structured siliceous feldspathic trace heavy minerals clay cemented closed framework.

Figure 37.19. Sample A176.2, 40X. Figure 37.20. Sample A176.2, 40XNic. Sandstone, medium textured well sorted poorly structured feldspathic siliceous minor heavy minerals and coal not quite closed framework clay matrix slightly dolopitic.

Figure 37.21. Sample A179.2, 40X. Figure 37.22. Sample A179.2, 40XNic. Sandstone, medium textured well sorted unstructured siliceous feldspathic trace heavy minerals slightly weathered closed framework clay matrix.

Figure 37.23. Sample B182.3, 40X. Sandstone, medium textured massive minor coal particles clay matrix closed framework siightly weathered.

Figure 37.24. Sample S43, 40X. Shale, medium-very fine grained disturbed laminated fractured coal partings bentonitic.

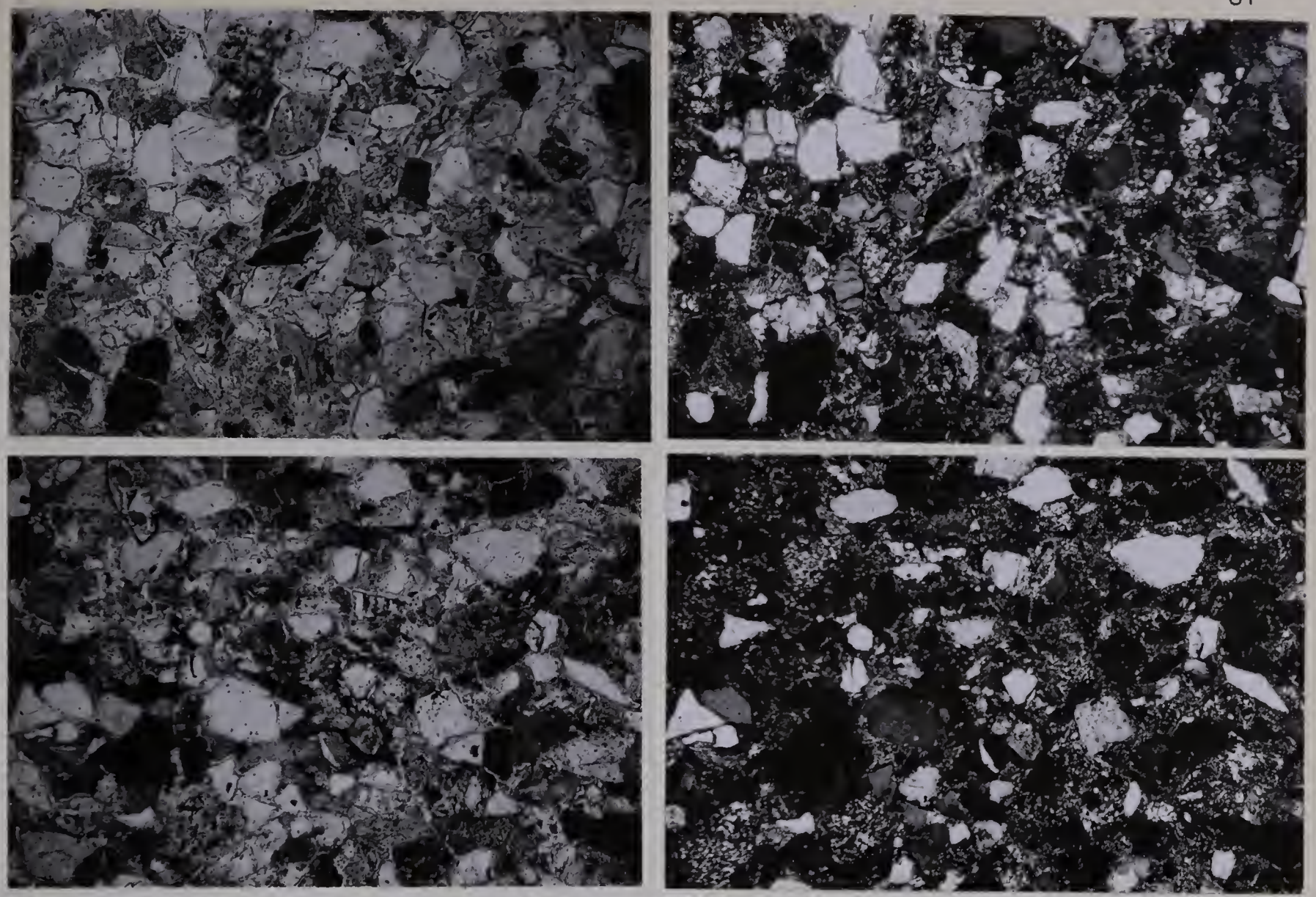

Figures 37.17 to 37.24. Photomicrographs of thinsections of bedrock.

APPENDIX D

CARTOGRAPHIC PRESENTATION OF VARIOUS ASPECTS OF THE SLIDE AREA

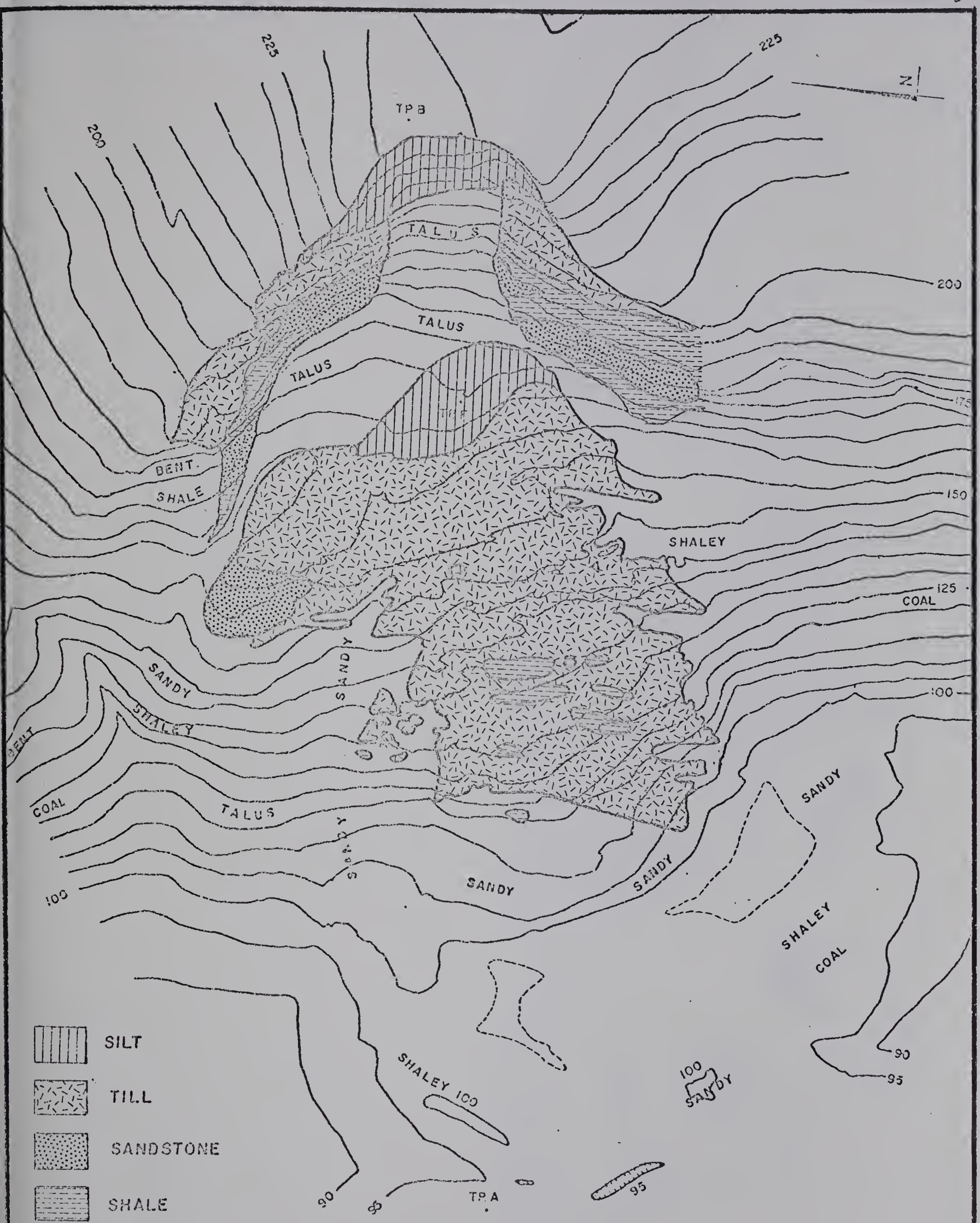

PRINCIPAL SURFICIAL MATERIALS

FIGURE: 39

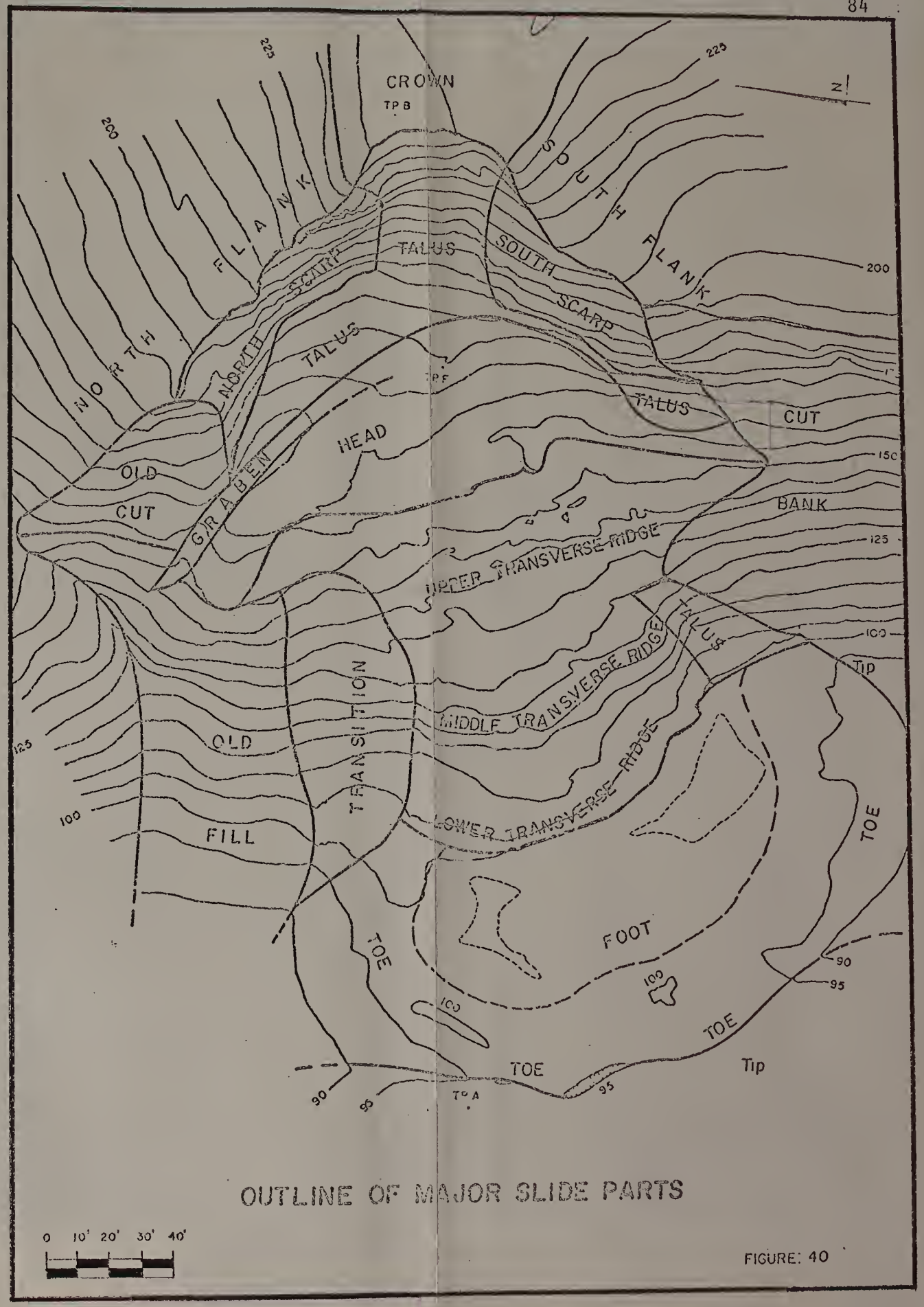

OUTLINE OF MAJOR SLIDE PARTS

0 10' 20' 30' 40'

FIGURE: 40

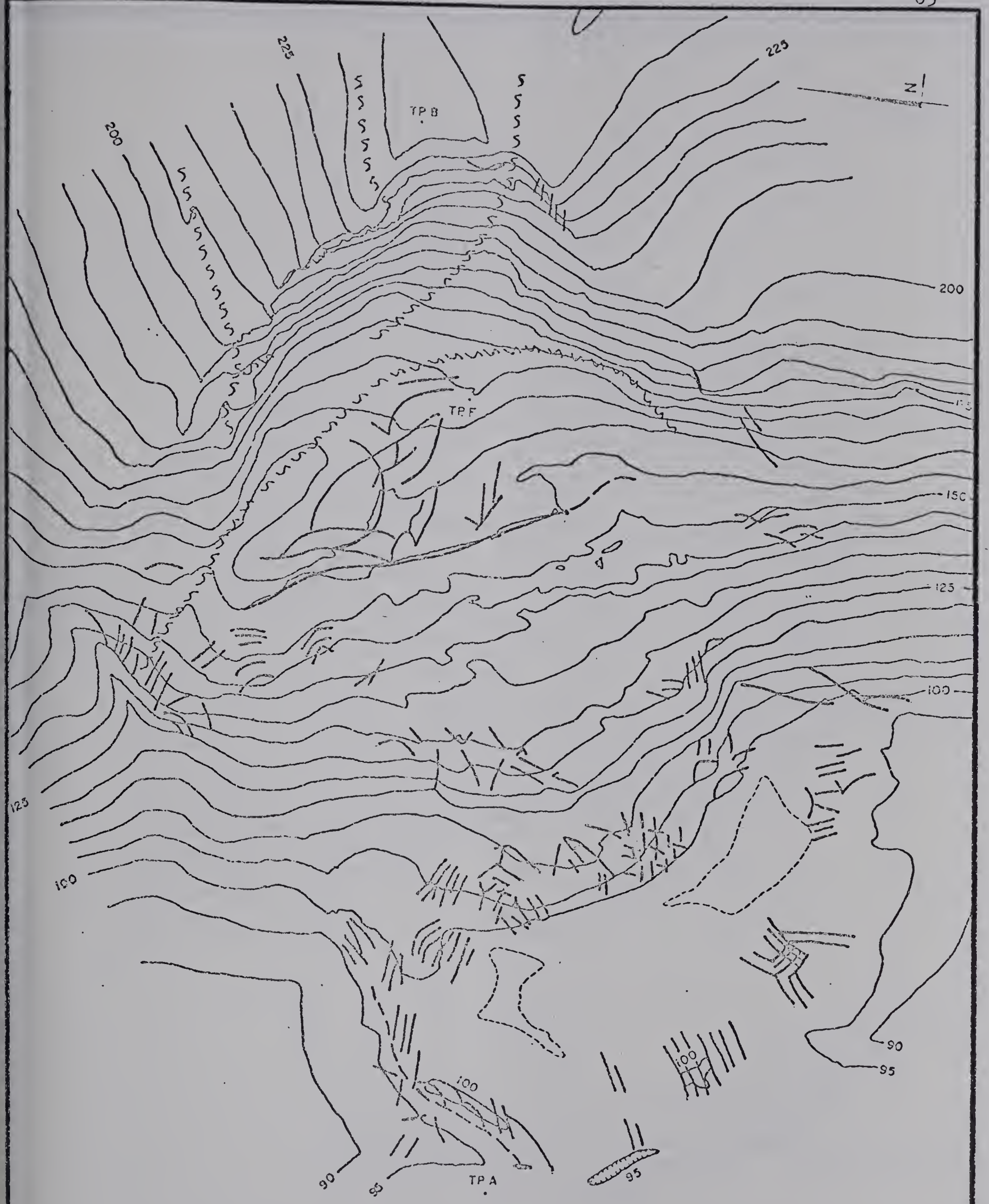

MAJOR ZONES OF FRACTURES

0 10' 20' 30' 40'

FIGURE: 41

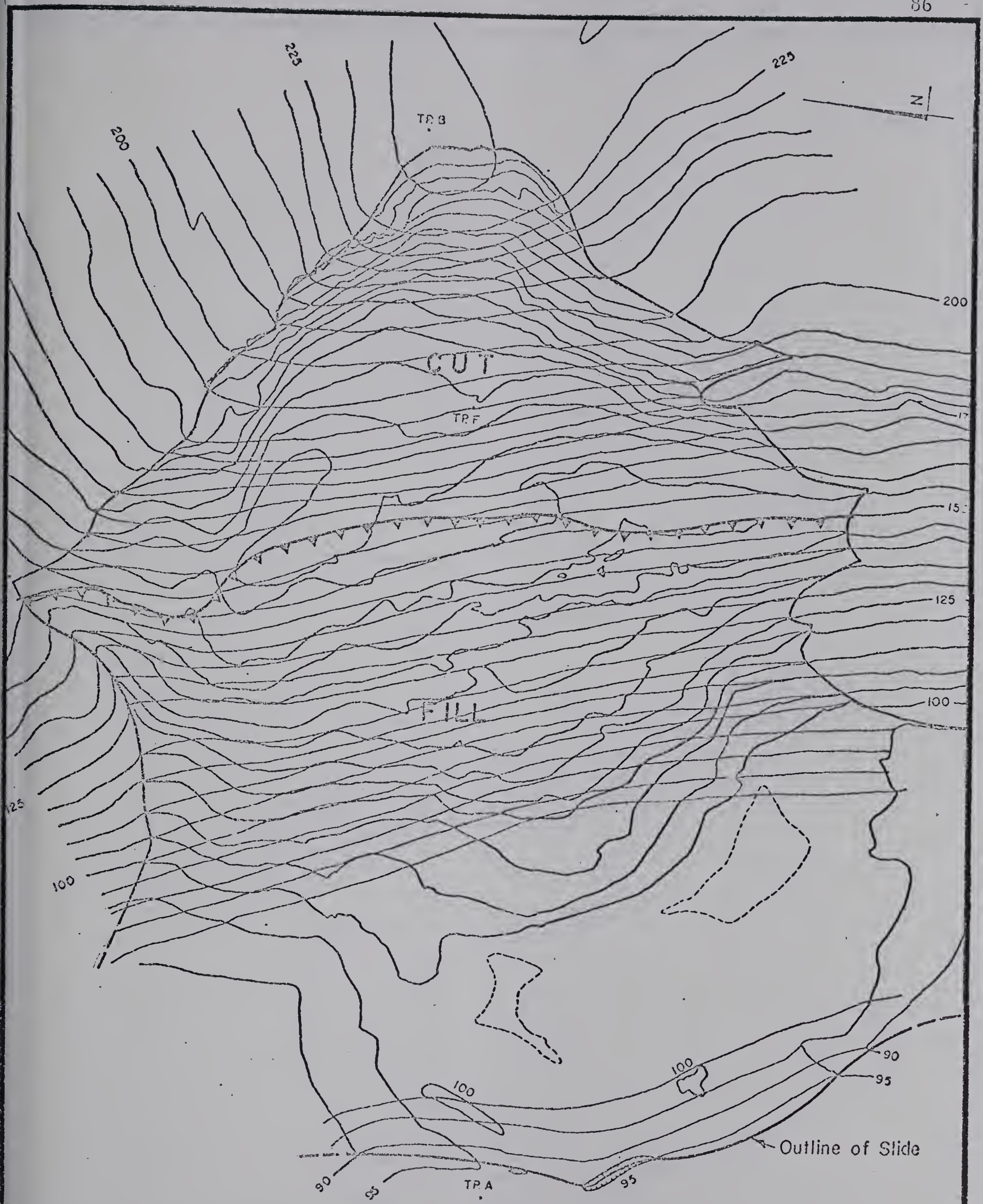

ESTIMATED SURFACE CONTOURS BEFORE SLIDE

0 10' 20' 30' 40

FIGURE: 42

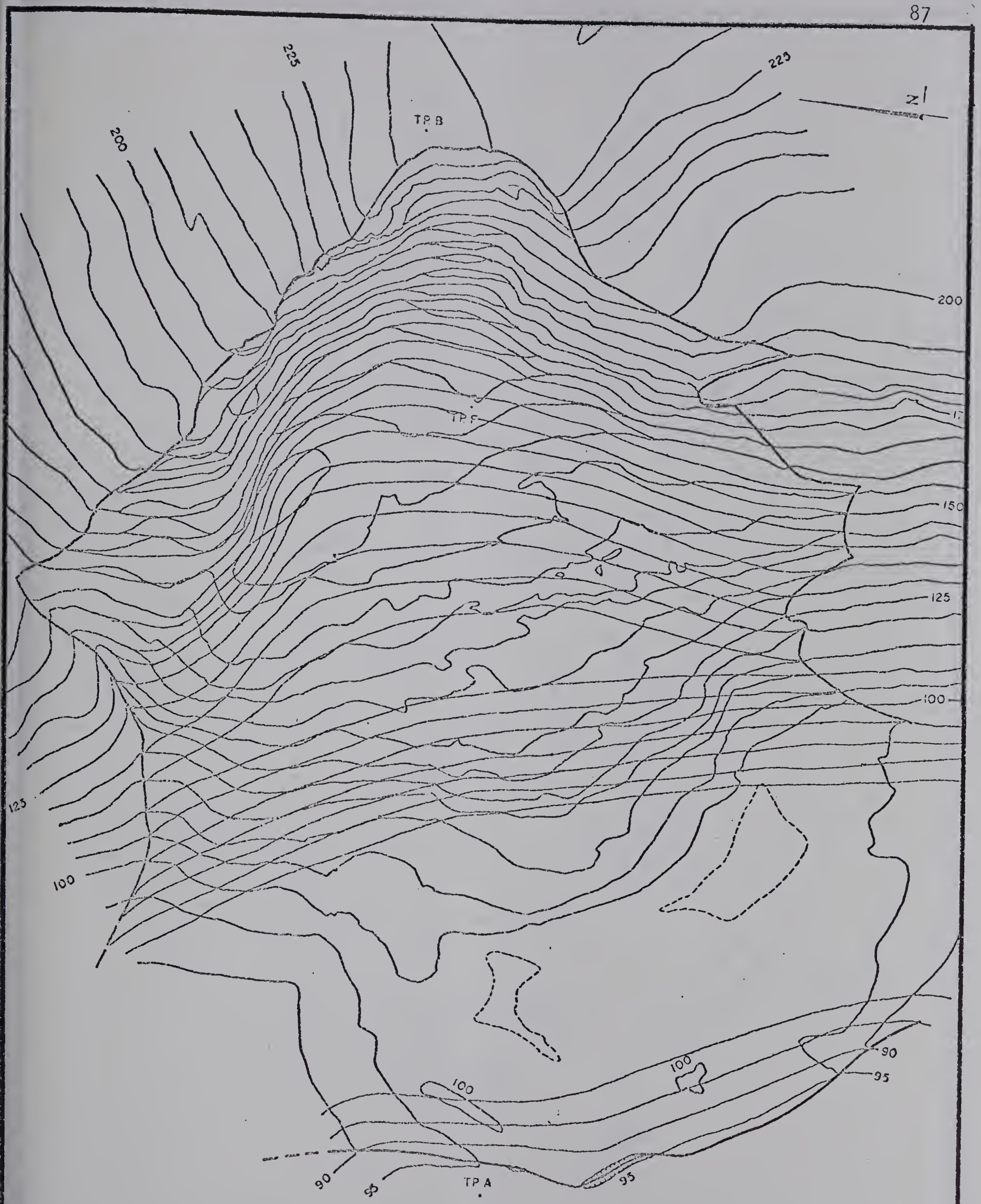

ESTIMATED SHEAR SURFACE CONTOURS

0 10' 20' 30' 40'

FIGURE: 43

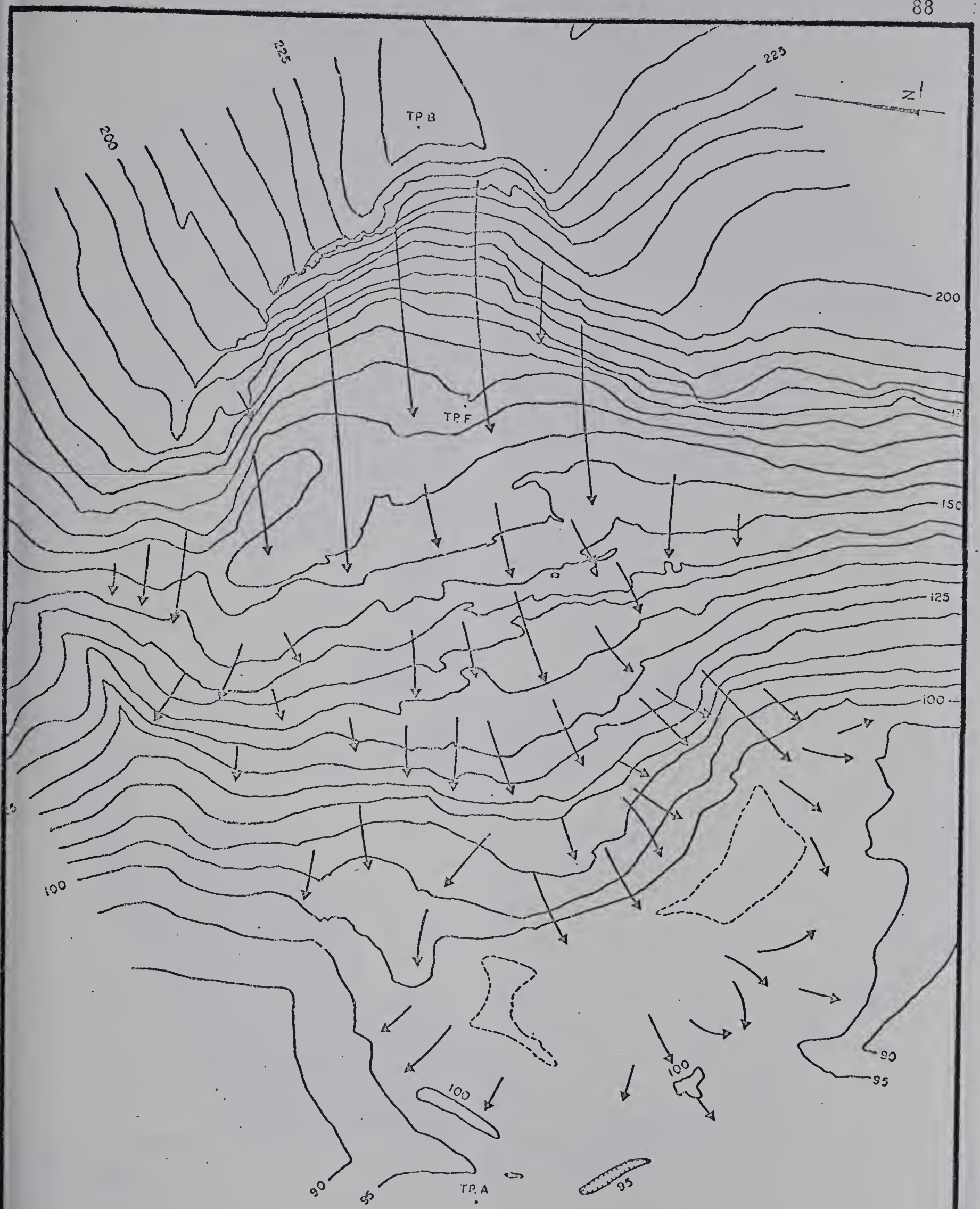

ESTIMATED MOVEMENT OF SLIDE MATERIAL

0' 10' 20' 30' 40'

FIGURE : 44

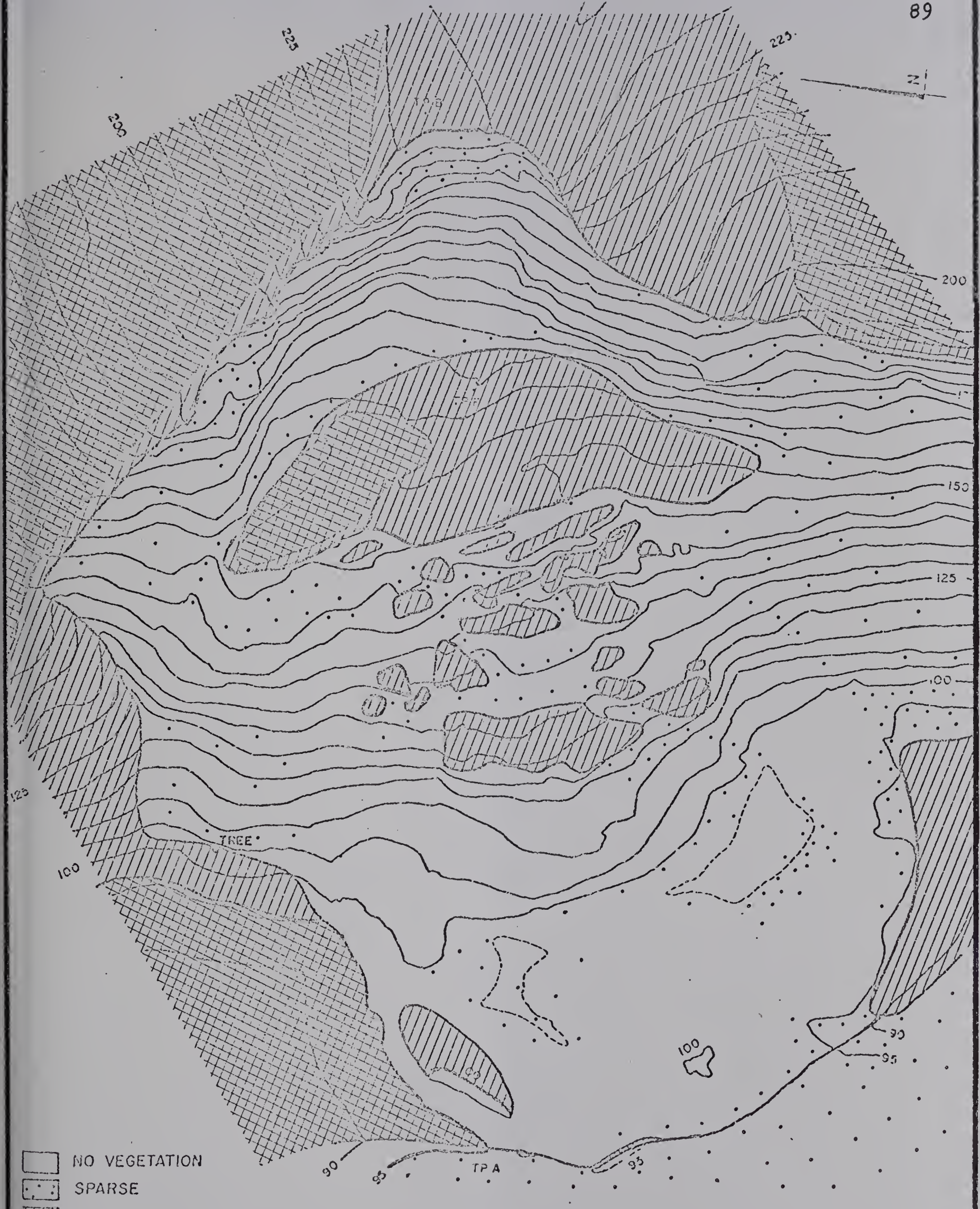

VEGETATION DENSITY

FIGURE : 45

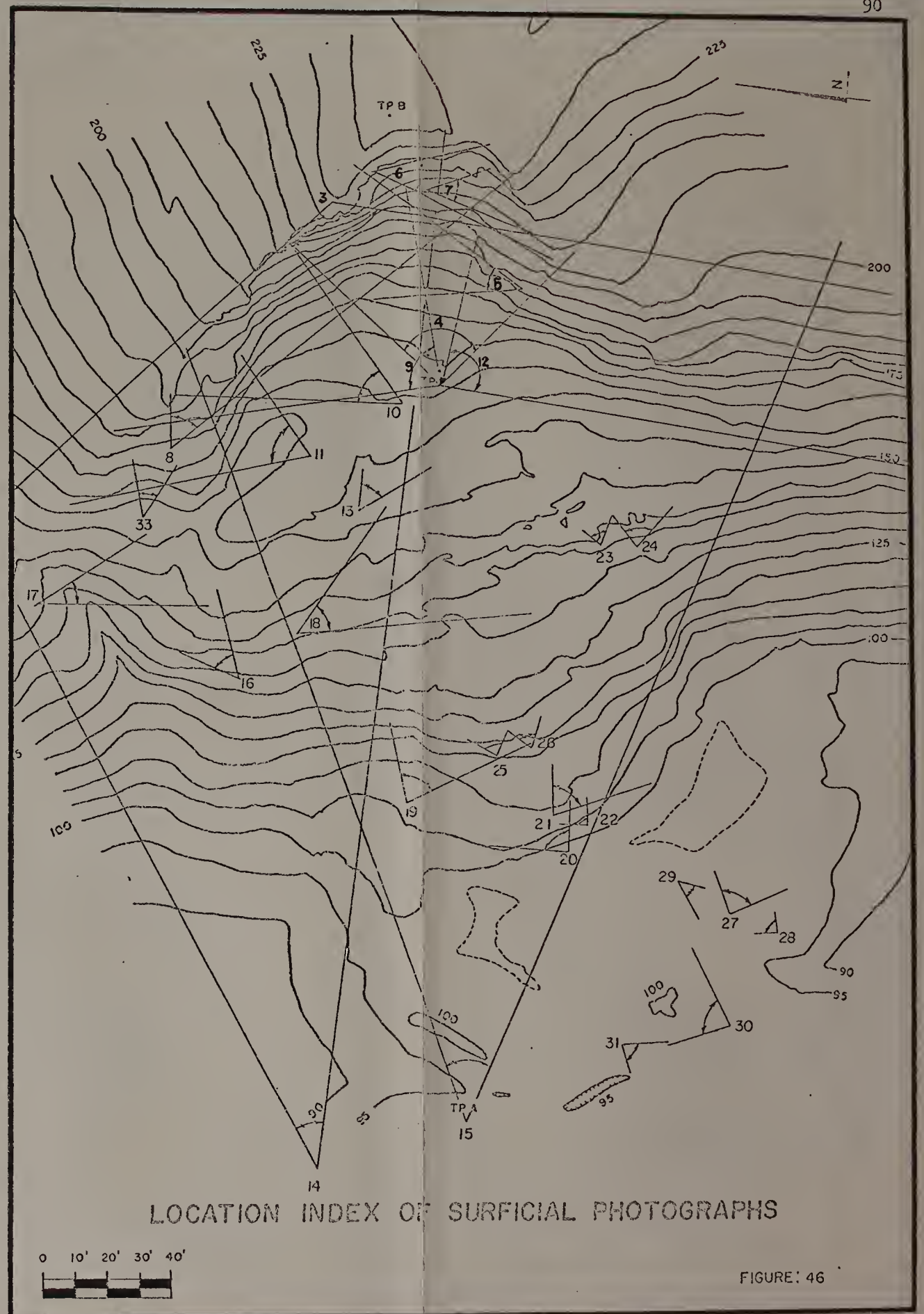

LOCATION INDEX OF SURFICIAL PHOTOGRAPHS

FIGURE: 46

APPENDIX E

PLASTICITY AND ACTIVITY CHARTS

OFF SCALE BENTONITES:
A130.3 – WI = 400; Ip = 344
A166.0 – WI = 372; Ip = 310

A-LINE

inorganic clays of high plasticity

inorganic clays of medium plasticity

inorganic silts of high compressibility and organic silts

inorganic silts of medium compressibility

LEGEND
x Clays
+ Till
• Shales

PLASTICITY CHART

FIGURE 47

INDEX OF PLASTICITY

Ip (%)

WI (%)

A

0 1.0 2.0 3.0 4.0 5.0 6.0

100 90 80 70 60 50 40 30 20 10 0

% Clay

A130.3
A166.0
A130.1
A131.1
A133.2
S92
A132.9
8187.4
A166.4
A138.2
8164.8
A147.0
A173.7
S53
S12
S53
S12
01-13.5
S83
8191.8
8190.0
S72
C2-13.7
S82
C2-8.3
S81
S74
S73
S71
x S3
C2-18.6
A136.0
A137.0
A129.5
A110.0
S51
A143.3
8193.5
A102.0
A108.1
A112.5
8196.2
A115.0
C4-18.7
S59
8170.0
A104.2
S19
A168.8
S68
A140.8
C2-9.3
S13
x C7-3.7
C5-28.8
A153.5
C3-32.7
S54
C3-13.6
01-18.6
S55
8197.0
C5-3.7
A165.6
A144.4
C7-18.7
01-23.5
S30
S29
S48
A106.4
C5-22.5
S44
C3-18.5
A138.8
S49
A118.8
A115.6
8186.0
S28
S41
A150.0
S66
A161.0
S59
C5-17.8
S40
C4-3.3
S50
S32
A152.1
S38
S65
S42
S93
S100
C1-8.8
C3-33.7
A172.3
8188.7
A116.6
C4-18.9
A95.8
8168.8
C7-13.1
S43
A146.3
C7-8.5 x
S97
A99.4
A158.0
S52
A162.8
C4-4.0
S94
A162.0
8182.5
A146.8
S6 x
D1-8.4
C5-3.2
S21
C3-8.4
S90
S35
C6-17.1
C6-22.3
C6-7.5
C6-4.9
S34
C6-12.9
C7-8.2
A119.3

LEGEND
× Cloys
+ Till
• Sholes

ACTIVITY CHART

FIGURE: 48

0 0.5 1.0 1.5 2.0 2.5 3.0 3.5 4.0 4.5 5.0 5.5 6.0

Activity A

APPENDIX F

DATA AND ROSE DIAGRAMS OF:

MACRO TILL FABRIC OF UPPER TILL,

SOUTH SCARP, AND AZIMUTH OF JOINT PLANES IN UPPER TILL,

NORTH SCARP.

Table 1. Data of macro till fabric of upper till, south scarp

Azi	Dip	Azi	Dip	Azi	Dip	Azi	Dip	Azi	Dip
030	01NNE	040	05 NE	325	10 NW	030	01NNE	225	23 SW
060	0	060	0	015	17 N	065	0	080	0
055	05 NE	235	31WSW	135	02 SE	235	12 SW	240	18WSW
045	21 NE	300	20WNW	320	02 NW	240	34WSW	240	43WSW
155	0	145	03 SE	015	0	215	07 SW	255	18 W
240	12WSW	240	17WSW	025	02NNE	350	01 N	040	0
270	06 W	015	16 N	200	45 SW	195	20 S	275	02 W
020	04 N	345	18 N	300	32WNW	335	11NNW	040	03 NE
055	08 NE	060	0	185	27 S	005	07 N	005	0
050	36 NE	145	05 SE	080	13 E	030	14NNE	080	06 E

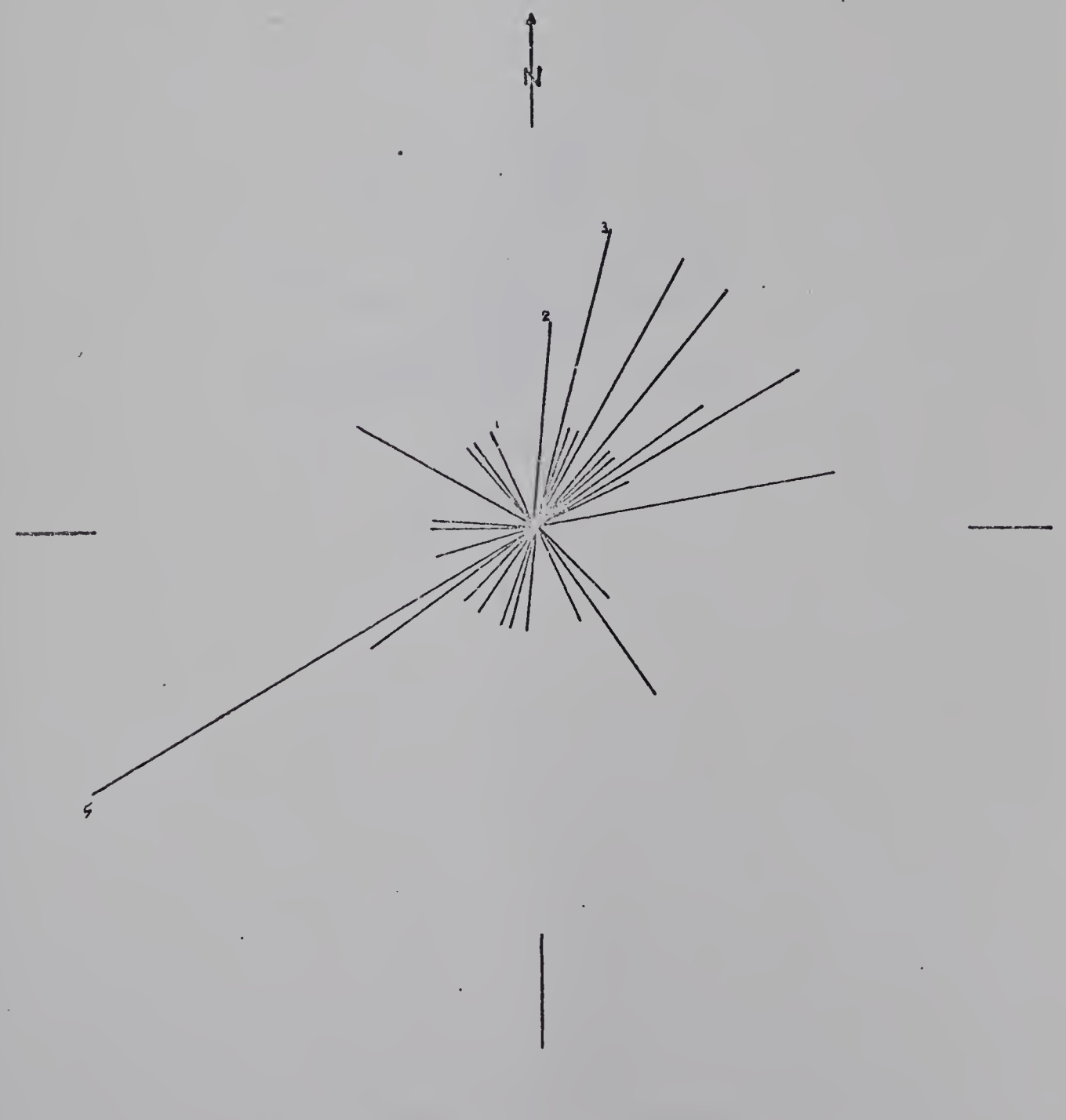

Fig. 49. Macro till fabric of upper till.

Table 2. Azimuth of joint planes in upper till, north scarp

103	062	074	053	104	000	158	009	020	028
142	132	000	068	163	022	022	081	078	

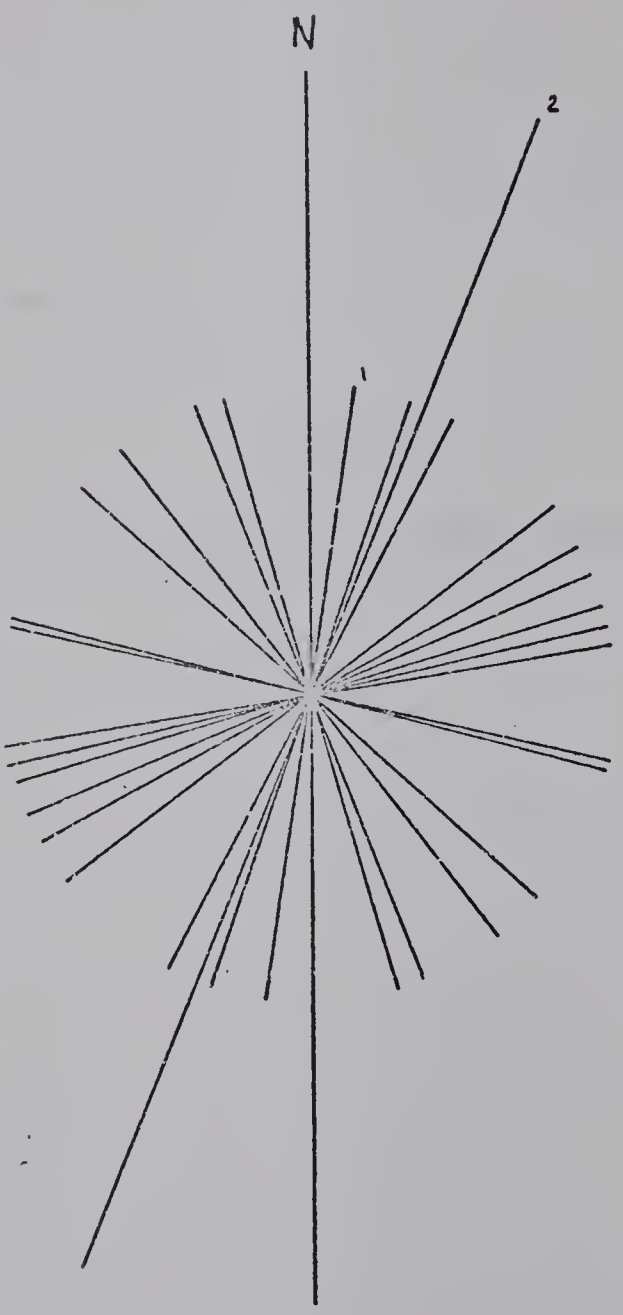

Fig. 50. Strike of joint planes of upper till.

APPENDIX G

TABULATED RESULTS OF LABORATORY ANALYSIS

Table 3 . Test Results of Samples, Trench A

Sample			TX	Wentworth Scale: % wt. coarser than $\phi = \log_2 (1/Dmm)$													Moist. Cont. by wt.			Index Property			Carb. % wt	
No.	Elev.	Material		UC	0	1	2	3	4	5	6	7	8	9	Md ϕ	Mn ϕ	sd σ	Skew α	Wn %	Wl %	Wp %	Ip %	Act.	It	Dol.	Calc.
A	95.8	shale		CH	0	0	3	16	28	38	45	52	58	65	6.8		3.8		27.8	94	23	71	2.03	+.07	0.9	5.8
A	96.4	sandst.		SC	0	0	20	64	71	73	75	77	79	81	2.6	6.8	4.5	+.922	16.3							
A	96.7	sandst.		SC															19.2							
A	97.1	sandst.		SC	0	0	1	14	37	46	50	55	60	66	4.8		1.7		18.0						1.0	5.2
A	97.4	sandst.		SC															13.5							
A	97.6	sandst.		SC															19.6						1.0	5.3
A	97.8	sandst.		SC															16.7						1.0	5.5
A	98.0	sandst.		SC															15.7							
A	98.2	sandst.		SC															18.8						1.3	7.3
A	98.4	sandst.		SC															16.8						1.2	5.2
A	98.7	sandst.		SC	0	0	3	28	63	71	74	77	80	81	3.3		0.6		14.5						0.7	29.6
A	99.0	sandst.		SC															20.0							
A	99.4	shale		CH	0	0	0	10	40	49	54	58	63	67	5.2		2.0		22.2	115	23	92	2.79	-.01	1.1	5.1
A	99.7	sandst.		SC															25.2							
A	100.0	sandst.		SC	0	0	0	7	45	55	60	64	66	69	4.4		1.2		18.7						1.1	5.1
A	100.6	shale		CH	0	0	0	2	15	27	36	43	50	58	8.0		3.9		25.3							
A	101.7	shale		CH															22.7							
A	102.0	shale		CH	0	0	0	0	6	17	27	37	46	55	8.4		3.3		25.8	97	35	62	1.38	-.15	0.7	5.3
A	102.5	shale		CH	0	0	0	0	9	22	33	42	50	58	8.0		3.5		20.9						1.1	5.1
A	103.3	shale		CH															25.5							
A	103.6	shale		CH															25.4							
A	104.2	shale		CH	0	0	0	0	8	20	31	39	49	58	8.1		3.4		23.6	92	28	64	1.52	-.07	0.0	5.1
A	106.4	shale		CH	0	0	0	1	11	27	36	44	52	60	7.7		3.4		21.2	80	23	57	1.42	-.03		
A	106.6	sandst.		SC	0	0	0	35	58	64	68	70	73	75	3.4		0.7		18.0							
A	107.0	shale		CH	0	0	0	3	20	35	42	49	56	63	7.2		3.4		23.0						0.9	5.0
A	107.6	shale		CH															24.1							
A	108.1	shale	T	CH	0	0	0	2	10	20	28	37	46	55	8.4		3.9		22.8	72	24	48	1.07	-.03	1.1	5.3
A	109.0	shale		CH															24.4							
A	110.0	shale		CH	0	0	1	5	11	19	25	31	41	53	8.7		4.2		22.3	71	26	45	0.96	-.08	0.8	5.6
A	110.5	shale		CH															18.6							

Note: T = thinsection made, X = x-ray analysis run

Table 3. Test Results of Samples, Trench A

Sample			TX	Wentworth Scale: % wt. coarser than $\phi = \log_2$ (1/Dmm)														Moist. Cont. by wt.			Index Property			Carb. % wt	
No.	Elev.	Material		UC	0	1	2	3	4	5	6	7	8	9	Mdϕ	Mnϕ	sdσ	Skew α	Wn%	Wl%	Wp%	Ip%	Act.	II	Dol.	Calc.
A	111.0	shale		CH															17.6							
A	112.5	shale		CH	0	0	0	0	0	10	16	23	38	55	8.7		1.9		16.9	62	29	33	0.73	-.37		
A	113.8	shale		CH															19.9							
A	115.0	shale	T	CH	0	0	0	0	1	5	11	25	45	56	8.4		2.1		18.1	72	26	46	1.05	-.17	1.1	4.7
A	115.2	sandst.		SC	1	8	22	35	51	61	68	74	78	82	3.9	5.8	4.2	+.452	8.9						1.9	19.0
A	115.4	sandst.		SC															20.5							
A	115.6	ss+sh		ML	0	0	0	0	7	21	35	45	54	61	7.5		2.8		19.5	63	26	37	0.95	-.18	1.2	5.3
A	116.0	ss+sh		ML	0	0	0	0	28	42	49	55	60	66	6.2		2.6		21.5						0.8	4.6
A	116.6	ss+sh		ML	0	0	0	0	11	25	38	48	56	65	7.2		3.0		20.0	59	26	33	0.94	-.18	0.8	4.7
A	116.9	sandst.		SC	0	0	0	1	33	48	55	60	66	70	5.2		1.6		20.2							
A	117.5	shale		CH															18.2							
A	118.8	shale		CH	0	0	0	0	2	10	25	38	50	61	8.0		5.4		19.3	55	26	29	0.74	-.23		
A	119.1	shale		ML															11.5							
A	119.3	shale	TX	ML	0	0	1	7	22	37	50	65	75	84	5.9	6.4	2.8	+.179	10.8	31	17	14	0.87	-.44		
A	119.4	shale		ML	0	0	0	2	10	22	36	51	68	80	6.9	7.0	2.5	+.040	17.0						0.9	4.9
A	124.5	sandst		SC	0	0	7	27	50	60	65	69	70	73	4.0		1.5		19.0						1.0	4.7
A	124.7	shale		CH	0	0	0	1	7	17	26	35	43	52	8.8		4.0		21.8						1.2	5.5
A	126.5	sandst.		SC															17.5						1.1	5.0
A	126.8	ss+sh		ML	0	0	0	1	11	35	46	51	55	61	5.8		2.6		20.1						1.3	6.0
A	127.9	sandst.		SC	0	1	7	27	50	56	60	64	66	70	4.1		1.6		17.2							
A	128.3	shale		CH															25.0							
A	129.0	shale		CH															27.5						1.1	5.6
A	129.5	shale		CH	0	0	0	0	5	21	35	41	46	52	8.6		3.8		26.3	200	28	172	3.58	-.01		
A	130.1	shale	X	CH	0	0	0	0	1	4	9	15	23	30					32.9	216	40	176	2.52	-.04	1.0	6.9
A	130.2	shale		CH															29.6						0.9	5.3
A	130.3	benton.		CH	0	0	0	2	5	8	11	15	19	24					48.5	400	56	344	4.52	-.02	0.9	5.2
A	130.5	shale		CH															37.0							
A	131.1	shale		CH	0	0	0	0	1	4	8	14	22	32	10.0		3.2		29.8	135	40	95	1.40	-.11	1.4	7.7
A	132.9	shale	T	CH	0	0	0	0	1	4	11	20	30	41	9.6		3.2		28.9	130	36	94	1.59	-.08		
A	133.2	shale		CH	0	0	0	0	1	5	13	21	30	40	9.7		3.4		34.0	151	36	115	1.92	-.02	1.1	6.8

Note: Thinsection of concretionary rock from elev. 125.1'

Table 3. Test Results of Samples, Trench A

Sample			TX	Wentworth Scale: % wt. coarser than $\phi = \log_2 (1/Dmm)$												Moist. Cont. by wt.			Index Property			Carb. % wt	
No.	Elev.	Material		UC	0	1	2	3	4	5	6	7	8	9	Mdφ	Mnφ	sdσ	Skew α	Wn%	Wl%	Wp%	Ip%	Act.	Il	Dol.	Calc.
A	136.0	shale		CH	0	0	0	0	9	17	26	35	44	52	8.8		4.0		26.3	150	32	118	2.46	-.05	1.9	5.6
A	137.3	shale		CH	0	0	0	0	6	18	26	35	44	53	8.7		3.8		26.8	142	30	112	2.38	-.03		
A	138.2	shale	T	CH	0	0	0	0	0	2	15	24	35	46	9.3		3.0		22.9	128	30	98	1.81	-.07	1.4	5.0
A	138.8	shale	T	CH	0	0	0	0	6	21	36	46	54	60	7.4		2.7		25.5	152	29	123	3.07	-.03	3.5	5.2
A	140.1	shale		CH	0	0	0	0	26	43	53	59	62	65	5.6		1.9		25.2						0.9	6.0
A	140.8	shale		CH	0	0	0	1	9	17	29	34	46	55	8.4		3.6		23.5	136	27	109	2.42	-.03		
A	142.1	shale		CH															25.6						1.0	4.8
A	142.8	shale		CH	0	0	0	12	25	30	36	43	50	57	8.0		4.8		28.1							
A	143.3	shale		CH	0	0	0	0	1	6	16	28	40	53	8.8		2.8		22.1	114	34	80	1.70	-.15		
A	143.8	sandst.		SC	0	0	0	16	49	55	58	61	64	67	4.2		1.2		24.5						0.8	5.7
A	144.4	shale		CH	0	0	1	4	14	21	27	35	46	59	8.2		4.0		26.0	97	32	65	1.59	-.09	1.0	5.4
A	145.0	shale		CH															27.6							
A	146.0	shale		CH															20.6						0.7	4.7
A	146.3	shale		CH	0	0	0	2	6	11	16	27	46	66	8.2		2.2		20.9	79	25	54	1.59	-.08	0.7	5.1
A	146.8	shale	TX	MH	0	0	0	3	8	16	24	38	56	71	7.7		2.7		22.8	76	32	44	1.52	-.21	0.8	4.6
A	147.0	shale		CH	0	0	0	0	0	0	2	10	30	47	9.2		2.0		23.5	121	23	98	1.85	+.01	0.9	5.8
A	148.3	sandst.		SC	0	0	8	25	55	61	65	69	71	73	3.8		1.2		20.9						1.7	5.0
A	149.6	sandst.		SC															19.9						1.2	6.1
A	150.0	shale		CH	0	0	0	1	21	34	43	50	56	61	7.0		3.2		21.2	115	28	87	2.13	-.08	0.9	4.9
A	150.5	shale		CH	0	0	0	0	5	38	53	60	65	69	4.7		1.4		21.7							
A	151.8	shale		CH	0	0	0	1	7	19	33	44	54	61	7.6		2.8		20.4						0.0	5.1
A	152.1	shale	T	CH	0	0	0	1	10	25	36	45	54	61	7.5		3.1		19.0	94	25	69	1.77	-.09	0.8	4.8
A	153.5	shale		CH	0	0	0	0	7	22	35	44	50	58	8.1		3.5		21.0	82	26	56	1.33	-.09		
A	155.0	shale		CH	0	0	0	1	7	15	26	39	51	61	7.9		2.8		19.7						0.7	5.2
A	156.0	shale		CH	0	0	0	3	34	46	51	54	57	64	5.8		2.4		19.9						0.7	5.3
A	157.0	shale		CH	0														17.9							
A	158.0	shale	T	Cl	0	0	1	11	25	36	45	50	58	68	7.0	6.5	3.2	-.146	16.0	52	23	29	0.91	-.24	0.0	4.6
A	158.5	shale		CH															15.5							
A	160.0	shale		CH															17.4						0.8	5.2
A	161.0	shale		CH	0	0	1	8	20	29	35	41	50	62	8.0		4.4		17.3	61	25	36	0.95	-.21	0.0	4.8
A	162.0	shale	T	CH	0	0	1	10	20	31	40	49	60	70	7.1	7.3	3.7	+.054	15.5	63	25	38	1.27	-.25	0.9	4.9
A	162.8	shale		CH	0	0	1	10	24	34	43	52	60	69	6.8	7.2	3.4	+.118	14.8	76	20	56	1.81	-.09		
A	164.4	shale		CH	0	0	1	11	25	36	45	52	59	69	6.8	6.9	6.6	+.023	16.1						1.0	5.1

Table 3. Test Results of Samples, Trench A

Sample			TX	Wentworth Scale: % wt. coarser than $\phi = \log_2$ (1/Dmm)														Moist. Cont. by wt.			Index Property			Carb. % wt	
No.	Elev.	Material		UC	0	1	2	3	4	5	6	7	8	9	Mdϕ	Mnϕ	sdσ	Skew α	Wn%	Wl%	Wp%	Ip%	Act.	II	Dol.	Calc.
A	164.7	shale		CH															19.3						0.8	5.6
A	165.6	shale	T	CH	0	0	1	8	17	27	35	43	50	59	8.0		4.2		18.9	80	25	55	1.34	-.09	1.2	5.5
A	166.0	benton.	X	CH	0	0	0	0	0	1	2	3	3	4					51.3	372	62	310	3.23	-.03	1.2	9.9
A	166.4	shale		CH	0	0	0	2	4	7	13	21	33	45	9.3		3.0		23.4	138	30	108	1.96	-.06		
A	168.0	shale	T	CH	0	0	0	0.	3	11	22	34	45	55	8.5		3.2		20.7	124	32	92	2.04	-.12	2.1	5.6
A	168.7	shale		CH	0	0	0	1	25	45	53	57	62	68	5.5		1.8		20.4						1.2	5.7
A	169.4	shale		CH															19.8							
A	170.3	shale		CH	0	0	0	0	11	25	34	43	51	59	7.8		3.5		20.0							
A	171.6	shale		CH															22.8							
A	172.3	shale	T	CH	0	0	0	1	23	36	46	53	59	64	6.6		2.9		20.9	138	27	111	3.08	-.06	2.0	5.2
A	172.4	shale		CH															21.0						1.2	5.6
A	173.7	shale		CH	0	0	0	0	1	4	10	23	38	48	9.2		2.6		21.4	115	26	89	1.71	-.05	1.1	5.7
A	174.2	sandst.	TX	SC	0	1	20	58	69	73	75	78	80	83	2.8	5.7	3.9	+.744	11.5						0.9	5.7
A	174.9	sandst.		SC	0	0	5	23	53	62	66	70	73	75	3.8		1.1		14.4							
A	176.0	sandst.		SC	0	0	17	61	72	75	77	80	82	83	2.7	6.1	4.7	+.724	11.3							
A	176.2	sandst.	T	SC	0	2	30	56	67	71	75	76	78	80	2.7		1.1		12.4						1.6	5.2
A	178.5	sandst.		SC	0	2	30	58	70	76	80	85	89	90	2.7	4.9	3.4	+.648	3.5						2.9	38.5
A	179.2	sandst.	T	SC	0	0	37	55	64	68	72	76	79	82	2.6	5.7	4.2	+.738	13.3						0.9	6.1
A	180.5	sandst.		SC															10.5							
A	181.6	sandst.		SC	0	0	33	6-	69	73	76	79	81	84	2.5	5.9	3.8	+.895	10.6						0.7	6.9

Table 3. Test Results of Samples, Trench B

Sample			TX	Wentworth Scale: % wt. coarser than $\phi = \log_2$ (1/Dmm)														Moist. Cont. by wt.			Index Property			Carb. % wt	
No.	Elev.	Material		UC	0	1	2	3	4	5	6	7	8	9	Md ϕ	Mn ϕ	sd σ	Skew α	Wn %	Wl %	Wp %	Ip %	Act.	Il	Dol.	Calc.
B	164.3	shale		CH	0	0	0	0	7	22	30	38	67	56	8.3		4.1		28.3						0.7	5.4
B	165.0	shale	TT	CH	0	0	0	0	2	5	10	20	34	47	9.2		2.7		35.6	102	28	74	1.40	+.10	1.2	5.8
B	166.3	shale		CH															29.8						1.4	5.8
B	167.5	shale		CH	0	0	0	0	2	16	30	40	49	56	8.2		3.2		29.0						1.8	5.3
B	168.2	shale		CH															25.3						1.9	5.3
B	168.8	shale		CH	0	0	3	10	29	40	49	55	60	65	6.2		2.9		45.7	109	24	85	2.42	+.26	1.3	5.1
B	170.0	shale		CH	0	0	0	2	7	17	25	35	45	57	8.4	7.8	3.0	-.200	26.5	88	27	61	1.42	-.01		
B	171.0	sandst.	T	SC	0	2	18	59	69	73	74	76	80	83	2.7	6.1	4.0	+.850	14.6						1.1	5.3
B	173.1	sandst.		SC	0	0	45	60	70	74	76	79	81	84	2.6	5.3	3.8	+.710	35.4						1.8	26.8
B	176.0	calc ss.		SC															16.3						1.0	5.1
B	177.7	sandst.		SC	0	0	29	61	68	69	71	74	76	79	2.5	6.3	4.6	+.826	21.5						1.0	5.1
B	178.8	sandst.		SC															18.5						0.8	5.1
B	181.0	sandst.		SC															19.8							
B	182.0	siltst.		ML	0	0	4	14	24	34	44	54	64	73	6.7	6.7	3.5	0.000	27.9						0.9	5.2
B	182.3	sandst.	T	SC	0	14	50	59	65	71	74	76	79	81	3.0	6.5	4.3	+.815	23.3						0.7	5.1
B	182.5	shale		CH	0	0	1	3	13	39	50	59	65	70	6.0		1.9		29.1	97	25	72	2.40	+.06	0.8	5.2
B	184.0	shale		CH															33.3						0.9	4.9
B	186.0	shale		CH	0	0	0	3	9	16	25	34	49	61	8.2		4.0		34.4	66	25	35	0.90	+.27	0.8	4.9
B	187.0	shale		CH															27.6						0.0	4.8
B	187.4	shale	TX	CH	0	0	0	0	1	4	7	17	30	44	9.4		2.6		24.9	58	29	29	0.52	-.14	0.7	5.1
B	187.6	siltst.		SM															21.3							
B	188.7	siltst.		SM	0	0	2	18	35	42	48	52	56	65	6.5	6.6	3.9	+.026	26.3	52	27	25	0.72	-.03		
B	190.0	shale		CH	0	0	0	0	1	3	9	25	35	50	9.0		3.0		27.5	54	28	26	0.52	-.02	1.0	5.9
B	191.8	shale		MH	0	0	0	3	7	14	19	26	36	50	9:1		3.6		29.4	54	32	22	0.44	-.12	0.8	5.2
B	193.5	shale		CH	0	0	1	2	5	10	19	30	41	54	8.6		3.0		28.3	59	28	31	0.67	+.01		
B	196.2	shale		CH	0	0	0	3	10	23	29	36	46	56	8.4		3.9		14.1	56	24	32	0.73	-.13	0.7	4.8
B	197.0	shale		MH	0	0	0	3	7	18	23	32	45	60	8.4		2.7		23.3	57	31	26	0.65	-.30		

Table 3. Test Results of Samples, Auger hole C-1

Sample			TX	Wentworth Scale: % wt. coarser than $\phi = \log_2 (1/Dmm)$													Moist. Cont. by wt.			Index Property			Carb. % wt	
No.	Elev.	Material		UC	0	1	2	3	4	5	6	7	8	9	Mdϕ	Mnϕ	sdσ	Scew α	Wn %	Wl %	Wp %	Ip %	Act.	Ii	Dol.	Calc.
C-1																									
3.0	93.1	sandst.		SC															30.0						1.1	5.2
3.4	92.7	sandst.		SC															36.0							
3.6	92.5	shale		CH															36.6						0.8	5.2
6.0	90.1	shale		CH	0	0	1	8	18	27	35	44	52	60	7.8		3.9								1.0	4.8
8.1	88.0	ss+sh		SC															28.1							
8.8	87.3	shale		CH	0	0	0	1	10	20	32	43	53	64	7.7		3.1		25.5	81	25	56	1.22	+.01	0.7	4.7
13.6	82.5	ss+sh		SC															17.3						2.1	19.8
13.9	82.2	shale		CH															40.0							
14.2	81.9	shale		CH															34.8						1.1	6.0
16.0	80.1	sandst.		SM	2	9	35	55	67	75	80	84	87	90	2.7		2.9								8.2	18.0
18.0	78.1	sand		SP	0	3	27	69	80	85	88	90	92	94	2.5		1.4								5.7	10.4

Table 3. Test Results of Samples, Auger hole C-2

Sample			TX	Wentworth Scale: % wt coarser than ϕ $\log_2$ (1/Dmm)													Moist. Cont. by wt.			Index Property			Carb. % wt	
No.	Elev.	Material		UC	0	1	2	3	4	5	6	7	8	9	Mdϕ	Mnϕ	sdσ	Skew α	Wn %	Wl %	Wp %	Ip %	Act.	II	Dol.	Calc.
C-2																									
2.0	95.8	sandst.		SC															12.8							
3.2	94.6	sandst.		SC	0	1	38	65	72	76	79	81	82	84	2.3	5.6	4.1	+.806	16.9						0.9	4.9
3.9	93.9	sandst.		SC															14.9							
4.0	93.8	sandst.		SC															19.0							
6.0	91.8	shale		CH	0	0	2	4	6	17	29	40	49	56	8.3		3.8		28.4						1.7	5.3
8.0	89.8	shale		CH															32.0							
8.3	89.5	shale		CH	0	0	0	1	8	20	30	38	45	51	8.9		4.3		34.0	155	32	123	2.51	+.02	0.9	5.2
9.3	88.5	shale		CH	0	0	1	3	13	26	36	44	50	55	8.0		4.2		25.2	150	23	127	2.82	+.02		
9.8	88.0	shale		CH															25.4						0.8	5.3
10.0	87.8	shale		CH															28.0							
11.0	86. 8	siltst.		CH	0	0	2	6	35	43	50	56	62	68	6.0		2.6		29.4						1.2	5.1
12.0	85.8	shale		CH															40.9							
13.0	84.8	shale		CH															31.4						1.4	5.2
13.7	84.1	shale		CH	0	0	0	1	2	5	14	22	40	50	9.1		3.8		35.8	140	34	106	2.12	+.02	0.8	5.5
14.0	83.8	shale		CH															31.4							
15.0	82.8	shale		CH	0	1	2	4	10	17	24	32	40	46	9.3		4.4		42.8							
16.0	81.8	shale		CH	0	0	2	5	13	27	34	40	47	53	8.5		4.2		37.6						1.1	5.3
17.0	80.8	shale		CH															38.5							
18.0	79.8	shale		CH	0	1	4	13	22	30	36	43	49	55	8.2		4.8		34.4						1.2	5.5
18.6	79.2	shale		CH	0	0	1	3	10	17	25	31	40	52	8.8		4.0		41.4	113	34	79	1.64	+.09		
18.9	78.9	ss+sh		SC															33.0						8.2	16.6
20.0	77.8	sand		SW	0	1	4	25	33	44	61	70	75	79	4.6	5.9	4.3	+.294	27.4						6.0	8.4

Table 3. Test Results of Samples, Auger hole C-3

Sample			TX	Wentworth Scale: % wt coarser than $\phi = \log_2$ (1/Dmm)													Moist. Cont. by wt.			Index Property			Carb. % wt	
No.	Elev.	Material		UC	0	1	2	3	4	5	6	7	8	9	Mdϕ	Mnϕ	sdσ	Skew α	Wn %	Wl %	Wp %	Ip %	Act.	II	Dol.	Calc.
C-3																									
2.0	109.1	sandst.		SC	0	3	23	45	54	63	68	74	78	80	3.5	5.9	4.1	+.576	9.8						2.7	26.4
3.0	108.1	siltst.		ML															12.3							
3.1	108.0	shale		CH															26.7						0.0	4.9
3.4	107.7	shale		CH	0	0	1	11	24	39	45	53	60	66	6.7		3.3		30.5						1.0	4.7
3.8	107.3	shale		CH															30.7						0.7	4.8
5.0	106.1	sandst.		SC															12.8						1.4	6.9
6.0	105.1	sandst.		SC	0	2	25	55	64	69	74	77	81	83	2.8	5.5	3.8	+.711	14.2						2.4	17.0
8.0	103.1	shale		CH															30.7							
8.1	103.0	shale		CH															32.1						0.9	4.7
8.4	102.7	shale		CH	0	0	1	10	25	44	54	63	70	74	5.6		2.3		19.3	70	25	45	1.73	-.13	1.1	4.9
10.0	101.1	shale		CH	0	0	3	9	19	29	37	47	56	65	6.2		2.5		24.2						1.0	4.9
12.0	99.1	shale		CH															24.9						1.1	4.9
13.2	97.9	shale		CH															24.0						1.0	5.8
13.6	97.5	shale		CH	0	0	0	3	9	19	30	40	50	58	8.0		3.3		33.2	101	28	73	1.74	+.07	0.7	5.4
13.9	97.2	shale		CH															23.7						1.1	5.1
14.0	97.1	shale		CH															28.6						1.3	5.7
16.0	95.1	sandst.		SC	0	0	2	41	60	66	70	74	77	80	3.3	6.8	4.2	+.845	21.4						1.3	5.1
17.0	94.1	shale		CH															35.6							
18.0	93.1	shale		CH															20.7							
18.5	92.6	shale		CH	0	0	0	2	15	31	41	48	54	60	7.2		3.1		18.6	117	27	90	2.25	-.09	0.9	5.3
20.0	91.1	shale		CH															21.8						1.2	5.8
22.0	89.1	shale		CH															19.9						1.6	5.2
23.4	87.7	shale		CH	0	2	6	14	21	30	39	46	54	61	7.5		4.2		15.7						1.8	6.8
24.0	87.1	shale		CH															23.1							
25.0	86.1	shale		CH															25.1						1.5	4.8
26.0	85.1	shale		CH	1	3	5	11	20	28	35	42	50	59	8.0		4.5		23.3						2.3	5.3
28.0	83.1	shale		CH															26.0						2.7	5.6
28.1	83.0	shale		CH	1	3	5	10	16	24	31	40	50	61	8.1		4.3		20.5						1.5	5.3
30.0	81.1	sandst.		SC	0	0	15	44	55	61	66	70	74	76	3.4		1.2		30.7						1.1	5.3
31.0	80.1	sandst.		SC	0	0	14	45	56	62	66	70	74	77	3.3		1.2		27.0						1.3	5.6
32.0	79.1	sandst.		SC															27.1						1.2	5.4
33.0	78.1	sandst.		SC															24.4							
33.2	77.9	shale		CH															22.7						1.3	5.5

Table 3. Test Results of Samples, Auger hole C-3

Sample			TX	Wentworth Scale: % wt coarser than $\phi = \log_2 (1/Dmm)$														Moist. Cont. by wt.			Index Property			Carb. % wt	
No.	Elev.	Material		UC	0	1	2	3	4	5	6	7	8	9	Mdϕ	Mnϕ	sdσ	Scew α	Wn %	Wl %	Wp %	Ip %	Act.	II	Dol.	Calc.
C-3																									
33.6	77.5	shale		CH	0	0	0	1	3	7	19	39	54	64	7.7		2.0		16.1	112	30	82	2.28	-.17	0.8	5.1
34.0	77.1	shale		CH															24.9						1.6	5.3
36.0	75.1	shale		CH															23.9							
37.0	74.1	sandst.		SC															12.3							
38.0	73.1	sandst.		SC	0	1	4	19	51	63	69	74	78	81	3.9		1.1		11.4						2.3	21.2

Table 3. Test Results of Samples, Auger hole C-4

Sample			TX	Wentworth Scale: % wt. coarser than $\phi = \log_2$ (1/Dmm)														Moist. Cont. by wt.			Index Property			Carb. % wt	
No.	Elev.	Material		UC	0	1	2	3	4	5	6	7	8	9	Mdϕ	Mnϕ	sdσ	Scew α	Wn %	Wl %	Wp %	Ip %	Act.	II	Dol.	Calc.
C-4																									
2.0	130.2	sandst.		SC	0	0	0	17	43	59	64	68	71	74	4.4		1.4		20.2						0.9	5.0
3.1	129.1	sandst.		SC															12.0						0.8	4.6
3.3	128.9	shale		CH	0	0	0	1	5	22	38	47	55	62	7.3		2.6		20.9	106	28	78	2.05	-.09	0.8	5.1
3.8	128.4	shale		CH	0	0	0	10	31	49	57	64	68	70	5.2		2.0		17.9							
4.0	128.2	shale		CH	0	0	0	0	8	40	54	61	66	69	5.7		1.4		22.9	120	27	93	3.00	-.04		
6.0	126.2	shale		CH	0	0	1	3	10	25	35	44	52	60	7.8		3.3		23.4						1.0	5.0
8.0	124.2	sandst.		SC															19.4						0.9	5.3
8.6	123.6	sandst.		SC	0	0	24	60	70	75	78	80	81	84	2.8	5.6	3.8	+.713	13.1							
10.0	122.2	sandst.		SC															19.7						1.7	5.3
11.0	121.2	sandst.		SC	0	0	31	60	70	74	76	79	81	84	2.6	5.6	3.9	+.761	18.2						2.4	5.3
12.0	120.2	sandst.		SC															18.4						1.3	5.8
12.5	119.7	sandst.		SC															16.5							
13.0	119.2	sandst.		SC	0	2	25	51	62	70	74	78	80	81	2.9	5.9	4.1	+.733	12.8						1.3	17.2
13.4	118.8	sandst.		SC															12.9						1.2	7.3
13.8	118.4	sandst.		SC	0	2	42	73	80	84	85	87	88	89	2.2	3.5	2.0	+.650	10.6						1.1	5.1
14.0	118.2	sandst.		SC															16.4						1.8	7.1
16.0	116.2	shale		CH	1	4	6	12	21	25	35	50	63	70	6.9		3.5		23.0						2.2	5.3
18.0	114.2	shale		CH															18.5							
18.1	114.1	shale		CH															17.0						1.2	5.5
18.7	113.5	shale		CH	0	0	0	0	2	19	27	39	49	56	8.2		3.5		12.4	93	40	53	1.20	-.52	2.3	5.1
18.9	113.3	shale		CH	0	0	1	7	20	30	37	45	55	65	7.4		3.5		18.0	74	28	46	1.31	-.22	0.7	5.1
20.0	112.2	shale		CH	0	1	10	22	32	40	46	54	60	68	6.4		3.9		18.0						1.7	5.3
21.0	111.2	shale		CH															18.0						1.7	5.1
22.0	110.2	shale		CH	0	0	1	20	30	37	41	47	54	60	7.4		4.6		36.2						1.1	5.1
23.6	108.6	sandst.		SC	0	0	0	3	49	60	64	68	71	74	4.1		0.8		17.7						0.7	4.8
25.0	107.2	sandst.		SC															17.3						1.1	4.8
26.0	106.2	sandst.		SC															16.7							
27.0	105.2	sandst.		SC	0	3	6	20	51	59	64	68	73	75	3.9		1.1		33.1						1.5	11.1
28.0	104.2	sandst.		SC	0	0	0	3	19	52	63	69	73	76	3.8		1.0		23.8							
28.1	104.1	sandst.		SC															11.7						1.4	9.1
29.0	103.2	sandst.		SC															14.1							

Table 3. Test Results of Samples, Auger hole C-5

Sample			TX	Wentworth Scale: % wt. coarser than $\phi = \log_2$ (1/Dmm)														Moist. Cont. by wt.			Index Property			Carb. % wt	
No.	Elev.	Material		UC	0	1	2	3	4	5	6	7	8	9	Mdϕ	Mnϕ	sdσ	Skew α	Wn %	Wl %	Wp %	Ip %	Act.	II	Dol.	Calc
C-5																									
2.0	139.2	till		CI	0	2	10	20	29	39	49	58	68	73	6.1		3.5		16.0						2.9	5.3
3.2	138.0	siltst.		MH	0	1	4	8	13	22	33	45	59	73	7.3	7.3	3.0	0.000	24.8	53	33	20	0.74	-.41	0.8	4.5
3.7	137.5	shale		CH	0	0	1	3	9	18	26	35	48	60	8.2		3.4		15.2	58	28	30	0.75	-.43	1.1	4.4
4.0	137.2	shale		CH															23.7						1.3	4.8
6.0	135.2	shale		CH	0	1	2	5	12	23	31	39	51	65	7.9		3.6		24.0						1.9	5.2
8.0	133.2	shale		CH															23.0							
8.3	132.9	sandst.		SC	0	0	5	41	63	69	73	75	78	80	3.3		0.9		16.9						0.7	4.8
8.5	132.7	sandst.		SC	0	1	17	57	68	75	78	79	82	84	2.7	5.6	3.7	+.784	23.6						1.4	43.0
8.7	132.5	sandst.		SC															8.5							
10.0	131.2	sandst.		SC	0	1	12	32	52	64	68	71	74	77	3.8		1.6		19.8						1.4	6.5
12.0	129.2	sandst.		SC															20.1							
12.1	129.1	sandst.		SC															5.0							
12.2	129.0	sandst.		SC	0	4	32	58	71	78	80	82	84	86	2.7	4.9	3.4	+.647	14.6						1.4	28.6
12.5	128.7	sandst.		SC															9.3						2.2	48.0
14.0	127.2	sandst.		SC					36	65	71	75	79	84	2.4	5.4	3.8	+.970	24.2						1.2	5.5
16.0	125.2	sandst.		SC	0	0	37	50	67	76	79	81	83	85	3.0	5.4	3.4	+.706	19.8						1.5	4.7
17.0	124.2	sandst.		SC															18.6							
17.3	123.9	sandst.		SC															28.3						2.6	11.2
17.4	123.8	shale		CH	0	0	1	6	14	23	31	41	52	62	7.8		3.6		21.1						1.1	4.8
17.8	123.4	shale		CH	0	0	0	0	0	2	6	18	41	62	8.4		1.5		12.6	89	22	67	1.76	-.14	0.9	5.6
20.0	121.2	shale		CH	0	1	7	16	27	36	42	48	54	60	7.3		4.4		19.9						1.2	5.5
22.0	119.2	shale		CH															19.3							
22.5	118.7	shale		CH	0	2	6	11	18	26	33	40	50	60	8.1		4.3		48.3	95	32	63	1.58	+.26	1.2	5.9
24.0	117.2	shale		CH	0	1	3	7	14	22	29	37	45	54	8.5		4.3		19.6						0.7	5.3
26.0	115.2	shale		CH	0	0	0	2	9	22	32	44	50	57	8.0		4.5		27.4						1.3	4.9
27.5	113.7	shale		CH	0	0	3	5	8	21	31	40	49	58	8.1		3.4		40.4							
28.6	112.6	shale		CH															16.5						1.2	5.9
28.8	112.4	shale		CH	0	0	1	3	13	20	26	34	44	57	8.5		4.2		22.6	78	25	53	1.23	-.05	0.9	5.3
30.0	111.2	shale		CH	0	0	0	3	11	20	28	37	46	57	8.3		3.9		15.8						0.9	4.7
32.0	109.2	shale		CH															15.8							
32.7	108.5	shale		CH	0	0	1	7	15	23	30	39	49	58	8.2		4.2		18.4	84	27	57	1.36	-.15	0.9	5.3

Table 3. Test Results of Samples, Auger hole C-6

Sample			TX	Wentworth Scale: % wt. coarser than $\phi = \log_2 (1/Dmm)$														Moist. Cont. by wt.			Index Property			Carb. % wt	
No.	Elev.	Material		UC	0	1	2	3	4	5	6	7	8	9	Mdϕ	Mnϕ	sdσ	Skew α	Wn %	Wl %	Wp %	Ip %	Act.	II	Dol.	Calc
C-6																									
2.0	154.8	till		Cl	0	0	3	10	32	43	53	63	71	76	5.7		3.5		16.0						3.1	6.9
3.0	153.8	till		Cl															10.7						3.0	6.8
4.9	151.9	till		Cl	2	8	18	29	41	53	61	68	74	79	4.8	6.2	4.4	+.432	12.0	30	15	15	0.71	-.20	3.2	5.7
6.0	150.8	till		Cl															12.6						1.0	4.6
7.0	149.8	till																	12.4							
7.5	149.3	till		Cl	0	2	8	18	28	39	53	64	70	79	4.8		3.0		11.2	28	18	10	0.48	-.68	3.1	5.3
10.0	146.8	till		Cl	2	6	19	42	59	70	78	82	85	87	3.4	4.8	3.0	+.467	7.7						3.4	4.7
12.0	144.8	till		Cl	1	5	19	37	51	67	75	81	86	88	3.9	4.7	2.9	+.276	8.7							
12.2	144.6	till		Cl															10.2						3.1	5.7
12.9	143.9	till		Cl	3	13	30	40	52	62	69	75	79	81	3.9		2.7		11.2	21	13	8			3.3	5.2
14.0	142.8	till		Cl	0	3	14	27	41	53	60	68	73	77	4.7		1.8		13.3						3.2	5.2
16.0	140.8	till		Cl	1	5	15	29	41	53	61	68	72	76	4.8		2.7		14.9						2.8	4.8
17.0	139.8	till		Cl	1	4	12	20	39	51	60	67	71	76	4.9		2.6		13.8							
17.1	139.7	till		Cl	2	10	21	33	45	55	63	69	73	76	4.5		3.0		15.5	27	16	11			2.8	5.1
17.4	139.4	sand		SP	0	0	6	28	74	84	87	91	92	93	3.5	3.4	1.3	-.077	10.8						3.3	5.7
17.5	139.3	till		Cl	1	5	17	40	59	73	78	82	86	88	3.5	4.8	2.8	+.464	14.0							
17.8	139.0	till		Cl	0	3	13	25	44	57	63	70	75	79	4.3	6.6	4.4	+.523	13.6						2.3	5.5
20.0	136.8	till		Cl	1	4	13	25	39	50	58	65	70	75	5.1		2.9		14.9						2.8	5.2
22.0	134.8	till		Cl															16.9							
22.1	134.7	till		Cl	2	9	19	30	40	50	58	66	71	76	5.1		3.4		16.7	35	18	17			2.8	5.6
23.0	133.8	till		Cl															21.2							
24.0	132.8	shale		CH	0	0	0	4	7	18	26	33	46	54	8.5		4.7		26.8						1.3	4.8
26.0	130.8	shale		CH															20.2							
26.4	130.4	shale		CH	0	0	0	2	13	28	35	41	48	54	8.2		4.0		18.4						1.5	5.3

Table 3. Test Results of Samples, Auger hole C-7

Sample			TX	Wentworth Scale: % wt. coarser than $\phi = \log_2 (1/Dmm)$													Moist. Cont. by wt.			Index Property			Carb. % wt	
No.	Elev.	Material		UC	0	1	2	3	4	5	6	7	8	9	Mdϕ	Mnϕ	sdσ	Scew α	Wn %	Wl %	Wp %	Ip %	Act.	II	Dol.	Calc
C-7																									
2.0	166.4	silt		Ml															15.8						8.2	9.1
3.5	164.9	silt		CL	0	0	0	0	1	4	17	29	41	55	8.6		2.7		21.2						5.7	11.2
3.7	164.7	silt		ML	0	0	0	1	6	46	63	69	74	78	5.7		0.9		17.5	38	18	20	0.91	-.03		
4.0	164.4	silt		CL	0	0	0	0	2	4	20	32	45	57	8.3		2.6		19.7							
6.0	162.4	silt		CL	0	0	0	0	2	7	17	33	46	56	8.3		2.5		19.3						6.1	9.2
8.0	160.4	silt		ML															15.5							
8.2	160.2	till		Cl	3	10	24	35	46	56	65	72	79	83	4.3	5.7	4.3	+.326	17.2	25	14	11	0.65	+.29		
8.5	159.9	silt		CH	0	3	5	9	13	20	29	45	59	67	7.3		2.9		16.4	38	22	16	0.49	-.35	1.8	6.4
10.0	158.4	till		Cl	0	2	6	13	21	30	39	49	58	66	7.2		3.9		20.5						2.8	5.3
12.0	156.4	till		Cl	0	0	2	4	6	14	26	38	47	56	8.3		3.2		16.4						3.4	5.1
13.0	155.4	till		Cl	1	4	8	13	20	30	40	50	58	66	7.0		3.7		19.0	44	21	12	0.68	-.09	2.2	5.2
13.5	154.9	shale		CH	0	0	0	0	2	6	15	25	37	50	9.0		2.9		15.9						2.0	5.7
14.0	154.4	shale		CH															15.7							
16.0	152.4	shale		CH	0	0	0	6	15	26	36	45	54	61	7.5		3.5		15.0						0.9	5.0
18.0	150.4	shale		CH															15.7						1.1	4.7
18.5	149.9	shale		CH	0	0	1	6	15	25	35	45	54	61	7.6		3.5		16.5	93	25	68	1.74	-.12	0.9	5.1
19.0	149.4	shale		CH															15.5							

Table 3. Test Results of Samples, Auger hole D-1

Sample			TX	Wentworth Scale: % wt. coarser than $\phi = \log_2 (1/Dmm)$												Moist. Cont. by wt.			Index Property			Carb. % wt	
No.	Elev.	Material		UC	0	1	2	3	4	5	6	7	8	9	Mdϕ	Mnϕ	sdσ	Scew α	Wn %	Wl %	Wp %	ip %	Act.	II	Dol.	Calc.
D-1																									
4.0	155.4	till		Cl	0	2	15	23	39	47	55	65	71	75	5.3		3.0		17.9						2.9	5.9
6.0	153.4	till		Cl															21.1						3.2	5.2
8.0	151.4	till		Cl															17.1							
8.2	151.2	till		Cl	1	6	15	23	31	38	47	57	68	73	6.3		4.2		12.2	34	15	19	0.70	-.15	2.1	5.7
10.0	149.4	till		Cl	0	3	10	20	35	53	63	70	75	79	4.8		2.2		13.7						3.4	5.2
12.0	147.4	till		Cl															21.2						2.8	5.3
13.0	146.4	sandst.		SC															24.6							
13.3	146.1	sandst.		SC	0	0	36	47	69	72	75	78	80	81	2.8	6.5	4.5	+.822	24.5						1.1	8.1
13.4	146.0	shale		CH															46.1						0.7	5.3
13.6	145.8	shale		CH	0	0	0	1	4	15	26	34	42	50	9.0		4.0		45.4	138	28	110	2.20	+.16	0.8	5.2
14.0	145.4	shale		CH															26.6							
15.0	144.4	till		Cl															26.2						2.1	5.7
16.0	143.4	sandst.		SC	0	0	5	23	39	45	50	56	62	65	6.0		3.3		25.2						1.3	5.1
17.0	142.4	sandst.		SC															20.5							
18.0	141.4	sandst.		SC															22.2							
18.3	141.1	sandst.		SC	0	0	18	44	61	68	72	74	76	77	3.3		1.4		18.6						0.8	5.1
18.5	140.9	shale		CH	0	1	4	7	14	23	31	38	46	56	8.4		4.1		23.1	170	32	138	3.14	-.06	0.8	5.1
19.0	140.4	shale		CH															23.0							
20.0	139.4	shale		CH															21.3						1.5	5.0
21.0	138.4	shale		CH	0	0	3	5	10	18	27	35	42	50	9.0		4.2		19.7						0.7	5.2
22.0	137.4	shale		CH															23.0						1.5	4.9
23.0	136.4	shale		CH															18.0							
23.5	135.9	shale		CH	0	0	0	0	2	15	30	42	51	59	7.9		2.8		24.2	108	30	78	1.91	-.07	1.0	5.2

Table 3. Test Results of Samples, Surface

Sample			TX	Wentworth Scale: % wt coarser than $\phi = \log_2 (1/Dmm)$														Moist. Cont. by wt.		Index Property			Carb. % wt	
No	Elev.	Material		UC	0	1	2	3	4	5	6	7	8	9	Mdϕ	Mnϕ	sdσ	Scew α	Wn %	Wl %	Wp %	ip %	Act.	Il	Dol.	Calc.
S1	234	clay		CL	0	0	0	0	0	6	18	35	49	59	8.2		2.4								11.1	16.6
S2	233.5	silt		ML	0	0	0	0	0	11	44	69	78	81	6.2	7.6	2.4								11.4	14.9
S3	233	clay	T	CL	0	0	0	0	1	9	20	30	41	42	8.8		3.1			50	25	25	0.43		5.1	12.4
S4	232	silt		ML	0	0	0	0	0	9	25	41	57	70	7.5		2.1								3.7	26.9
S5	224	clay																								
S6	223.5	silt	T	ML	0	0	0	0	1	2	8	38	64	73	7.4		1.1			47	31	16	0.59		2.3	4.2
S7	216	till,Up	T	CI	0	3	11	22	35	44	53	63	71	76	5.7		3.3								2.6	5.3
S8	210	sand		SP	0	0	5	25	74	93	95	96	97	98	1.6	1.5	0.9	-.111							2.1	6.9
S9	207	sand		SP	0	0	31	86	93	94	95	96	97	98	2.2	2.3	0.6	+.083							2.2	5.2
S10	199	silt		ML	0	0	0	1	2	6	27	54	79	89	5.8	6.1	1.6	+.187							4.0	4.6
S11	184	sandst.	T	SC	0	0	25	64	74	77	81	83	84	85	2.5	4.9	3.1	+.775							1.4	5.1
S12	182	shale		CH	0	0	0	0	2	5	11	30	39	49	9.1		3.6			112	25	87	1.71		0.0	5.0
S13	180	siltst.		CH	0	0	0	3	11	22	35	44	50	55	8.0		3.5			181	31	150	3.33		0.9	5.3
S14	177	sandst.		SC	0	0	31	60	69	74	76	78	80	83	2.6	5.8	4.7	+.681							1.1	4.7
S15	176.5	sandst.																								
S16	166	sandst.	T	SC	0	0	0	20	59	69	74	77	79	83	2.8	5.8	4.0	+.763							0.9	4.5
S17	163	ss+coal		SC	0	0	44	67	75	79	81	83	85	87	2.2	4.4	3.1	+.738							0.9	4.7
S18	187	sandst.																								
S19	186	tuff		CH	0	0	0	1	14	30	40	48	53	57	7.4		3.2			100	30	70	1.63		0.7	5.3
S20	175	ironst.																								
S21	151	sh+fer,		MH	0	0	1	4	11	25	39	51	63	72	6.9		2.6			66	37	29	1.04		0.7	4.7
S22	146.5	sandst.		SC	0	0	29	50	61	66	70	73	75	77	3.0		1.4									
S23	137	ss+sh		SC	0	0	20	60	70	74	76	79	81	84	2.7	5.6	3.7	+.782							0.8	4.7
S24	109	ss+sh		SC																						
S25	99	ss+fer.		SC																					2.4	43.0
S26	100	ss+fer.		SM																					1.5	9.3
S27	100.5	ss+sh		SC	0	0	8	53	65	70	73	75	77	79	3.0		0.8									
S28	98	sh+fer.		CH	0	1	3	8	18	28	38	46	54	61	7.4		3.6			102	28	74	1.90			
S29	129	shale		CL	0	0	1	3	8	18	29	40	50	60	8.01		3.2			80	33	47	1.17		0.9	4.6
S30	167	shale		CH	0	0	0	0	2	10	26	39	49	58	8.2		2.8			135	20	115	2.74		1.8	5.0
S31	181	ss+fer.	T	SC	0	0	0	0	41	68	75	79	80	85	2.2	5.0	3.4	+.823							1.4	5.6
S32	187	shale		CH	0	0	0	1	3	10	20	35	49	63	8.1		2.5			99	37	62	1.68		0.7	5.0
S33	188	sandst.	T	SC	0	0	5	30	54	64	67	70	73	75	3.8		1.3								1.0	5.0

Table 3. Test Results of Samples, Surface

Sample			TX	Wentworth Scale: % wt. coarser than $\phi = \log_2 (1/Dmm)$														Moist. Cont. by wt.			Index Property			Carb. % wt	
No.	Elev.	Material		UC	0	1	2	3	4	5	6	7	8	9	Mdϕ	Mnϕ	sdσ	Skew α	Wn %	Wl %	Wp %	Ip %	Act.	II	Dol.	Calc.
S34	198	shale		ML	1	4	8	22	28	34	45	55	68	80	6.5	6.6	2.9	+.035		57	26	31	1.55		0.0	4.7
S35	202	till, L	T	CI	0	4	10	21	32	45	54	61	71	75	5.5		3.0			34	17	17	0.68		2.0	5.4
S36	109	sandst.		SC	0	0	21	63	72	77	81	84	88	90	2.7	4.4	2.6	+.665	12.9						0.9	21.4
S37	111	sandst.		SC	0	0	42	51	60	71	75	79	84	87	2.6	4.8	3.2	+.687	6.8						1.2	5.9
S38	110	shale		CH	0	0	2	5	11	21	33	44	55	62	7.5		3.1		28.0	100	25	75	1.97	-.04	1.0	4.8
S39	114	sandst.	T	SM	0	31	45	57	68	75	79	83	84	86	3.3	5.0	3.5	+.484	10.5						0.7	4.6
S40	114.5	shale		CH	0	0	1	4	9	19	30	43	54	62	7.6		2.9		23.2	95	21	74	1.94	+.03	0.7	4.8
S41	116	shale		CH	0	0	0	0	6	20	33	44	54	61	7.6		2.8		29.5	102	25	76	1.95	+.05	0.0	4.8
S42	116.5	shale		CL	0	0	1	3	9	20	30	39	51	64	7.9		3.3		24.2	78	24	54	1.50	0.00	0.7	5.0
S43	117	shale	T	CL	0	0	3	7	14	21	30	41	57	66	7.7		3.5		33.2	68	32	36	1.06	+.01	0.7	4.6
S44	118	shale		CH	0	0	0	0	1	9	24	39	51	60	7.8		2.3		29.2	104	24	70	1.75	+.07	0.7	5.1
S45	116.5	shale		ML	0	0	0	1	26	50	61	67	69	72	5.0		1.25		21.2						0.7	4.8
S46	119	sandst.		SC	0	0	5	17	42	55	62	66	68	72	4.5		1.7		23.9						0.7	4.6
S47	121.5	shale		CL	0	0	0	0	10	35	50	58	64	67	6.0		1.8		55.7						0.7	5.1
S48	123	shale		CH	0	0	0	1	5	15	25	36	48	60	8.2		3.1		28.6	87	34	53	1.33	-.10	0.9	4.8
S49	136	shale		CH	0	0	0	6	16	27	38	46	53	60	7.5		3.5		22.4	153	29	124	3.10	-.05	0.0	4.5
S50	137	shale		CH	0	0	0	10	25	33	40	48	56	63	7.2		3.9		32.3	85	29	56	1.51	+.06	0.7	4.7
S51	138	shale		CL	0	0	0	5	13	20	29	36	45	53	8.7		4.3		22.6	75	25	50	1.06	+.05	0.7	4.7
S52	140	shale		CH	0	0	1	7	16	27	37	47	57	68	7.3	7.4	3.4	+.029	17.7	60	30	30	0.94	-.41	0.9	4.5
S53	141	shale		CH	0	0	0	0	0	3	10	22	35	48	9.2		2.7		22.0	132	35	97	1.86	-.13	1.2	5.3
S54	140.5	shale		CH	0	0	0	5	15	22	31	41	49	58	8.1		3.9		38.4	100	28	72	1.71	+.14	0.8	5.1
S55	142	shale		CH	0	0	0	0	4	14	30	42	50	57	8.0		2.8		63.7	134	29	105	2.44	+.33	1.8	4.7
S56	144	sandst.		SC	0	0	14	54	70	73	75	78	79	80	2.8		0.7		14.9						1.1	4.5
S57	144.5	sandst.		SC	0	0	3	10	35	54	61	66	69	72	4.7		1.2		22.0						0.7	4.8
S58	145.5	shale		CL	0	0	0	0	2	15	39	41	50	57	8.0		2.9		52.0	88	30	58	1.35	+.38	1.0	4.8
S59	146	shale		ML	0	0	1	5	11	20	30	40	50	62	8.0		3.5		19.6	64	28	36	0.95	-.23	0.7	4.3
S60	142	benton.		CH	0	0	0	1	2	3	4	5	6	7					47.9	148	40	108	1.16	+.07	1.4	8.8
S61	140.5	shale		ML	0	0	0	3	8	31	37	42	52	65	7.8		3.4		34.0						1.2	4.8
S62	140	shale		ML	0	0	0	2	6	14	23	34	45	59	8.3		3.2		27.6						1.5	4.8
S63	138.5	shale		ML	0	0	0	1	15	36	51	60	64	68	5.9		1.8		23.6						0.7	4.8
S64	136.5	sandst.		SC	0	0	6	8	77	78	80	82	84	86	3.3	5.8	2.6	+.962	17.2						0.9	4.6
S65	136.5	shale		CH	0	0	0	1	9	35	40	51	57	63	6.8		2.3		17.9	121	26	95	2.57	-.09	1.1	4.8
S66	134	shale		ML	0	0	0	1	3	10	25	39	51	62	7.9		3.1		20.6	67	32	35	0.92	-.33	0.7	4.8

Table 3. Test Results of Samples, Surface

Sample			TX	Wentworth Scale: % wt. coarser than $\phi = \log_2 (1/Dmm)$													Moist. Cont. by wt.			Index Property			Carb. % wt	
No.	Elev.	Material		UC	0	1	2	3	4	5	6	7	8	9	Mdϕ	Mnϕ	sdσ	Scew α	Wn %	Wl %	Wp %	Ip %	Act.	II	Dol.	Calc.
S67	133	sandst.		SC	0	0	0	4	33	49	58	54	66	68	5.1		1.6		27.9						0.7	4.8
S68	164	shale		CH	0	0	0	0	3	15	29	40	50	55	8.1		3.0		26.6	134	30	104	2.31	-.03	1.5	5.0
S69	165	sandst.		SC	0	0	31	62	73	77	80	83	85	87	2.5	4.7	3.1	+.710	2.8						1.0	5.0
S70	171	sandst.		SC	0	0	0	30	63	73	78	81	84	86	2.5	4.6	3.0	+.701	3.9						0.9	4.8
S71	171	shale		CH	0	0	0	1	8	21	32	41	47	51	8.8		4.2		26.3	183	29	154	3.14	-.02	0.0	5.9
S72	172	shale		CH	0	0	0	0	1	7	16	27	38	50	9.0		3.1		21.4	129	33	96	1.92	-.12	0.7	5.9
S73	172.5	shale		CH	0	0	0	0	1	37	41	46	49	51	8.4		4.9		30.2	180	29	151	3.08	+.01	0.7	6.0
S74	174	tuff		CL	0	0	0	1	4	8	18	30	40	51	8.9		4.1		22.4	86	32	54	1.10	-.18	0.9	5.7
S75	175	sandst.		SC	0	0	20	66	75	78	80	81	83	84	2.5	6.0	4.1	+.854	13.7						0.7	5.1
S76	176	sandst.		SC	0	0	4	12	40	50	56	60	65	68	5.0		1.8		23.0						1.7	5.5
S77	175	sandst.		SC	0	0	20	61	71	74	76	78	79	81	2.7	6.4	4.6	+.805	14.2						0.9	5.2
S78	180	sandst.		SC	0	1	30	56	70	75	77	79	81	83	2.8	5.8	4.2	+.727	10.1						1.0	4.8
S79	181.5	sandst.		SC	0	0	10	54	66	72	75	78	80	83	2.8	5.9	3.7	+.838	13.1						2.7	4.7
S80	182	shale		CH	0	0	0	1	20	32	41	47	51	55	7.7		3.9		24.0						0.8	5.5
S81	182.5	shale		CH	0	0	0	0	6	18	30	38	43	50	9.1		4.3		26.2	167	28	139	2.78	-.01	0.8	5.6
S82	184	shale		CH	0	0	0	0	15	30	40	46	49	52	8.5		4.4		23.3	146	31	115	2.40	-.07	0.7	5.4
S83	183	shale		CH	0	0	0	0	0	3	15	25	41	49	9.4		4.0		26.1	165	32	133	2.61	-.04	0.7	5.7
S84	185.5	shale		CH	0	0	0	1	2	5	15	27	37	49	9.1		3.0		22.0						1.2	5.9
S85	186	sandst.		SC	0	1	26	65	75	77	80	82	84	85	2.5	5.8	3.4	+.942	7.0						0.0	5.7
S86	190	sandst.		SC	1	8	39	65	77	82	85	88	90	91	2.4	3.5	2.2	+.501							0.7	68.0
S87	193	sandst.		SC	0	0	20	57	70	74	76	78	80	83	2.8	5.9	4.0	+.788	4.3						0.9	5.7
S88	191	sandst.		SC	0	0	0	10	55	66	71	74	78	80	2.6		0.6		18.5						0.7	5.0
S89	194.5	sandst.		SC	0	0	3	25	55	64	66	69	72	74	3.8		1.1		19.1						0.7	5.2
S90	195	tills,L	T	CI	1	6	13	25	40	50	59	67	72	75	5.0		2.7		14.7	29	16	13	0.52	-.10	2.7	5.6
S91	196	sand		SP	0	1	7	55	92	95	97	98	99	99	1.9	2.0	0.7	+.143	4.2						2.2	5.8
S92	200	shale		CL	0	0	0	0	0	0	5	15	27	41	9.4		2.3		26.6	65	27	38	0.65	-.01	1.0	5.2
S93	198	shale		ML	0	0	1	4	11	20	29	40	52	64	7.8		3.2		25.6	64	26	38	1.06	-.01	0.7	5.2
S94	196.5	shale		ML	0	0	1	3	10	20	30	43	56	70	7.5	7.3	2.2	+.091	27.2	58	33	25	0.83	-.23	0.8	4.6
S95	196	shale		ML	0	0	1	5	14	25	35	45	55	64	7.5		3.3		26.8						0.7	5.0
S96	195.5	sandst.		SC	0	0	1	7	47	58	63	67	70	73	4.2		0.8		20.8						1.0	5.1
S97	195	shale		ML	0	1	2	7	16	26	36	46	57	67	7.3		3.4		23.6	56	28	28	0.85	-.16	0.7	5.0
S98	193	sandst.		SC	0	0	7	32	55	62	71	75	77	79	3.7		1.3		18.9						1.0	5.6
S99	188	sandst.		SC	0	0	28	52	65	68	73	76	79	81	2.8	6.3	4.7	+.735	5.6						0.8	4.8
S100	187.5	shale	T	CL	0	0	2	5	12	19	26	37	53	64	7.9		3.3		14.6	77	26	51	1.42	-.22	1.1	5.0

Table 3. Test Results of Samples, Shear test

Sample			TX	Wentworth Scale: % wt. coarser than $\phi = \log_2 (1/Dmm)$														Moist. Cont. by wt.			Index Property			Carb. % wt	
No.	Elev.	Material		UC	0	1	2	3	4	5	6	7	8	9	Mdϕ	Mnϕ	sdσ	Scew α	Wn %	Wl %	Wp %	Ip %	Act.	II	Dol.	Calc.
SHEAR TEST SAMPLES																									
CE	172.5	sandst	X	SC	0	0	36	65	71	75	78	80	83	85	2.4	4.9	3.4	+ .75							1.0	4.7
#14	165	shale	X	CH	0	0	0	0	1	6	15	27	41	52	8.8		2.2			135	28	107	2.23		1.5	4.7

APPENDIX H

X-RAY REFRACTOGRAMS OF CLAY-SIZED FRACTIONS OF BEDROCK

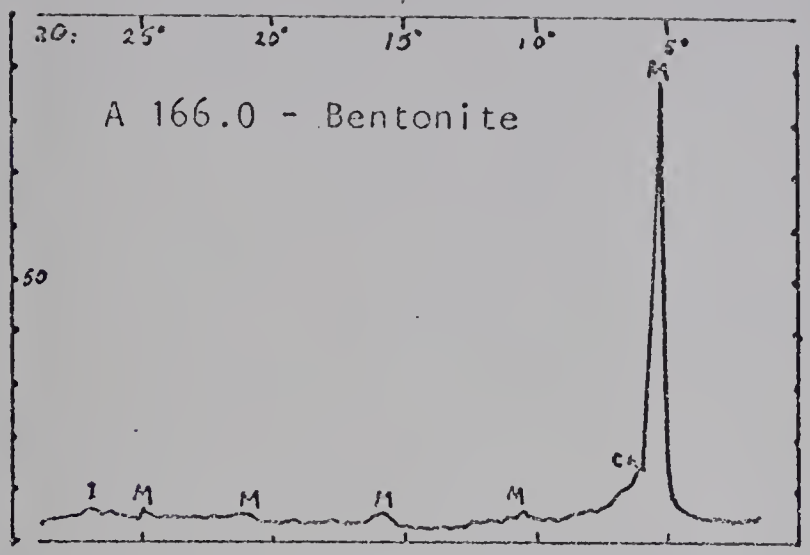

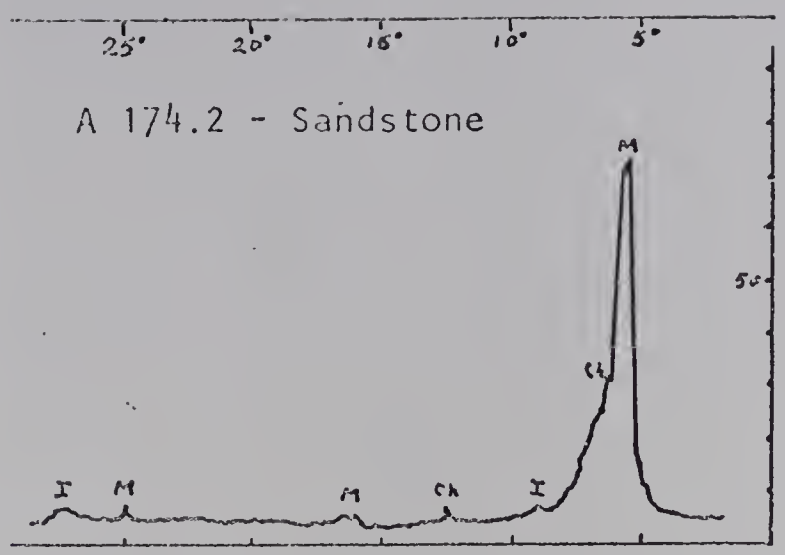

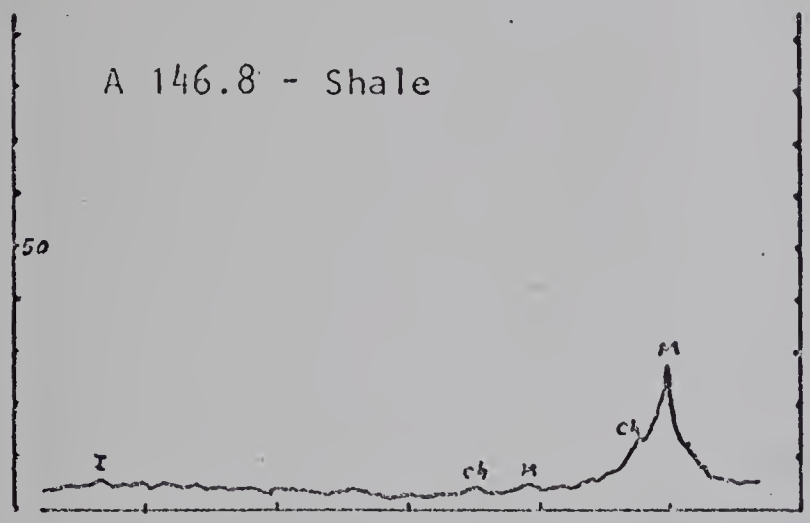

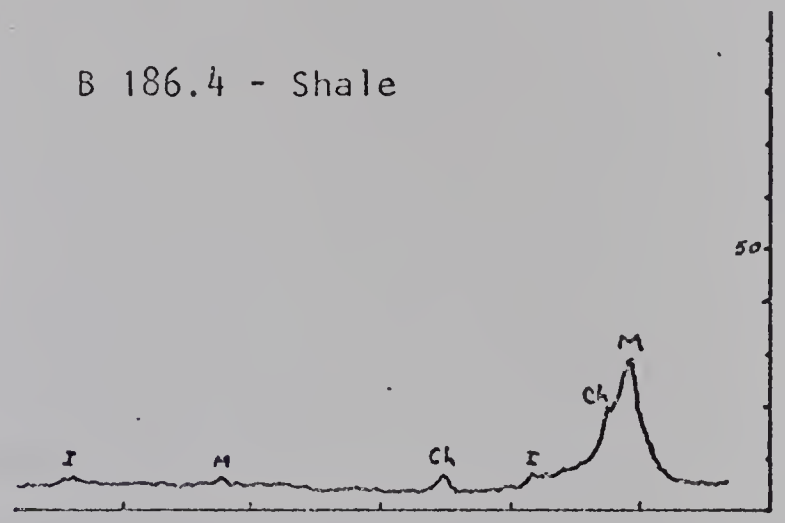

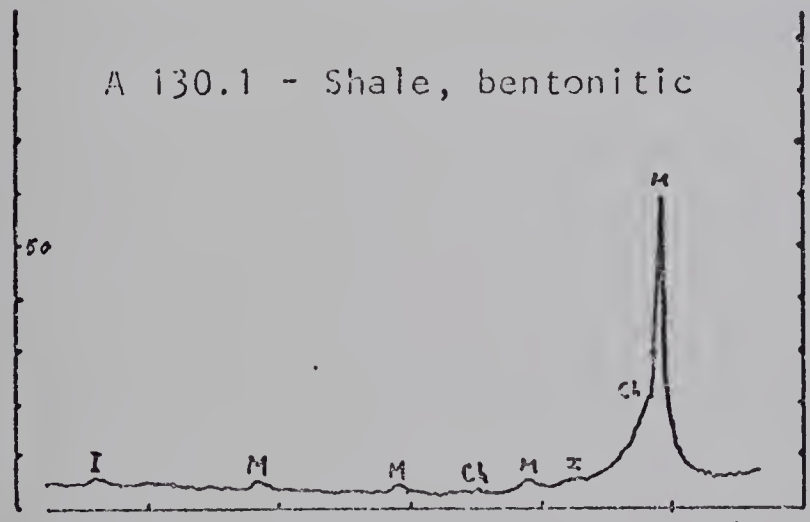

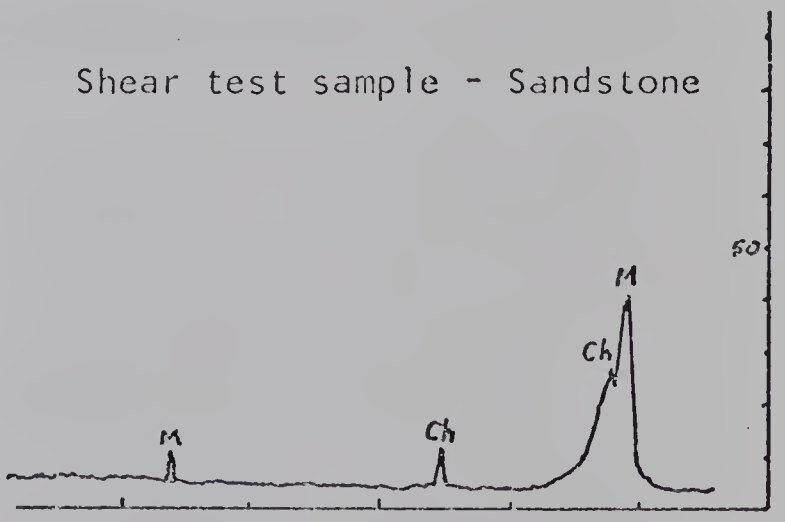

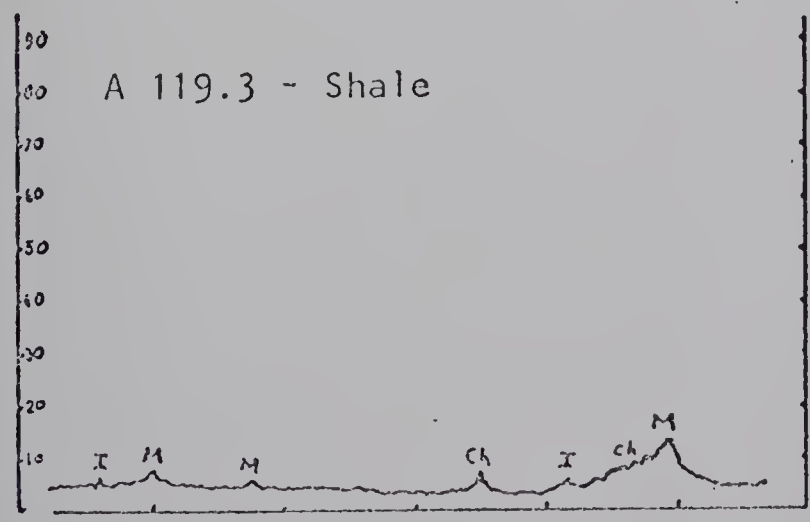

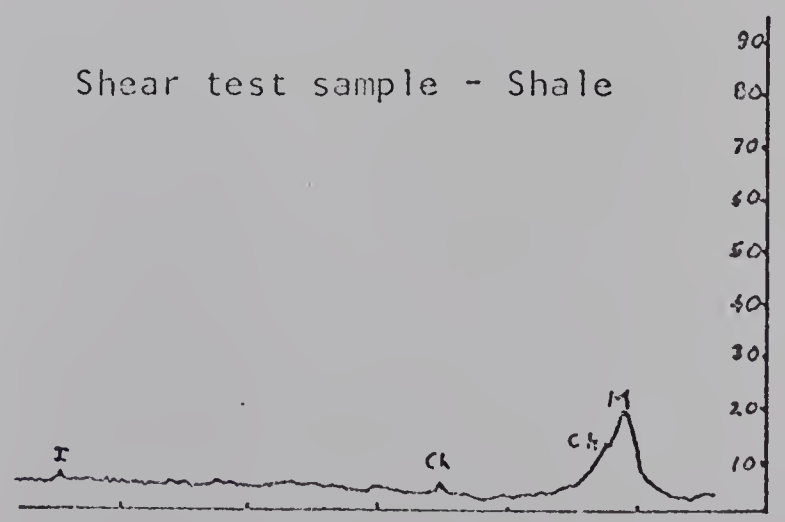

Machine setting, Cu: 16/1.0/2. Ch = Chlorite, I = Illite, M = Montmorill.

Table 4. X-ray refractograms of clay-sized fraction of bedrock

APPENDIX I

LEGEND TO PLATES III TO XII

LITHOLOGY

PRIMARY

- GLACIO - LACUSTRINE SILT & CLAY
- TILL
- SHALE
- SANDSTONE
- COAL
- CALCAREOUS SANDSTONE
- BENTONITE TUFF
- OVERBURDEN

SECONDARY

- SILTY
- JOINTED
- SHALEY SHALEY PEBBLES
- SANDY
- COALLY
- CALCAREOUS
- BENTONITIC TUFFACEOUS
- IRONSTONE CONCRETIONS
- DEVOID OF SECONDARY MAT'L

LEGEND TO PLATES III to XII

FIGURE: 51

NORTH

C

B

A

SILT TALUS

SILT & TILL TALUS

SANDSTONE & SHALE TALUS

TALUS

SANDY

SHALEY

BENTONITIC

COALLY

SILTY MUD

MUD

CLAY IRONSTONE

G-2

LEGEND

STRUCTURE

FRACTURE

BOUNDARY OF GEOLOGICAL MAPPING

LITHOLOGY

SHALE

BENTONITIC SHALE

SANDSTONE

CALCAREOUS SANDSTONE

COAL

IRONSTONE CONCRETIONS

UNDIFFERENTIATED

EDMONTON FORMATION

MAP OF STUDY AREA

SURFICIAL STRUCTURE AND LITHOLOGY
AND
LOCATION OF AUGER HOLES, TRENCHES AND SURFICIAL SAMPLES

ARBITRARY DATUM

PLATE I

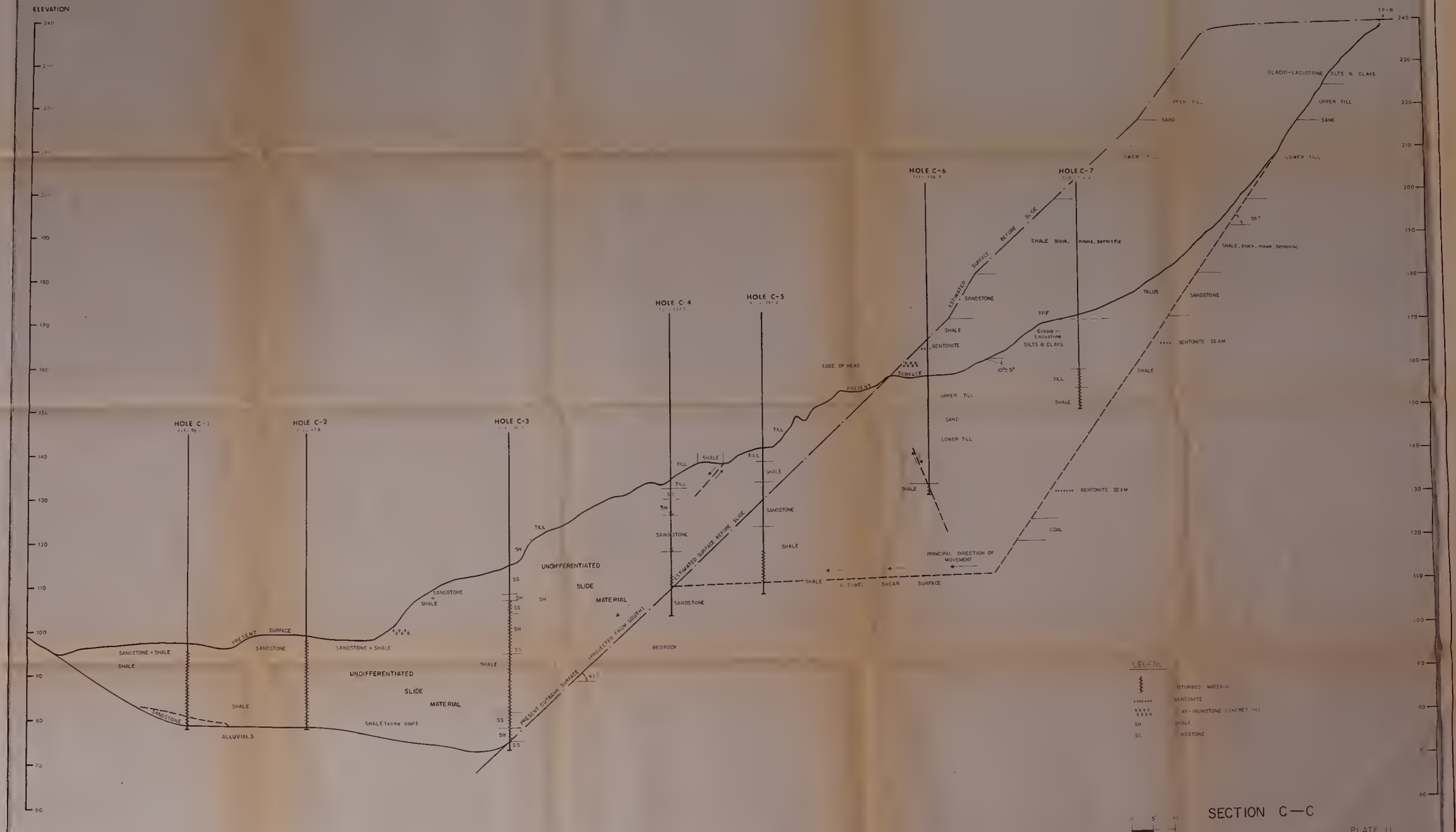
ELEVATION
HOLE C-1
HOLE C-2
HOLE C-3
HOLE C-4
HOLE C-5
HOLE C-6
HOLE C-7
TP-8
PRESENT SURFACE
SANDSTONE + SHALE
SANDSTONE
SHALE
ALLUVIALS
SHALE (some coal)
UNDIFFERENTIATED SLIDE MATERIAL
TILL
SH
SS
BEDROCK
EDGE OF HEAD
ESTIMATED SURFACE BEFORE SLIDE
PRESENT CUTBANK SURFACE (PROJECTED FROM SOUTH)
ESTIMATED SURFACE BEFORE SLIDE
PRINCIPAL DIRECTION OF MOVEMENT
R. SLIMEL SHEAR SURFACE
SHALE block, mows, bentonitic
BENTONITE
SANDSTONE
TPF
Glaco-Lacustine SILTS & CLAYS
UPPER TILL
SAND
LOWER TILL
TALUS
BENTONITE SEAM
COAL
GLACIO-LACUSTRINE SILTS & CLAYS
SHALE, black, mowe, bentonitic
LEGEND
DISTURBED MATERIAL
BENTONITE
SHALE
SANDSTONE
0 5' 10
SECTION C—C
PLATE II

HOLE Nº C-1

PLATE III

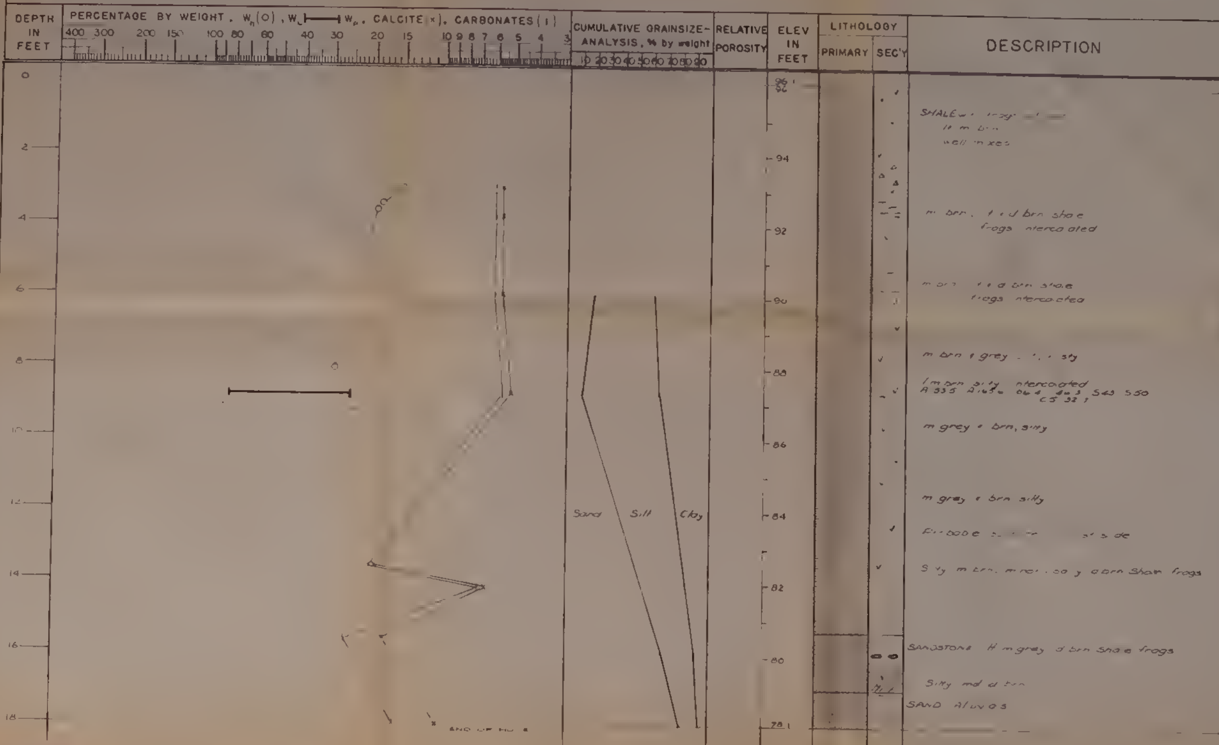

HOLE Nº C-2

PLATE IV

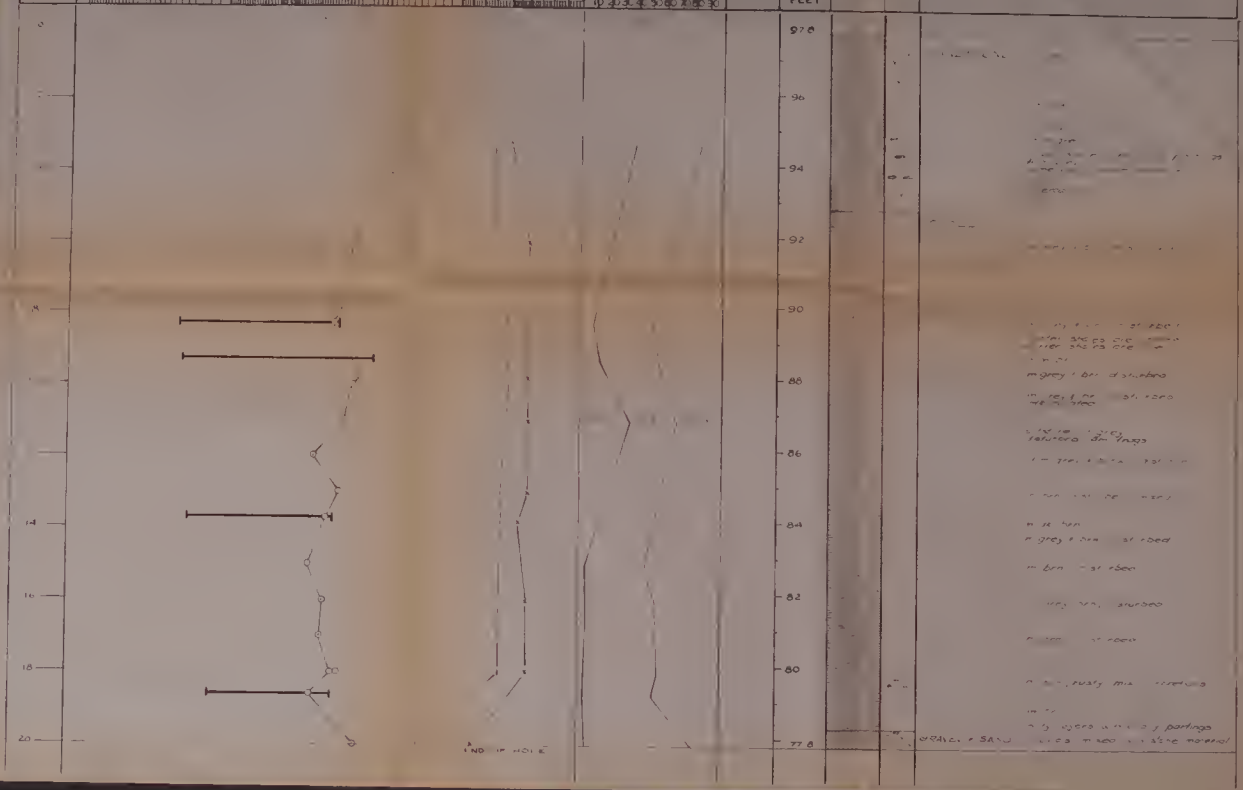

HOLE Nº C-3

PLATE V

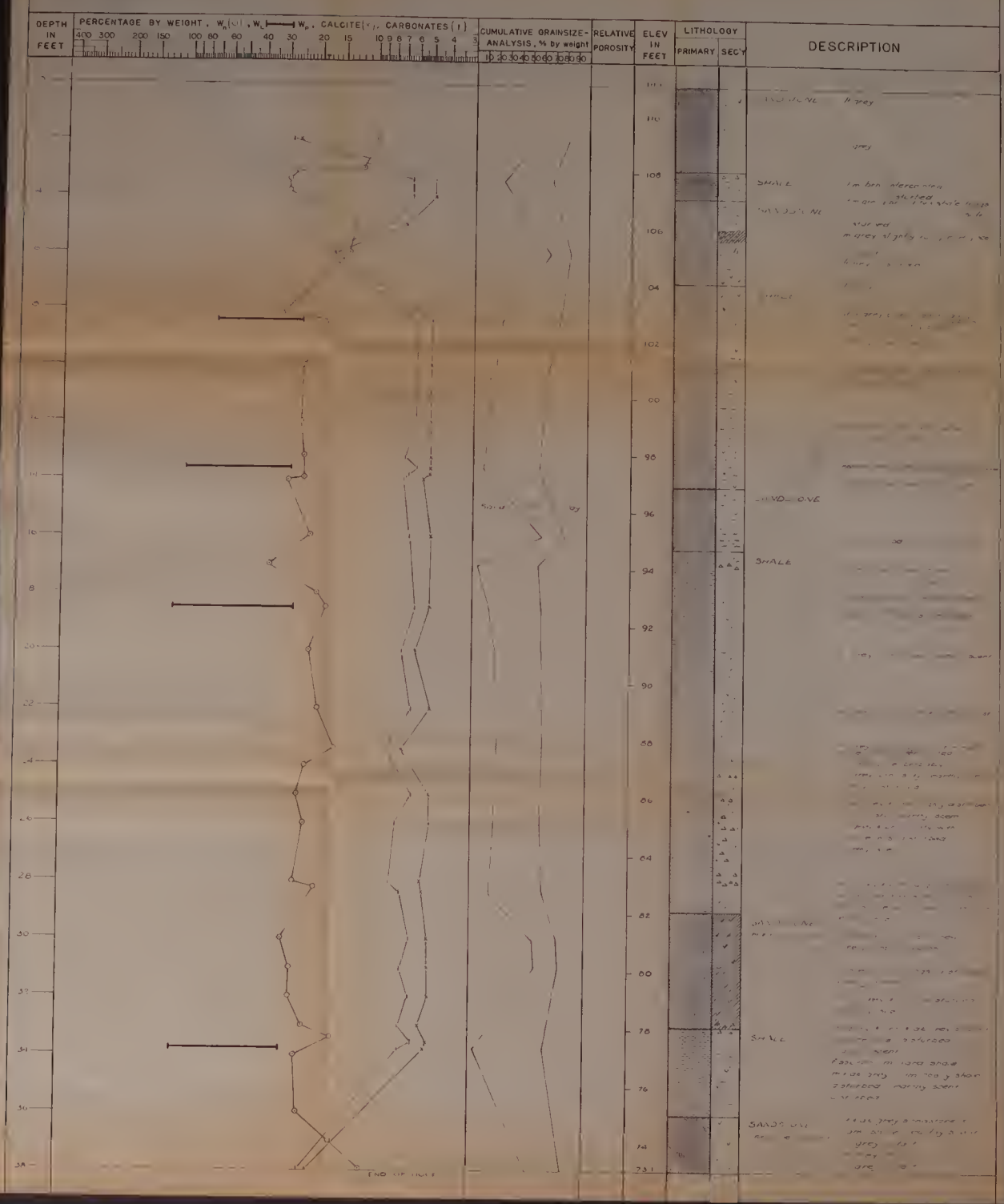

PLATE VI

HOLE Nº C-4

DEPTH IN FEET	PERCENTAGE BY WEIGHT, W_s / W_w, ATTERBERG LIMITS, CARBONATES (%)	CUMULATIVE GRAINSIZE ANALYSIS, % by weight	RELATIVE POROSITY	ELEV IN FEET	LITHOLOGY PRIMARY SEC'Y	DESCRIPTION
	400 300 200 150 100 80 60 40 30 20 15 10 8 7 6 5 4 3	10 20 30 40 50 60 70 80 90				
0						
1						
2						
3						
4						
5						
6						
7						
8						
9						
	END OF HOLE					

HOLE Nº C-5

PLATE VII

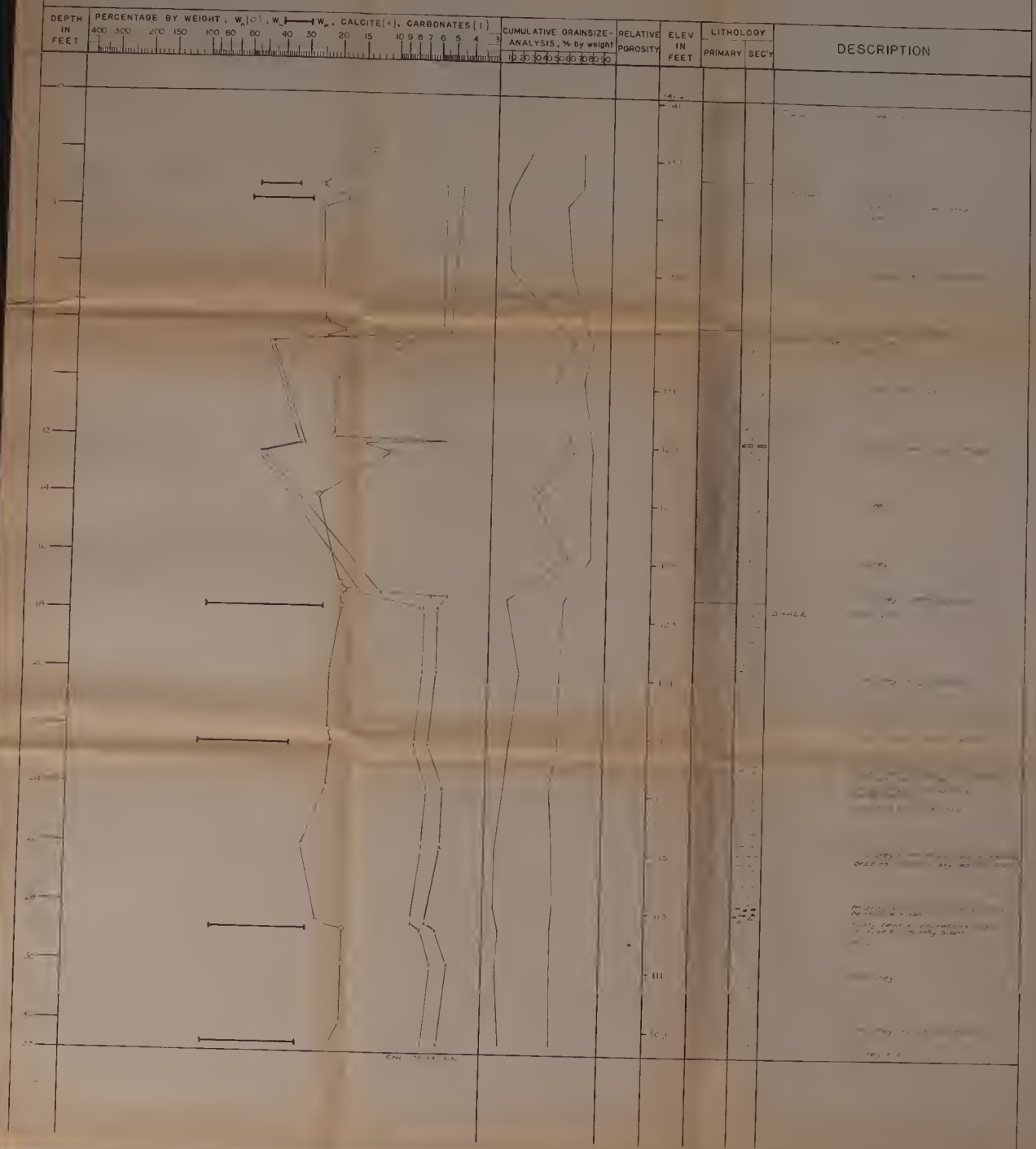

PLATE VIII

HOLE Nº C-6

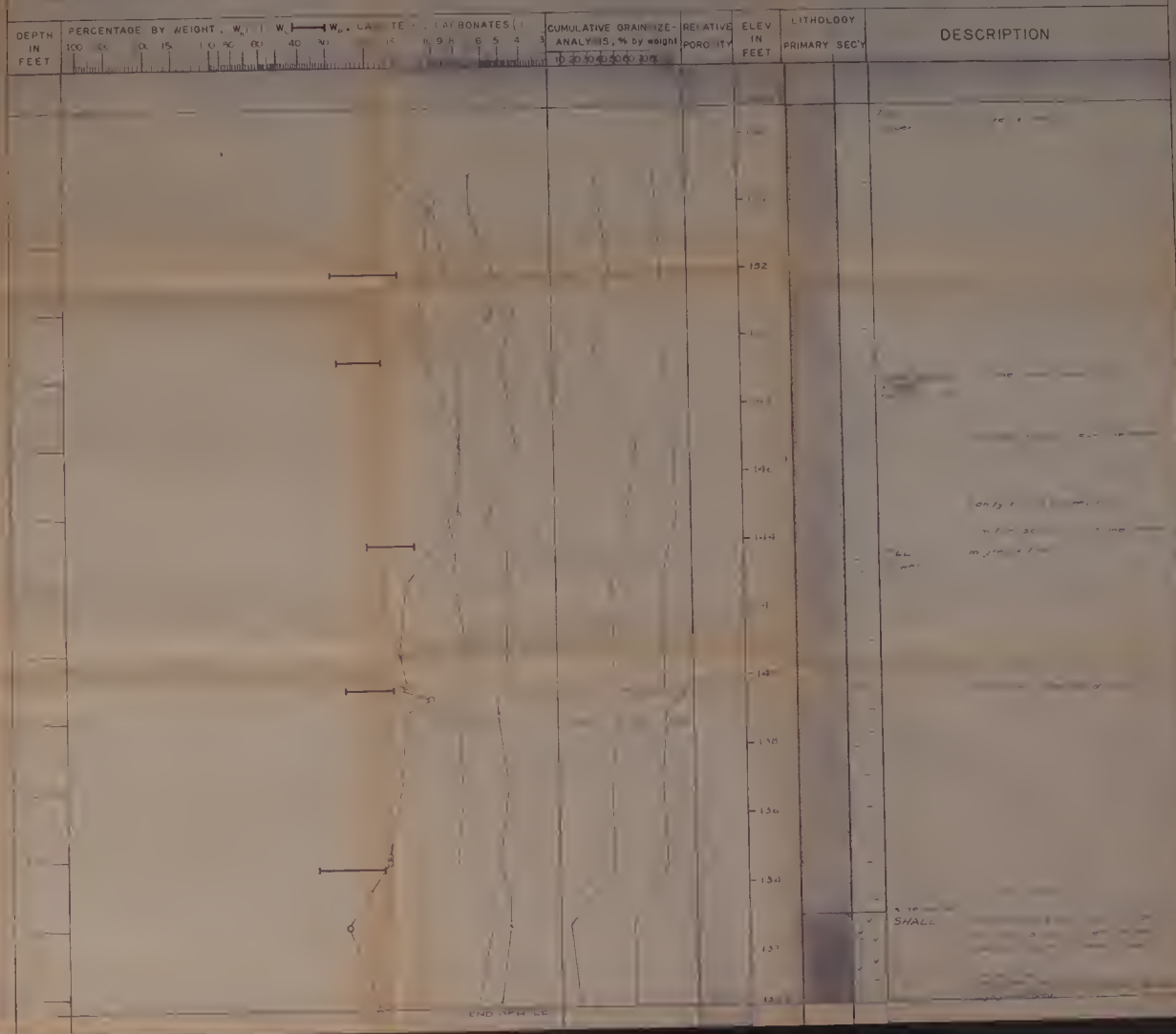

HOLE Nº C-7

PLATE IX

DEPTH IN FEET	PERCENTAGE BY WEIGHT, W_n(○), W_L ⊢—⊣ W_p, CALCITE(×), CARBONATES(↕) 400 300 200 150 100 80 60 40 30 20 15 10 9 8 7 6 5 4 3	CUMULATIVE GRAINSIZE-ANALYSIS, % by weight 10 20 30 40 50 60 70 80 90	RELATIVE POROSITY	ELEV IN FEET	LITHOLOGY PRIMARY	LITHOLOGY SEC'Y	DESCRIPTION
				168.4			
				160			LA E LDML N
				140			
				130			SHALL
				120			
				110			
				100			
10							

PLATE X

HOLE Nº D-1

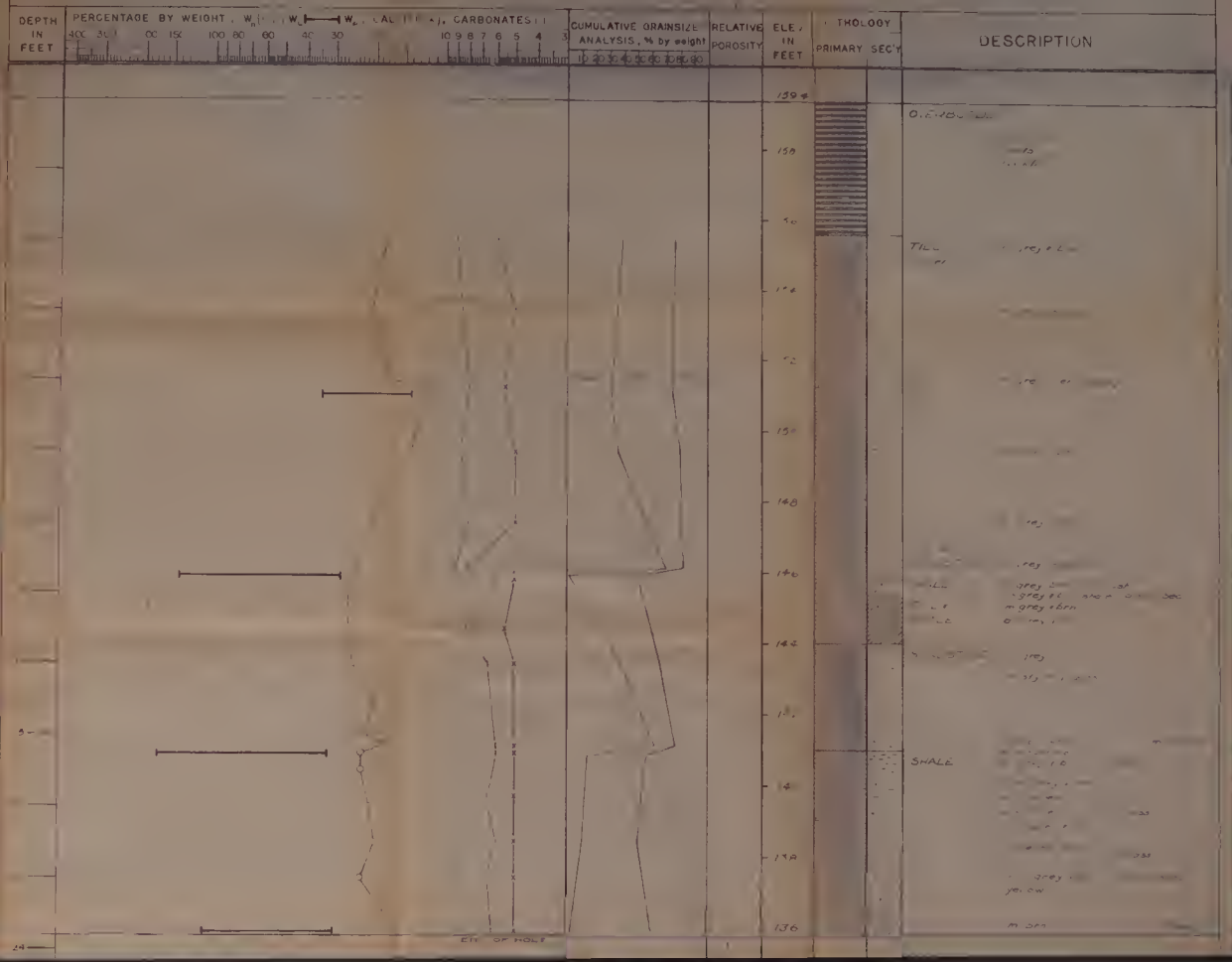

TRENCH Nº A

PLATE XI

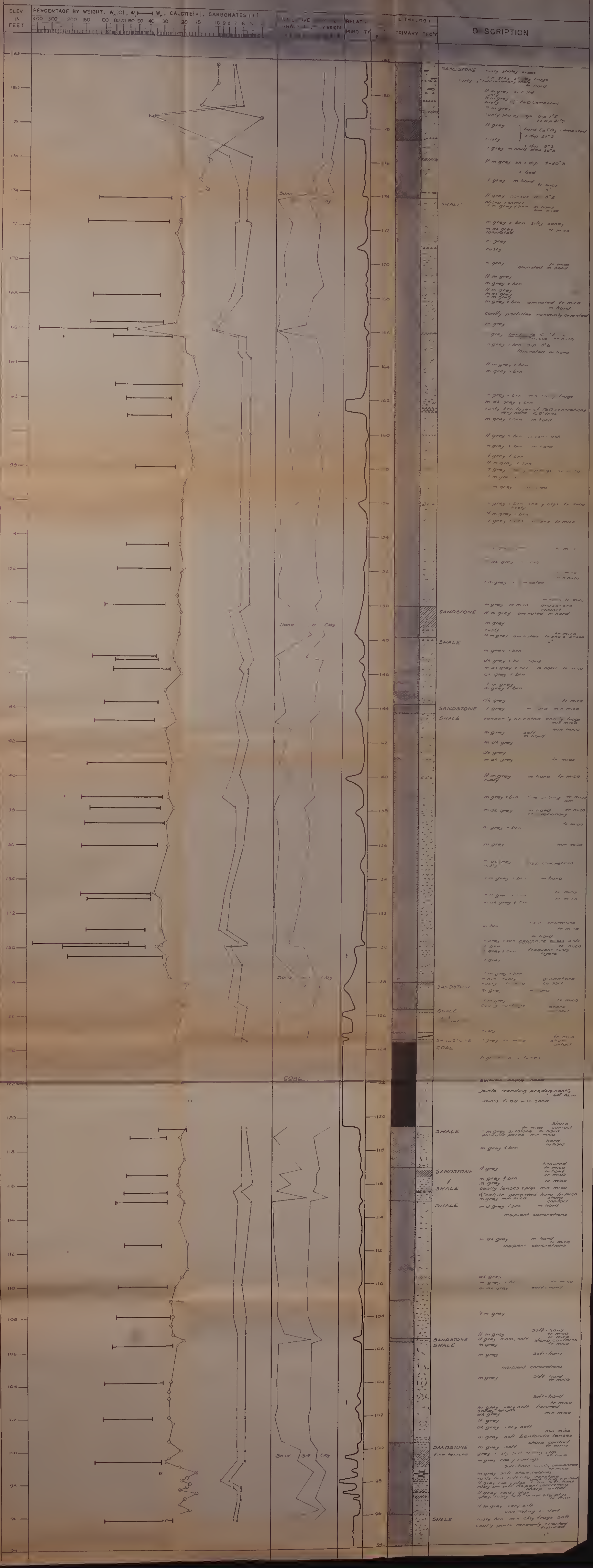

TRENCH Nº B

PLATE XII